© Copyright 2019

Anna Kathleen McLaskey

Multiple effects of ocean change on crustacean zooplankton: A coupled field-laboratory approach

Anna Kathleen McLaskey

A dissertation

submitted in partial fulfillment of the

requirements for the degree of

Doctor of Philosophy

University of Washington

2019

Reading Committee:

Julie E. Keister, Chair
Evelyn J. Lessard
Terrie Klinger

Program Authorized to Offer Degree:

Oceanography

University of Washington

Abstract

Multiple effects of ocean change on crustacean zooplankton: A coupled field-laboratory approach

Anna Kathleen McLaskey

Chair of the Supervisory Committee:
Associate Professor Julie E. Keister
Oceanography

In this dissertation I combine laboratory experiments and field observations across natural oceanographic gradients to investigate how crustacean zooplankton will be affected by ocean acidification (OA) and other co-occurring ocean changes. Anthropogenic emissions are increasing carbon dioxide concentrations in the atmosphere and ocean, causing declining seawater pH, increasing ocean temperatures, and decreasing dissolved oxygen concentrations. These changes have the potential to influence the metabolism, growth, and survival of crustacean zooplankton, such as copepods and krill, that act as critical prey items for higher trophic levels. Puget Sound, WA is a large coastal estuary with a wide range of pH and oxygen levels present in

different areas and seasons. By coupling laboratory methods and field observations, a wide range of drivers and mechanisms of ocean change can be considered, forming a powerful research approach. In Chapters 2 and 3, I characterized the pH exposure of the copepod *Calanus pacificus* and the krill *Euphausia pacifica* in Puget Sound and reared their eggs and larvae under a range of pH conditions in the laboratory. I found that krill larvae are sensitive to reduced seawater pH and may already be affected by pH conditions in some areas of Puget Sound. In Chapter 4, I investigated the effects of elevated CO_2 on the phytoplankton-copepod trophic link at two different temperatures, using the marine cryptophyte *Rhodomonas salina* and the calanoid copepod *Acartia hudsonica*. I observed complex shifts in phytoplankton fatty acid content and evidence of direct effects of CO_2 on copepods, as well as indirect effects mediated through changes in the phytoplankton. In Chapter 5, I used enzyme activities as physiological indicators of how adult *E. pacifica* are affected by pH and oxygen in controlled laboratory conditions and across natural oceanographic gradients in Puget Sound. To characterize the high inter-individual variability displayed by this species, I used an individual-based approach that had not previously been used with these indicators. In Chapter 6, I examined the use of aminoacyl-tRNA synthetases (AARS) activity in individual krill, explored the biochemistry underlying the assay, and suggested a modification to the method. This dissertation increases our understanding of how key zooplankton taxa are affected by seawater pH and the multiple pathways by which they can be affected. Additionally, this dissertation provides a basis for understanding how *E. pacifica* may be affected by OA in the future.

TABLE OF CONTENTS

LIST OF FIGURES

LIST OF TABLES

ACKNOWLEDGEMENTS

Thank you to my advisor Julie for her unwavering support in me along the varied paths I decided to take. I am incredibly grateful for everything she taught me about conducting research at sea, which has become something I truly love. She has been a wonderful example of adapting plans on the fly in response to conditions or results, and keeping an upbeat attitude no matter what happens.

I would also like to thank the members of my committee, Evelyn Lessard, Steve Emerson, and Terrie Klinger, for many helpful conversations and always making me think critically and realistically about my ideas.

I was able to accomplish this research because of several important collaborations. Thank you to Shallin Busch, Paul McElhany, Brady Olson, and Brooke Love for being wonderful mentors and for sharing their varied knowledge and experiences. Also thank you to Ted Packard and Lidia Yebra for mentoring me in the specifics of enzyme activities from across the world.

Amanda has been an amazing coworker these past seven years. It has been a pleasure to spend so many days at sea and at the microscope together; she is a confident, ferocious woman, with infectious energy. BethElLee also started working with me early on as a volunteer and I am lucky she never left because she is strong, compassionate, and always there to just get the job done. I am grateful for the community that they gave me.

Thank you to all the Ocean staff that make so many things possible, especially Shelly, Su, Kathy, and Aaron and Kathy K. All the students that I have mentored make the research happen, and also so much fun. My time at sea has been some of the most important experiences I've had during grad school. Huge thanks to all the captains and crew I have worked with, and especially Ken Pinnell and Brian Bare.

Frieda Taub has been a mentor, colleague, and friend for over ten years. She has helped me see the long game and keep a level head in what has sometimes seemed like a crazy world to try and live in. I am forever grateful for being welcomed into her lab and family.

The graduate student community has been a sustaining force for me over the past seven years, united by shared loves of beer, biking, costumes, dancing, and a firm belief that we have a role to play in understanding the ocean and its place in society, as well as in improving higher education. Special thanks and love to my cohort, Team Z: Dewey, Earle, Miguel, Evan, Diane, Owen, and Lisa. Special thanks to my wonderful officemates for complaining with me, drinking with me, and finding ways to laugh at our stresses. Earle and Dewey have truly become family. My adopted lab mates: Max, Sasha, Robert, and Amy. Also Ashley, Hilary, Katherine, Hally, Elizabeth, Jake, Angie, Isaiah, and Robin. The IGERT program and all of its fellows has been an amazing source of knowledge and friendship, and extended my community across the university. Thank you Christine, Eliza, Eleni, Elizabeth, Adam, Merrill, and Alex Lowe. But truly, I cannot name everyone who has added to every BBT, Toaster, First Friday, Tea Time, Thunderfjords game, and shared struggle. Thank you team!

And finally, thank you to my family. To my parents for always encouraging me to get outside and keep questioning, and my brother and sister-in-law for sharing their experiences, frustrations, and joys along their paths with me. And to my other family—BJ, Emma, Sydney, Sarah, Laura, Gillie, Russell, Stephen, Daniya, Hannah, Sara, and Austin—thank you for helping keep my eyes on the stars, my feet in the mud, and the wind at my back.

DEDICATION

For BJ, my biggest champion. To the stars and back, my love.

Chapter 1

INTRODUCTION

The oceans are currently experiencing a period of rapid environmental change. Anthropogenic carbon dioxide emissions have increased CO_2 concentrations in the atmosphere, causing global temperatures and ocean CO_2 concentrations to rise (IPCC 2014). When CO_2 dissolves in seawater, a series of chemical reactions occur that reduce pH and decrease the availability of carbonate ions in a process called ocean acidification (OA). In addition, the physical and biological responses to rising temperatures in the ocean are causing dissolved oxygen (DO) concentrations to decrease (Breitburg et al. 2018). These three main areas of global ocean change are occurring simultaneously and will likely have widespread effects on marine organisms and ecosystems.

Crustacean zooplankton, like copepods and krill, are critical components of marine ecosystems. They link primary production to higher trophic levels by serving as an abundant and nutritious prey source for fish, seabirds, and mammals. Zooplankton also play a significant role in marine biogeochemical cycling. They are major consumers within the euphotic zone, producing rapidly-sinking fecal pellets that are biological hotspots and transport organic matter to the deep ocean. Given their pivotal role in marine systems, understanding how their populations will be affected by ocean change is an important research priority.

Although many crustaceans are tolerant to OA (Whiteley 2011; Kroeker et al. 2013), some crab (Swiney et al. 2016, Miller et al. 2016) and krill species (Kawaguchi et al. 2013) are sensitive. Early OA research on adult copepods showed that they are generally resilient; however, early life stages can be more sensitive to pH shifts (Lewis et al. 2013; Cripps et al. 2014b). Sensitivity to pH is also affected by other stressors such as temperature, which has a broad influence on organism physiology (Kroeker et al. 2013). Similarly, oxygen concentrations constrain the overall metabolism of an organism and can reduce its ability to maintain processes such as acid-base balance. These concurrent ocean changes influence organism physiology, community structure and diversity, and ultimately, affect marine ecosystem functioning (Doney et al. 2012).

Krill and copepods display a variety of behaviors and life cycle traits that influence their exposure and sensitivity to environmental drivers. As adults, they undertake diel vertical migration over hundreds of meters depth, experiencing a wide range of conditions on short time scales. Many species, including those studied in this dissertation, release their negatively-buoyant eggs at the surface, after which they sink down into the water column to hatch. The first few life stages do not feed but rather rely on endogenous energy sources. As they molt into progressively older stages they develop mouthparts, digestive tracts, and stronger swimming appendages, eventually making their way up to the food-rich surface waters. These changes in depth can correspond to different environmental experiences across life stages, and the large morphological changes larvae undergo are accompanied by physiological shifts that influence their tolerance to environmental conditions.

Zooplankton are influenced by ocean change through a complex combination of drivers and mechanisms. In coastal waters, pH, DO, and temperature are often correlated with each other

(Reum et al. 2014) because they are driven by similar process, e.g., low pH and low DO conditions co-occur because they are both exacerbated by respiration and low mixing. As a result, organisms are often exposed to multiple stressors at once. Crustacean zooplankton may also be affected by ocean change through indirect mechanisms, which are caused by changes in other species such as competitors, predators, or prey. Change in the availability and nutritional quality of phytoplankton is hypothesized to be one way through which OA will affect marine ecosystems. Increased CO_2 and temperature can both affect phytoplankton in ways that influence the quantity and quality of food available for zooplankton by modifying growth rate and biochemical content.

Laboratory experiments provide detailed characterization of specific processes under controlled conditions, while field observations integrate multiple pathways and drivers simultaneously with little control. Integrating both approaches requires the use of biomarkers that can characterize the state of zooplankton in both lab studies and the field. Enzyme activities are promising biomarkers because they are proxies for the physiological rates that determine the physical state of an organism and are often more sensitive to environmental changes than biochemical content (Pan et al. 2015). Laboratory results provide evidence for where and how we expect biomarkers to change in the field, and observations from the field can shed light on how field-specific processes might modulate responses observed in the lab.

The long-term OA, warming, and deoxygenation trends are occurring on a global scale, but ocean conditions also display a high degree of spatial and temporal variability across smaller scales (Hofmann et al. 2011; Chan et al. 2017). Coastal waters are highly variable environments as a result of freshwater inputs, eutrophication, and dynamic circulation patterns. The California Current Ecosystem (CCE) is an area where naturally low pH conditions occur due to seasonal

upwelling, which brings cold, low DO, high CO_2, and low pH waters up onto the continental shelf (Feely et al. 2008). Seawater pH levels that are predicted for the open ocean in the future are found in areas of the CCE today, making it an informative system to investigate the biological and ecological effects of these conditions.

Puget Sound (PS) is a large coastal estuary connected to the northern CCE, with complex morphology, bathymetry, and circulation patterns that gives rise to a wide range of oceanographic conditions within close physical proximity (Feely et al. 2010; Pelletier et al. 2018). Deep water that is upwelled onto the shelf enters PS where estuarine processes such as freshwater inputs and respiration act to further modify seawater chemistry. In particular, Hood Canal is a deep basin fronted by a shallow sill that develops low pH and DO conditions at depth. In summer, strong stratification, restricted mixing, and high productivity in the surface layers lead to CO_2 accumulation and O_2 drawdown in deeper waters. In some areas, waters with pH 7.32 have been observed (Feely et al. 2010), while low DO conditions regularly develop over the course of the summer leading to seasonal hypoxia (Newton et al. 2002). This provides a natural analogue for future ocean conditions where responses to environmental variability in space can substitute for changes over time.

This dissertation integrates lab and field approaches to investigate copepod and krill responses to a changing ocean. The primary focus is on OA, but it is considered in the context of concurrent changes in oxygen and temperature. Using these two main groups of holozooplankton, I explore their exposure and sensitivity to changing conditions across life stages, investigate indirect effects mediated by changes in their phytoplankton prey, and compare physiology across natural environmental gradients and under controlled laboratory conditions.

In Chapters 2 and 3, I characterized the pH exposure and sensitivity of early life stages of the copepod *Calanus pacificus* and the krill *Euphausia pacifica*. This was the first evaluation of how these two abundant and ecologically important species may be affected by OA. In the 4th chapter of this dissertation, I investigated the direct and indirect effects of elevated CO_2 on the phytoplankton-copepod trophic link at two different temperatures, using the marine cryptophyte *Rhodomonas salina* and the calanoid copepod *Acartia hudsonica*. Chapters 5 and 6 investigate *E. pacifica* using Electron Transport System (ETS) and aminoacyl-tRNA synthetases (AARS) activity as physiological indicators in an individual-based approach that has not before been used with these indicators. In Chapter 5 I characterized krill physiology in relation to seawater pH and DO concentrations both in the laboratory and across a broad range of oceanographic conditions present in Puget Sound. In Chapter 6, I explored the details of measuring AARS activity in individual *E. pacifica*, and examined the biochemistry underlying the assay. Finally, in Chapter 7, I explore important considerations outside the scope of this dissertation, summarize the open questions that still remain, and identify priorities for future research.

Chapter 2

DEVELOPMENT OF *EUPHAUSIA PACIFICA* (KRILL) LARVAE IS IMPAIRED UNDER CO_2 LEVELS THAT ARE CURRENTLY OBSERVED IN THE NORTHEAST PACIFIC

(This manuscript has been previously published as: McLaskey A.K., Keister J.E., McElhany P., Olson M.B., Busch D.S., Maher M., Winans A.K. (2016) Development of Euphausia pacifica (krill) larvae is impaired under pCO_2 levels currently observed in the Northeast Pacific. Marine Ecology Progress Series 555: 65-78)

2.1 ABSTRACT

Despite the critical importance of euphausiids in marine food webs, little ocean acidification (OA) research has focused on them. *Euphausia pacifica* is a dominant and trophically important species of euphausiid throughout the North Pacific and the California Current Ecosystem, where low pH conditions are occurring in advance of those in the global ocean. We assessed the impact of reduced pH on the hatching and larval development of *E. pacifica* in the laboratory and characterized the pH that *E. pacifica* eggs and larvae are currently exposed to in Puget Sound, WA, a large estuary connected to the California Current. In two independent sets of laboratory

experiments that lasted 6-22 days and involved 110 different females' broods, we found that hatching is robust to a wide range of pH levels, but larval development and survival are reduced at pH levels that are currently observed within their habitat. Survival from three days post hatch to the calyptopis 2 stage was reduced by an average of 20% at pH 7.69 compared to pH 7.96. Even though this population experiences a range of pH conditions on seasonal and daily timescales, it may be living near the limits of its pH tolerance. Continued OA may push these organisms past their threshold, which could have cascading negative consequences for higher trophic levels.

2.2 INTRODUCTION

Ocean acidification (OA) is a reduction in the pH of the ocean over time that is primarily caused by the ocean's uptake of carbon dioxide from the atmosphere (IPCC 2011). Average surface ocean pH has declined 0.1 pH units (from 8.2 to 8.1) since the industrial revolution (Caldeira & Wickett 2003) and is predicted to decline an additional 0.3 pH units by 2100 (Feely et al. 2009). This predicted change represents a 150% increase in ocean acidity since the beginning of the industrial revolution. OA is happening at a faster rate than any time during the past 50 million years (Hönisch et al. 2012) and has the potential to affect marine ecosystems throughout the world (Hofmann et al. 2010; Kroeker et al. 2013). Increased CO_2 affects both calcification and acid-base physiology in marine organisms; in some species, the increased metabolic costs of compensating for decreased pH can divert energy away from growth and reproduction (Melzner et al. 2011; Thomsen et al. 2013; Pedersen et al. 2014a). In general, increased CO_2 decreases survival, calcification, growth, and development in marine invertebrates, but with highly variable responses among different groups (Kroeker et al. 2013).

Regional patterns of pH and aragonite saturation state vary; high latitude waters and some coastal areas such as upwelling systems will experience harmful pH conditions sooner than the rest of the ocean due to a combination of natural and anthropogenic factors (Orr et al. 2005; Hauri et al. 2013). The California Current Ecosystem (CCE) is an ecologically productive and economically important upwelling system that has low and declining pH throughout the water column (Gruber et al. 2012, Hauri et al. 2013). During upwelling events in the CCE, high pCO_2/low pH deep water is driven up onto the continental shelf (Feely et al. 2008). Although this is a natural phenomenon, the CO_2 load of the upwelled waters is increasing over time as the oceans absorb anthropogenic CO_2, leading to increasingly acidified waters. The current anthropogenic carbon load has led to the shoaling of the aragonite saturation horizon (where dissolution and precipitation of the aragonite form of calcium carbonate are equally favored) by about 50 m across the shelf and to even reach the surface at times (Feely et al. 2008). Carbonate chemistry in the CCE has already shifted significantly from its pre-industrial range, and even greater changes are predicted in the near future (Hauri et al. 2013). In estuaries within the CCE, OA is exacerbated by runoff of low-pH freshwater and the respiration of organic matter, which increases CO_2 loading and drives the pH down even further (Feely et al. 2010). Organisms living in regions like the CCE where ocean pH is naturally low and declining could give insight into species responses to the chemical conditions expected elsewhere in the future. Are these species sensitive to the changes expected with OA or do they display adaptation to the low and variable pH conditions currently experienced in their environment?

Despite their ecological importance, very few OA studies to date have focused on euphausiids. Experiments have shown that *Euphausia superba*, a keystone species in Antarctic ecosystems, has reduced hatching at 1250 µatm pCO_2 (pH 7.50) compared to 380 µatm and

complete hatching failure at 2000 µatm pCO_2 (pH 7.36-7.40); however, larval swimming activity is not affected by three days post hatch at 1000 µatm pCO_2 (Kawaguchi et al. 2011, 2013). Even at moderate levels of 672 µatm pCO_2 (pH 7.84), adult *E. superba* increase feeding and nutrient excretion rates, which may indicate shifts in metabolism associated with acid-base regulation (Saba et al. 2012). Sub-adults of the north Atlantic krill *Nyctiphanes couchii* have reduced survival at pCO_2 concentrations between 1100 and 1700 µatm pCO_2 (pH 7.63 and 7.47), but other life stages have not been tested (Sperfeld et al. 2014). The few published studies on euphausiids are not sufficient to generalize the effects of increased CO_2 across species, especially without an evaluation of equivalent life stages. Early life stages generally have narrower physiological tolerances than other life stages and are predicted to be the most vulnerable to OA and other environmental changes (Kurihara 2008; Byrne 2011). The current literature characterizes crustaceans as generally tolerant to OA (Whiteley 2011, Kroeker et al. 2013, Wittmann & Pörtner 2013). However, very few holoplanktonic crustaceans have been studied to date and those that have been tested are primarily copepods (Riebesell and Tortell 2011).

Euphausia pacifica is a dominant zooplankton species throughout the North Pacific and the northern CCE (Brinton 1962), and an important prey item for fish, whales, and seabirds (Field and Francis 2006). The goals of this study were to characterize the pH conditions currently experienced *in situ* by *E. pacifica* eggs and larvae in Puget Sound, a large estuary adjoined to the northern CCE, and to test in the laboratory the influence of current and future pH levels on the development of this important species. During development from eggs to juveniles, *E. pacifica* pass through two nauplius stages and one metanauplius stage which are non-feeding, then three calyptopis stages (C1-C3) followed by seven furcilia stages which are all feeding. *E. pacifica* has been successfully reared under laboratory conditions from egg to adulthood, but they have not

been successfully mated in the lab to our knowledge. There are currently no published studies on the effects of increased pCO_2 on *E. pacifica*, however, sensitivity to pCO_2 can vary within and among species based on the organism's exposure to pCO_2 in their environment (Maas et al. 2012; Lewis et al. 2013; Kelly et al. 2013), and the population tested in this study inhabits an environment with large seasonal and geographic variation in pCO_2 and pH. Therefore, we hypothesized that the hatching and early development of Puget Sound *E. pacifica* populations would be robust to the intermediate pCO_2 levels they currently encounter in the field, but would be reduced at higher pCO_2 levels they may encounter in the future. We tested this hypothesis by sampling the pCO_2 conditions they experience in the field and simulating those and projected future levels in the laboratory.

2.3 METHODS

2.3.1 *Field chemistry and euphausiid distributions*

We characterized the pH environment currently experienced by *E. pacifica* eggs and larvae at two stations in the northern end of Hood Canal in Puget Sound, WA (47.61˚N 122.94˚W and 47.66˚N 122.86˚W; known as Puget Sound Regional Synthesis Model (PRISM) stations P14 and P15; Figure 2.1). Samples were collected during the day and night on 9-10 April and 15-16 June 2012. This design was chosen to sample during *E. pacifica's* spawning season (approximately February to July) in an area where low pH waters occur (Feely et al. 2010). We collected physical and chemical data using a conductivity temperature depth (CTD) profiler equipped with a pH sensor (SBE 18, Sea-Bird Electronics) and Niskin bottles, which were used to collect water at six depths for spectrophotometric pH, total dissolved inorganic carbon (DIC), and total alkalinity (TA) analyses. The CTD's pH sensor was not accurate, so it was only used to

determine the shape of the pH profile relative to discrete measurements. Spectrophotometric pH was measured shipboard immediately after water sampling (Ocean Optics USB 2000+ Fiber Optic Spectrometer; m-cresol purple dye from Sigma Aldrich). TA was measured by open-cell potentiometric titration (according to SOP 3b in Dickson et al. 2007) and DIC was measured by acidification and quantification either using a Licor-700 CO_2 detector at the University of Washington's Friday Harbor Laboratory, or a CO_2 coulometer (UIC model CM5015) at the University of Washington's School of Oceanography. All chemistry samples from the field and experiments were analyzed according to Dickson et al. (2007) and Riebesell et al. (2010). We calculated full carbonate system parameters using CO2sys version 2.1 (Lewis & Wallace 2012) with K1 and K2 constants from Lueker et al. (2000), $KHSO_4$ constant from Dickson (1990), $[B]_T$ from Uppström (1974), and the total pH scale.

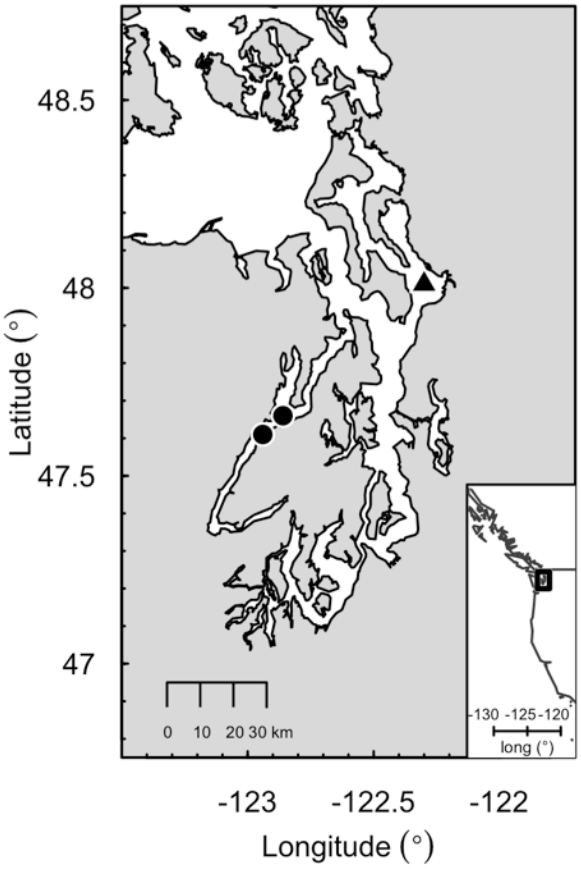

Figure 2.1. Location of study area in Puget Sound, WA. Field sampling stations P14 (southwest) and P15 (northeast) are shown with circles. Possession Sound, the location for experiment organism collections, is shown with triangle.

We collected zooplankton samples at the same locations where carbon chemistry was measured through a series of depth-stratified net tows. Larger life stages were quantified from oblique net tows using a five-net, 335-μm mesh, 0.25-m^2 Hydro-Bios Multinet sampler; smaller life stages were sampled with a 60-cm diameter, 75-μm mesh, closing ring net lifted vertically over discrete depth ranges. For all collections, a flowmeter was used to monitor the volume of water filtered. Samples were preserved in a 5% buffered formalin and seawater solution. In the laboratory, samples were diluted to 4-8 times the settled volume and subsampled with a 10-ml

Stempel pipette. Four to nine subsamples were counted: *E. pacifica* larvae were speciated and identified to the developmental stage.

2.3.2 *Laboratory Tests*

We report findings from two sets of experiments. The first set of experiments (hereafter, Experiment 1) characterized the sensitivity of *E. pacifica* hatching and development to the first feeding stage (calyptopis 1) across a wide range of pH conditions. The second set of experiments (Experiment 2) targeted a refined range of pH conditions based on Experiment 1, and the development tests were extended to the second feeding stage (calyptopis 2).

Ovigerous female *E. pacifica* were collected at night in May and June 2013 (Experiment 1) and 2014 (Experiment 2) from Possession Sound, WA (Fig. 1) between 22:00-01:00 using a 1-m diameter, 2000-μm mesh ring net with a non-filtering cod end towed obliquely through the upper 50 m of the water column at 2-3 knots. Krill were kept in a cooler and transported back to the lab within 4 hours. There, we distributed one healthy female per 500-ml jar of pre-equilibrated treatment water (described below), which was capped and held at 12˚C. The following morning, all females were removed and any eggs were counted and left undisturbed in the 500-ml hatching jars.

Experiment 1 was conducted at the National Oceanic and Atmospheric Administration Northwest Fisheries Science Center (NOAA NWFSC) in Seattle, WA. Treatment conditions were chosen to cover the broad range of pH conditions that *E. pacifica* currently experiences in Puget Sound (pH 8.0, 7.7, 7.4/ pCO_2 400, 800, 1600 μatm, based on our field measurements described below) and may experience in the future (pH 7.3, 7.2/ pCO_2 2400, 3200 μatm). The difficulty of collecting large numbers of ovigerous females from the field prevented us from populating all treatment conditions simultaneously. Instead, we conducted five separate trials to

complete Experiment 1, each with two pH treatments (Table 1). Hatching jars containing incubating krill eggs (or after hatching, larvae) were kept sealed in a 12˚C water bath, with partial water changes every two days (described below) for seven days, until approximately half of the larvae had reached the first feeding stage (calyptopis 1). The eggs take approximately 36 hours to hatch so after seven days the larvae are approximately five days post hatch. At the end of the experiment, living and dead larvae were sorted into separate groups and preserved in 5% buffered formalin for counting and staging. Hatching success was calculated from the initial egg counts and the number of hatched larvae (live + dead) found at the end of the experiment; survival was calculated over the duration of the larval phase (excluding egg mortality) as the proportion of hatched larvae that were alive at the end of the experiment; development was calculated as the proportion of the hatched larvae that had reached calyptopis 1.

Seawater for each treatment was pH-conditioned by bubbling CO_2 gas and CO_2-free air generated with CO_2 adsorbers (Twin Towers Engineering) in 20-μm filtered natural seawater maintained at 12˚C. pH Durafets (Honeywell Process Solutions) calibrated with a pH-certified Tris buffer (Dickson Laboratory, Scripps Institution of Oceanography) were used to monitor treatment water for the target values. Seawater for all treatments in a trial was conditioned in a single equilibration container, from which jars were filled when target pH levels were reached. Every two days, each jar was sampled for pH using a spectrophotometer (Ocean Optics USB 2000+ Fiber Optic Spectrometer) and m-cresol purple dye (Sigma Aldrich), after which 80% of the water was removed and replaced with freshly pH-conditioned treatment water. This resulted in four measurements of pH from each jar over the course of each 7-day trial. Discrete samples for TA of the treatment water were collected at the beginning and end of each experimental trial

and measured by open-cell potentiometric titration according to SOP 3b in Dickson et al. (2007) at the NOAA NWFSC.

Experiment 2 was conducted at the Shannon Point Marine Center in Anacortes, WA, in a system of airtight Plexiglas boxes supplied with atmospheric gas of pCO_2 treatment concentrations. This system can control pCO_2 in many individual containers through air-seawater diffusion, which allows tracking of individual larval development with minimal disturbance. Experiment 2 consisted of three trials with three treatment levels; treatment conditions targeted pH 8.0, 7.7, and 7.6 (~400, 800, and 1200 μatm pCO_2). Eggs were spawned and counted as in Experiment 1. On Day 5 of the experiment (3 days post hatch), a portion of the larvae were gently pipetted from the hatching jars into glass petri dishes of pre-equilibrated seawater at a concentration of one larva/20 ml. 50% of the water in the hatching jars was then exchanged with seawater that had been pre-equilibrated to the treatment conditions and the remaining, undistributed larvae were left in these jars until Day 7, then were sorted, preserved, and analyzed as in Experiment 1.

On Day 6 (4 days post hatch), larvae in petri dishes were checked for life stage and mortalities, 50% of the water in their dish was exchanged with pre-equilibrated seawater, and larvae were fed the alga *Heterocapsa triquetra* at 150 μg C/L. The krill larvae grown on this food source had visibly full guts, indicating that they fed well on it. Feeding and a 50% water change continued every second day for the remainder of the experiment. Survival and molting were tracked approximately daily for each individual. When larvae either died or molted to the calyptopsis 2 stage, they were removed from the experiment, so survival was tracked to the calyptopis 2 stage, but not beyond. Experiment 2 consisted of three trials of 18, 23, and 19 days duration, by which time 85-100% of the larvae had either molted to calyptopis 2 or died.

Treatment pCO_2 -enriched seawater for experiment set-up and water changes was generated by stripping compressed (oil-less rotary compressor, Powerex) ambient air of CO_2 using CO_2 adsorbers (Twin Towers Engineering), and then mixing this CO_2-free air with pure CO_2 in precise concentrations using mass flow controllers (Sierra International Inc.). Ambient and CO_2 enriched air were bubbled into large containers of 0.2-µm filtered natural seawater for 24 h, or until the pCO_2 of headspace gas equaled the desired pCO_2 concentration. Treatment water was generated in a single equilibration container for each treatment level and then used to fill all jars in that treatment. CO_2 concentrations of the headspace gasses and gas streams into the headspace were measured using a Li-COR Li-820 CO_2 sensor. The hatching jars and petri dishes of larvae were left open inside airtight Plexiglas boxes (one per pCO_2 level) supplied with atmospheric gas of the equivalent pCO_2 treatment concentrations in a 12˚C temperature controlled room. By supplying the airtight boxes with treatment gas, air-water gas exchange controlled the pCO_2 and bubbling was not needed. Carbonate chemistry of treatment conditions was verified with discrete DIC and pH samples taken in duplicate from the pre-equilibrated water each time it was dispensed, from the hatching jars on Days 1 and 5, and in the petri dishes prior to all feedings and water changes. Total DIC was measured using a Model AS-C3 total dissolved inorganic carbon analyzer, and spectrophotometric pH was measured using an Agilent 8453A UV-VIS diode array spectrophotometer.

2.3.3 *Statistical Analyses*

In Experiment 1, for which we have data only from the start and end of each trial, we assessed whether pH affected 1) the proportion of eggs that hatched, 2) the proportion of larvae that survived, and 3) the proportion of larvae that developed to calyptopis 1 stage. A mixed effects logistic regression on a logit scale was used with the lme4 package (Bates et al. 2014) in R

statistical software (R Core Development Team 2014). The four measurements of pH for each jar over the course of an experiment were averaged to define each jar's treatment conditions, and pH was converted to $[H^+]$ to define the model's fixed effect. Experimental trial and brood were considered as random effects in the model. Because *E. pacifica* eggs are sensitive to handling (Ross 1981) we did not split any broods and therefore brood and jar effects were confounded. Best-fit models were selected based on AICc values (Burnham & Anderson 2002), and Hosmer-Lemeshow tests were used to verify the fit of the models.

In Experiment 2, for which we have nearly continuous data on development and survival through each trial, survival and molting rates were analyzed using the survival package (Therneau 2014) in R statistical software (R Core Development Team 2014). Survival probabilities represent survival from three days post hatch (Day 5), when live nauplii were initially moved to petri dishes for tracking, to the calyptopsis 2 stage. We tested for differences between discrete treatments with a Cox proportional hazards model using robust variance estimates, which allowed the data to be clustered by brood. As in Experiment 1, broods were not split, so brood and jar effects were confounded until Day 5 when larvae were distributed into petri dishes. This model doesn't allow for comparison of clustering by different factors but preliminary data exploration indicated that petri dish alone, or together with brood, was not as predictive as brood alone. The Cox model gives the hazard ratio for two treatments, which describes the relative risk due to a treatment at any particular point in time. We also tested for pairwise correlations between hatching, survival, and development proportions of different broods with a logistic regression using the lme4 package (Bates et al. 2014) and Bonferroni correction in R statistical software (R Core Development Team 2014).

2.4 RESULTS

2.4.1 *Field chemistry and euphausiid distributions*

In June, surface waters were warmer and less saline than in April, while deep waters had greater DIC, pCO_2, and lower pH. There was also a larger phytoplankton bloom in June than in April (chl max. 10.9-22.7 mg m^{-3} and 1-2.2 mg m^{-3}, respectively), which corresponded with higher pH and lower pCO_2in the surface waters in June. In April, pH measured by spectrophotometry was 8.11 in the surface waters and pCO_2 (calculated from DIC and pH) was 320 µatm; in June, pH was 8.24 and $pCO_2$was 209 µatm. Water chemistry was similar between the two stations except in June when bottom waters at the deeper station (P14, 180 m) had higher DIC, pCO_2, and lower pH than at the shallower station (P15, 130 m; Figure 2.2). Deep waters in April reached pH 7.61 (1101 µatm pCO_2) while in June, bottom waters were pH 7.56 (1241 µatm pCO_2) at station P15, and pH 7.48 (1516 µatm pCO_2) at station P14. When pH was calculated from TA and DIC, the profile was similar to that measured by spectrophotometry, but the absolute values were consistently lower (Figure 2.3). Likewise, pCO_2 calculated from TA and DIC (not shown) was consistently higher than pCO_2 calculated from DIC and spectrophotometric pH (shown in Figure 2.2). Water chemistry profiles were similar between day and night samplings; all profiles shown in Figure 2.2 are from day samplings.

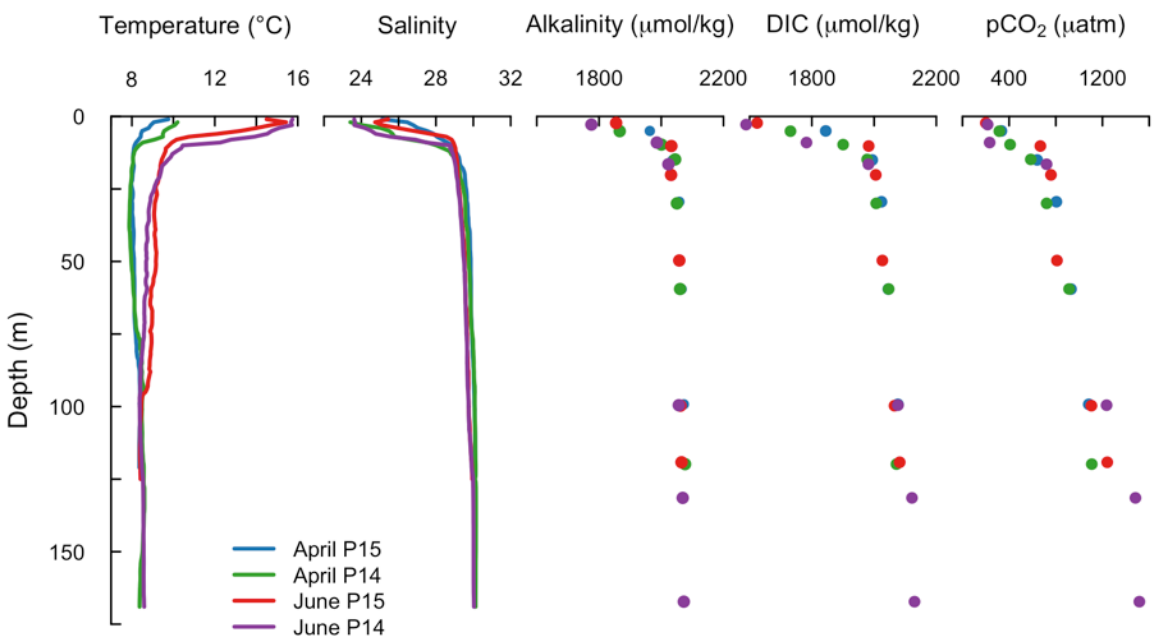

Figure 2.2. Seawater chemistry in Puget Sound, WA. Depth profiles of temperature, salinity, total alkalinity, total dissolved inorganic carbon (DIC) and pCO_2 from stations P14 and P15 during April and June. Temperature and salinity were measured continuously with a CTD while alkalinity and DIC were measured from discrete water samples. pCO_2 is calculated from discrete DIC and spectrophotometric pH measurements. April samples are shown in blue and green; June samples in red and purple.

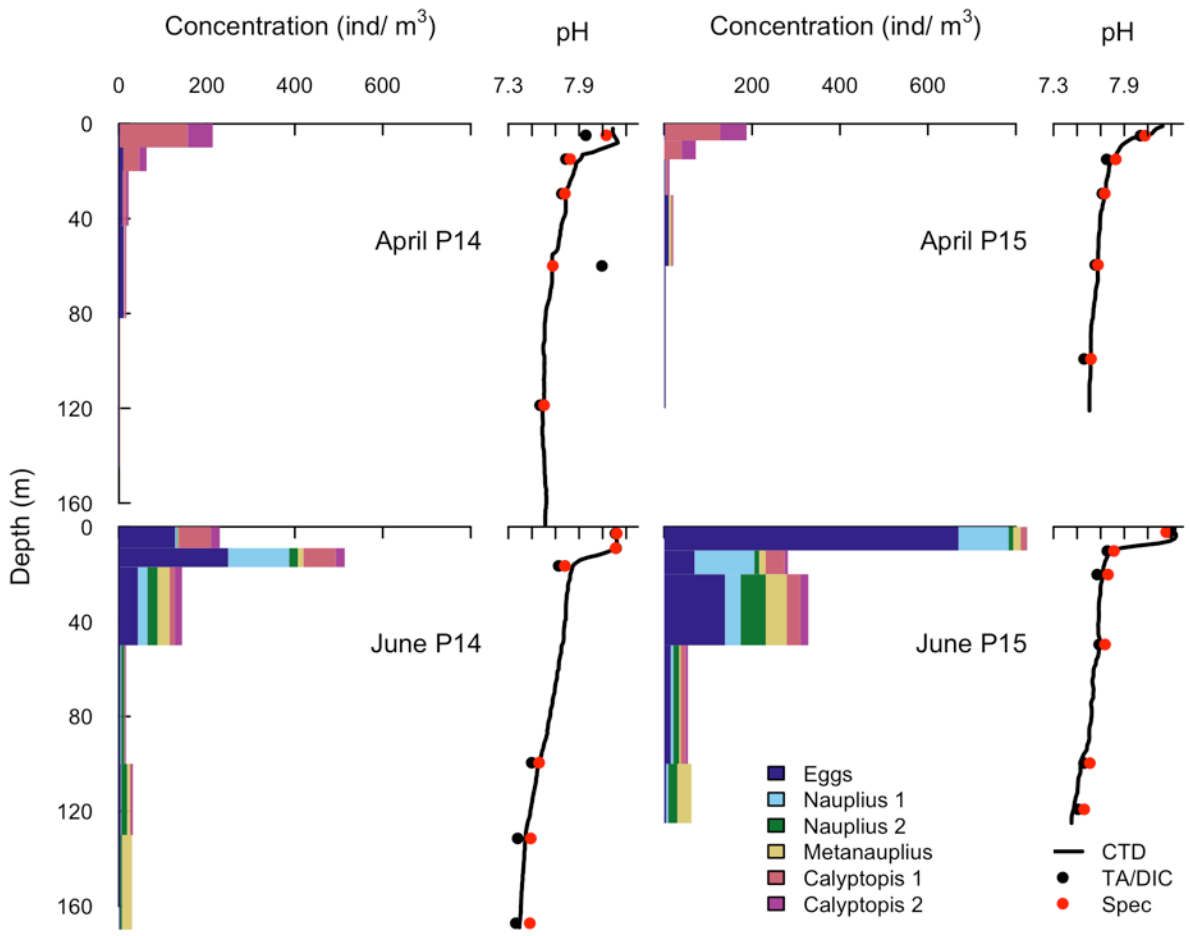

Figure 2.3. Vertical distribution of *E. pacifica* early life stages and their pH exposure in Puget Sound, WA. Life stages listed youngest to oldest, with eggs closest to the y-axis and increasingly older stages to the right. Depth profiles of pH were calculated from discrete total alkalinity and dissolved inorganic carbon samples (black points), and measured by spectrophotometry from discrete samples (red points). Continuous measurements from the CTD pH probe (black line) show the shape of the curve but have been shifted to approximately fit the discrete samples. The CTD probe was not calibrated for absolute measurements.

We observed much lower overall abundances of *E. pacifica* eggs and larvae in April compared to June. The majority of larvae in April were calyptopis 1 and 2 stages, which were concentrated in the surface waters (Figure 2.3). In June, all early life stages were abundant. Again, the highest concentrations were observed towards the surface, but a large proportion of

the population was also found below the pycnocline; approximately 37-42% of the eggs and nauplius 1 (first larval stage) were found below 20 m depth where the pH was <7.7, while 89-95% of nauplius 2 and metanauplius (second and third stages), 30-73% of calyptopis 1 (fourth stage), and 68-89% of calyptopis 2 (fifth stage) were below 20 m (Figure 2.3). The nauplius 2 and metanauplius stages were distributed deepest, with 38-68% of nauplius 2 and 36-52% of metanauplii found below 50 m. Distributions of these early stages did not show differences between day and night samplings; all distributions shown in Figure 2.3 are from day samplings.

2.4.2 *Experiment 1*

Temperature was relatively stable within and between trials, averaging 12.4˚C with a standard deviation of 0.31˚C (Table 2.1 and Table S2.1). Salinity was constant over the course of a trial (±0.26) and similar among trials, ranging from 29.1 to 30.0. The alkalinity of the source water behaved similarly to salinity, staying relatively stable over the course of a trial (~14 μmol/kg) and ranging from 2002 to 2041 μmol/kg among trials. In both Experiments 1 and 2, treatment conditions did not achieve our experimental targets with high accuracy, but were generally close and similar within treatments. pH conditions in Experiment 1 varied among jars within a treatment as well as between water changes in the same jar (0.02-0.25 pH units); however, pH of the different treatments were distinct from each other (Table 2.1; Table S2.1). Average pH measured in the jars for the five target treatments was 7.88, 7.65, 7.40, 7.27, and 7.09; pCO_2 calculated from pH and TA was 565, 1004, 1833, 2509, and 3814 μatm, respectively.

Table 2.1. Treatment conditions during Experiment 1. Average conditions grouped by experimental trial and target pCO_2 treatment, with the standard deviation of (n) measurements. Temperature, salinity, alkalinity, and pH were measured; pCO_2 and DIC were calculated.

Trial	Target pCO_2	# Broods	Temperature (˚C)	Salinity	Alkalinity (µmol/kg)	pH	pCO_2 (µatm)	DIC (µmol/kg)
1	400	5	12.2 ± 0.1 (20)	29.1	2030	7.87 ± 0.03 (19)	585 ± 47 (19)	1938 ± 10 (19)
	3200	1	12.2 ± 0.1 (4)			7.08 ± 0.04 (4)	3890 ± 358 (4)	2173 ± 17 (4)
2	800	4	12.2 ± 0.1 (11)	29.2 ± 0.1 (2)	2022 ± 28 (2)	7.68 ± 0.06 (12)	942 ± 149 (12)	1989 ± 30 (12)
	2400	5	12.2 ± 0.1 (14)			7.29 ± 0.03 (15)	2397 ± 188 (15)	2096 ± 24 (15)
3	800	10	12.7 ± 0.9 (40)	29.2 ± 0.1 (2)	2022 ± 28 (2)	7.64 ± 0.03 (40)	1037 ± 77 (40)	2001 ± 20 (40)
	2400	5	13.1 ± 1.0 (20)			7.26 ± 0.07 (20)	2621 ± 484 (20)	2108 ± 29 (20)
4	400	4	12.3 ± 0.1 (16)	30	2021	7.89 ± 0.04 (16)	547 ± 55 (16)	1918 ± 13 (16)
	3200	4	12.3 ± 0.1 (16)			7.09 ± 0.04 (16)	3796 ± 402 (16)	2158 ± 19 (16)
5	400	10	12.2 ± 0.1 (40)	29.5 ± 0.2 (2)	2029 ± 6 (2)	7.88 ± 0.03 (38)	560 ± 37 (38)	1931 ± 7 (38)
	1600	9	12.3 ± 0.1 (36)			7.40 ± 0.03 (35)	1837 ± 114 (35)	2063 ± 8 (35)

All three biological responses varied significantly among broods. Model results indicated that survival and development, but not hatching, were also significantly affected by pH (Figure 2.4; Table S2.2). Average hatching in the 400, 800, 1600, 2400, and 3200 µatm pCO_2 target treatments was 31%, 42%, 34%, 33%, and 21%, respectively. The proportion of larvae that survived decreased at pH levels <7.4 (Figure 2.4b); average survival in the 400, 800, 1600, 2400, and 3200 µatm pCO_2 target treatments was 90%, 94%, 58%, 83%, and 86%, respectively. The proportion of larvae to reach the calyptopis 1 stage strongly decreased as pH declined, starting at pH <7.8 and declining rapidly below pH 7.6 (Figure 2.4c). Results from Hosmer-Lemeshow tests indicate that all three best-fit models fit the data (Hatching $\chi^2 = 0.1046$, Survival $\chi^2 = 3.1262$, Development $\chi^2 = 1.2078$; number of groups = 10).

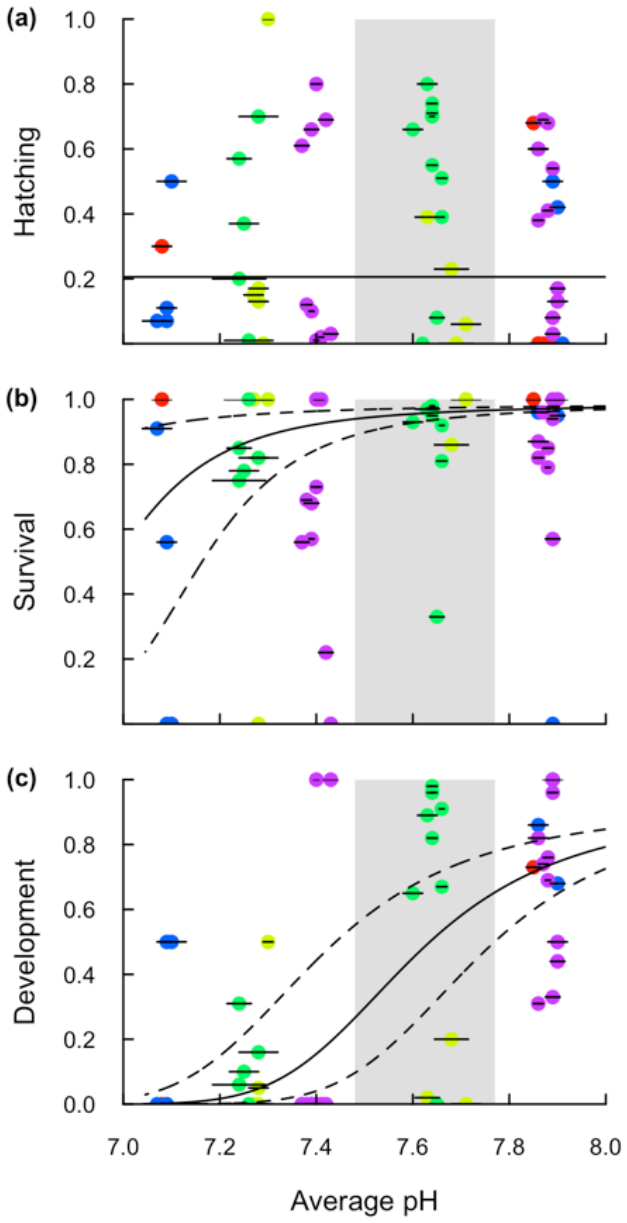

Figure 2.4. *E. pacifica* hatching, survival, and development to the calyptopis 1 (C1) stage as a function of pH in Experiment 1. Each point represents the final proportion of a single female's brood that hatched (a), survived (b), and developed to the C1 stage (c). Broods that were tested during the same trial share the same color. Horizontal error bars show the standard deviation from four pH measurements taken in each jar over the trial. Solid lines show the best fit model and dashed lines show the 95% CI for the effect of $[H^+]$ (no effect of $[H^+]$ detected on hatching). Shaded area shows the range of pH values observed in Hood Canal below the pycnocline in June.

2.4.3 *Experiment 2*

Salinity and alkalinity in Experiment 2 varied among source water, hatching jars, and larvae dishes of the same treatment due to evaporation in the petri dishes (Table 2.2). Measured pH and calculated pCO_2 conditions also varied among different water types of the same treatment, but were generally consistent among broods and trials (Table 2.2; Table S2.3). Average pH measured in the source water was higher than that measured in the hatching jars and petri dishes. Most of the larval development (three days post hatch to end of experiment) occurred in the petri dishes, where average pH was 7.96, 7.69, and 7.58 and calculated pCO_2 was 492, 956, and 1279 μatm; hereafter, these values are used to describe the treatment conditions, recognizing that the conditions the larvae experienced varied over time.

Table 2.2. Treatment conditions during Experiment 2. Average conditions grouped by water type and target pCO_2 treatment with the standard deviation of (n) measurements taken over three trials. Temperature, salinity, DIC, and pH were measured; alkalinity and pCO_2 were calculated.

	Target pCO_2	Temperature (˚C)	Salinity	Alkalinity (µmol/kg)	DIC (µmol/kg)	pH (total scale)	pCO_2 (µatm)
Source water	*400*		31 ± 1 (87)	2060 ± 46 (87)	1931 ± 50 (29)	7.98 ± 0.01 (29)	435 ± 3 (29)
	800				2005 ± 38 (29)	7.72 ± 0.03 (29)	846 ± 11 (29)
	1200				2030 ± 35 (29)	7.59 ± 0.03 (29)	1144 ± 15 (29)
Egg Jars	*400*	12.2 ± 0.4 (121)	31 ± 1 (33)	2110 ± 77 (33)	1991 ± 50 (10)	7.90 ± 0.04 (10)	553 ± 14 (10)
	800				2058 ± 74 (12)	7.69 ± 0.04 (12)	922 ± 21 (12)
	1200				2113 ± 86 (11)	7.55 ± 0.04 (11)	1318 ± 34 (11)
Larvae dishes	*400*	12.3 ± 0.6 (1235)	33 ± 2 (110)	2239 ± 109 (109)	2092 ± 83 (37)	7.96 ± 0.05 (37)	492 ± 10 (37)
	800				2161 ± 81 (36)	7.69 ± 0.03 (36)	956 ± 9 (36)
	1200				2228 ± 120 (36)	7.58 ± 0.05 (36)	1279 ± 23 (36)

Hatching in Experiment 2 was, again, variable among broods and not significantly different among treatments (Figure 2.5a; Table S2.4); average hatching in 400, 800, and 1200 µatm pCO_2 target treatments was 60%, 72%, and 68%, respectively. The larvae that were tested for survival and development through the calyptopis 1 stage (as done in Experiment 1 under a wider range of pH treatments) had high survival to five days post hatch across all treatments and no differences among treatments (Figure 2.5b; Table S2.4); average survival in the 400, 800, and 1200 µatm pCO_2 target treatments was 95%, 97%, and 97%, respectively. The proportion of larvae that had reached the calyptopis 1 stage by five days post hatch decreased as pH declined (Figure 2.5c; Table S2.4). Results from Hosmer-Lemeshow tests indicate that the models fit the data (Hatching $\chi^2 = 0.01$, Survival $\chi^2 = 0.255$, Development $\chi^2 = 0.079$, number of groups=10).

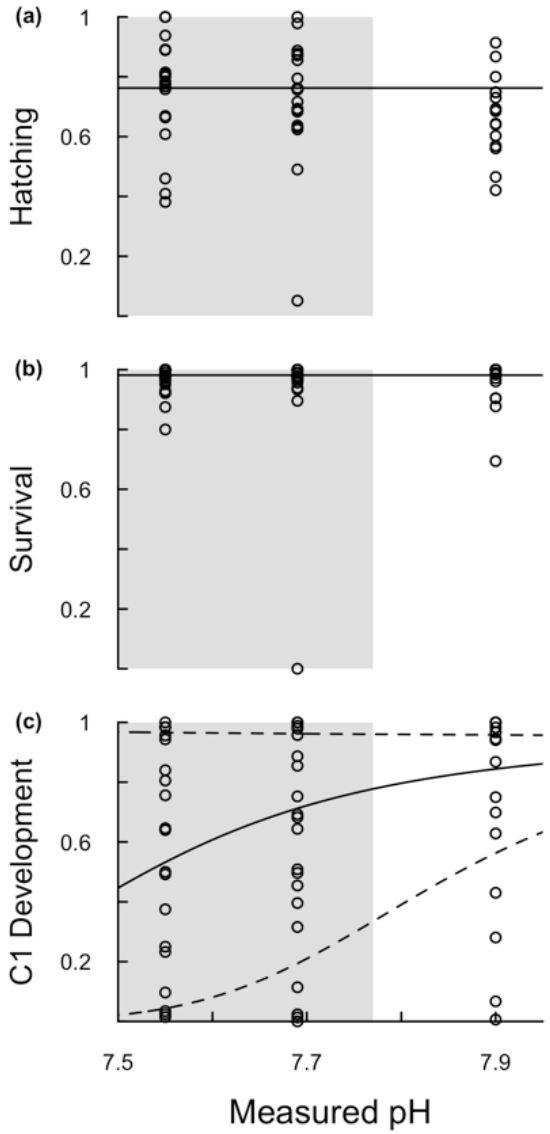

Figure 2.5. *E. pacifica* hatching, survival, and development to the calyptopis 1 stage as a function of pH in Experiment 2. Each point represents the proportion of a single female's brood that hatched (a), survived (b), and developed to the calyptopis 1 (C1) stage (c) at five days post hatch. Solid lines show the best fit model and dashed lines show the 95% CI for the effect of $[H^+]$ (no effect of $[H^+]$ detected on hatching or survival). Shaded area shows the range of pH values observed in Hood Canal below the pycnocline in June.

The probability of larvae surviving to the calyptopis 2 stage decreased at pH 7.69 (956 μatm pCO_2) and pH 7.58 (1279 μatm pCO_2), compared to pH 7.96 (492 μatm pCO_2). Average mortality before the calyptopis 2 stage in 400, 800, and 1200 μatm pCO_2 target treatments was 26.5%, 50%, and 45.7%, respectively. Survival probability in pH 7.69 and pH 7.58 treatments was similar (Figure 2.6a; log rank test: pH 7.96–7.69 contrast: χ^2=44.4, df=1, p= <0.0001; pH 7.96–7.58 contrast: χ^2=38.1, df=1, p=<0.0001; 7.69–7.58 contrast: χ^2=0.3, df=1, p=0.59). The Kaplan-Meier survival estimates shows the point-wise 95% CI for the pH 7.96 treatment does not overlap with either the pH 7.69 or the pH 7.58 treatments until after Day 17 when the number of remaining larvae (n) became very small, indicating that survival was higher in the pH 7.96 treatment from Day 6 through the duration of the experiment (Figure 2.6a). Survival data (Fig. S2.1) supports the proportional hazards assumption and use of the Cox Proportional Hazards model because the estimated –ln(–ln) survivor curves are nearly parallel (Kleinbaum & Klein 2005). The model yielded a survival hazard ratio of 2.29 (95% CI 1.66–3.16) for the pH 7.69 treatment compared to pH 7.96, and 2.08 (95% CI 1.42–3.04) for the pH 7.58 treatment compared to pH 7.96. In this application, hazard ratios describe the relative risk of dying at any particular point in time, with a higher ratio describing lower survival in the lower pH treatment compared to pH 7.96.

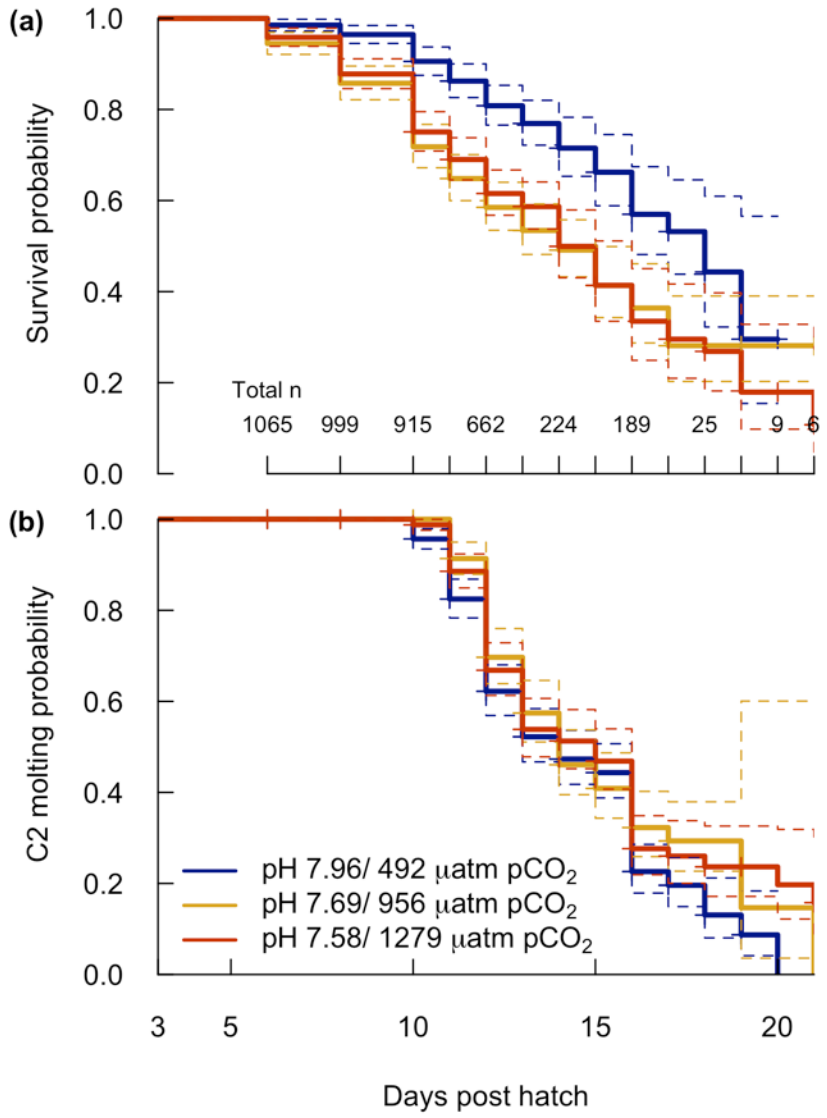

Figure 2.6. Survival probability and probability of molting to the calyptopis 2 (C2) stage in Experiment 2. (a) Survival probability (thick lines) of larvae from three days post hatch to the C2 stage raised at pH 7.96 (blue), pH 7.69 (yellow), and pH 7.58 (red). (b) Probability of larvae molting to the calyptopis 2 (C2) stage (thick lines). Dashed lines show 95% CI**.** Total number of larvae remaining in all treatments (n) shown above x axis in (a).

The probability curves for molting to calyptopis 2 are statistically distinguishable among treatments (log rank test: χ^2 =5.99, df=2, p=0.05), but visual examination of the curves indicates that there was little difference until the end of the experiment, when the number of animals in each treatment group was very small (Figure 2.6b). Log rank tests put more weight on differences towards the end of the data set; to test for the influence of this weighting on our results, we truncated the dataset to Day 17 and re-ran the log rank test. With the truncated dataset, differences among treatment groups were no longer significant (χ^2 = 4.5, df=2, p=0.11). The Wald and likelihood ratio tests were both non-significant on the entire data set (5.98 and 5.93, df=2), indicating that molting probabilities were similar among treatments.

There was a significant negative relationship between the proportion of a female's brood that reached the calyptopis 1 stage at five days post hatch and the proportion that died before reaching the calyptopis 2 stage ($p<0.0001$; Figure 2.7). There were also statistically significant relationships between hatching success of broods and their development to the calyptopis 1 stage at five days post hatch in both experiments, but the direction of the correlation was not consistent (Experiment 1: positive relationship, p=0.041; Experiment 2: negative relationship, p=0.022; Figure 2.7). There were no significant relationships between hatching success and the proportion that died before reaching the calyptopis 2 stage or the proportion alive at five days post hatch.

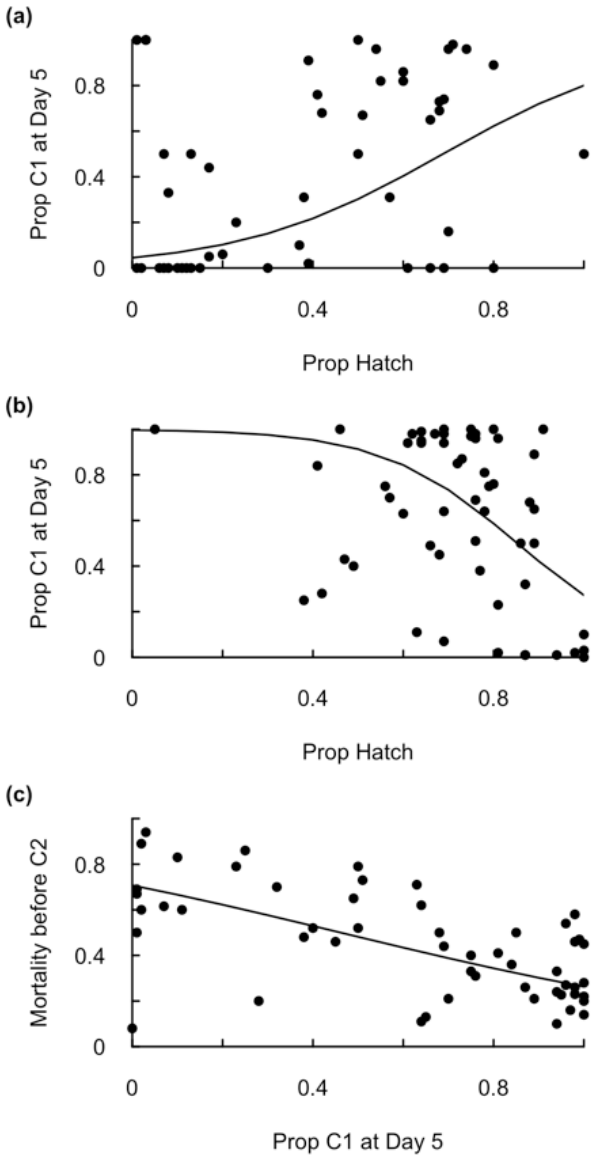

Figure 2.7. Relationships among measured parameters of different broods. Statistically significant relationships were found between (a) the proportion of larvae that reached calyptopis 1 (C1) by five days post hatch and the proportion that hatched in Experiment 1 (adjusted $p=0.04$), (b) the proportion of larvae that reached C1 by five days post hatch and the proportion that hatched in Experiment 2 (adjusted $p=0.02$), and (c) the proportion of larvae that died before reaching the calyptopis 2 (C2) stage and the proportion that reached the C1 stage by five days post hatch in Experiment 2 (adjusted $p<0.0001$).

2.5 DISCUSSION

We found that the early life stages of *E. pacifica* are naturally exposed to a wide range of carbonate chemistry conditions in Puget Sound, ranging from pH 8.3 to pH 7.5 during their egg to calyptopis 2 stages. Two sets of experiments in the laboratory indicated that the pH conditions that this species is currently exposed to in sub-surface waters of Puget Sound can lead to developmental delays and decreased larval survival.

Our field surveys showed that in June, significant proportions of *E. pacifica* early life stages are found between 20-50 m water depth, where they are exposed to low pH/high CO_2 waters. Vertical distributions of *E. pacifica* early life stages are not commonly reported in the literature, but the depth distributions we observed are similar to a published distribution in the Southern Yellow Sea, where *E. pacifica* eggs are distributed below 20 m in the high chlorophyll layer, nauplius 1 are distributed below 10 m, nauplius 2 and metanauplius extend nearly the whole water column, and most calyptopis 1 and 2 are restricted to the upper 30 m (Liu & Sun 2010). We observed pH values of 7.7 to 7.5 below the pycnocline in Hood Canal, which are similar to those observed by Feely et al. (2010) in the same region in 2008, indicating that such low pH conditions frequently occur in this area. Seawater pH values below 7.7 are also observed below the pycnocline in the Strait of Juan de Fuca (Feely et al. 2010) and on the continental shelf of the US west coast (Feely et al. 2008), where *E. pacifica* is abundant. Salinity and total alkalinity profiles were similar among months, whereas DIC concentrations in mid and deep waters were higher in June than in April—likely due to increased respiration—and contributed to lower pH and higher pCO_2 at depth at the time when *E. pacifica* was also more abundant.

E. pacifica hatching in the laboratory was similar across a wide range of pH conditions, but exposure to low pH slowed development and decreased survival of their larvae. In contrast,

E. superba hatching success decreased at pH 7.5/ pCO_2 1250 μatm in laboratory studies (Kawaguchi et al. 2011, 2013). Our study is the first to look at larval development of krill under increased pCO_2 through several life stages; *E. superba* larvae have only been observed under elevated CO_2 (1000 μatm) for up to 3 days post hatch, with no observed effects on larval swimming activity (Kawaguchi et al. 2011). We observed developmental delays in non-feeding stages (development to the calyptopis 1 stage) and increased mortality in feeding stages (mortality before the calyptopis 2 stage). In this study, 50% of the larvae reared at pH 7.69 died before the calyptopis 2 stage, compared to 27% of larvae reared at pH 7.96. This decline occurred over just the first 20 days of life; it takes *E. pacifica* an average of 45 days to reach the juvenile stage (Ross 1981). Both developmental delays and increased mortality are ecologically important for *E. pacifica* populations. Although some general trends in pH sensitivity across taxa are emerging (Dupont et al. 2010, Hofmann et al. 2010, Kroeker et al. 2013), the idea that crustaceans are generally tolerant (Whiteley 2011, Kroeker et al. 2013) should be carefully considered and re-examined after more species and life stages have been studied.

Our results indicate that *E. pacifica* developmental stages are differently affected by low pH conditions. Larvae were slower to molt into the calyptopis 1 stage at lower pH levels in both experiments; the highest pH at which this occurred was pH 7.69 (956 μatm pCO_2) in Experiment 2. However, we did not find a difference in time to molt to the calyptopis 2 stage at this pH level (as measured by molting probability), an apparent conundrum that is discussed below. Larval survival decreased with pH in both experiments, but again with differences between stages. Survival to five days post hatch was not affected by pH 7.69 or 7.58 (956 and 1279 μatm pCO_2), but survival to the calyptopis 2 stage was decreased at those pH levels (as indicated by hazard ratios >1). The calyptopis 1 stage is one of the longest developmental stages in *E. pacifica's*

early life cycle; as the first feeding stage, it involves a large change in physiology and behavior, and may represent a bottleneck for their larval development (Feinberg et al. 2006). The transition to calyptopis 1 is also the first true molt; although we did not determine whether the observed mortalities occurred during the molting process, increased pCO_2 has been reported to increase the frequency of molting-related deaths in sub-adults of Atlantic krill (Sperfeld et al. 2014), so the differences in mortality among treatments we observed after transition to calyptopis 1 may have been due to the energetic requirements associated with molting.

Increased energy expenditures early in life can lead to latent or carryover effects that influence later performance (Pechenik 2006). The mono-algal diet supplied in this laboratory study was potentially less nutritious than food available in the field, which could increase the importance of carry-over effects from non-feeding stages; however, we observed slowed development to the calyptopis 1 stage during life stages when larvae are completely dependent on endogenous energy sources, indicating that the larvae were stressed by reduced pH even before they began feeding. The mortality and development rates we observed in our control conditions are similar to those reported in previous laboratory studies, giving no clear indication of extra stress induced by the rearing methods (Ross 1981; Feinberg et al. 2006).

Females' broods that developed faster over the first five days post hatch had higher survival to the calyptopis 2 stage, as indicated by the negative correlation between the proportion of a female's brood that reached calyptopis 1 by five days post hatch and the proportion that died before reaching calyptopis 2**.** This may indicate that there are different inherent susceptibilities to pH in the population, which could explain the differences observed between the effects of pH on development rate to calyptopis 1 and calyptopis 2 stages. If individuals which had slower growth to the calyptopis 1 stage were also more likely to die before reaching the calyptopis 2 stage, our

measure of time to molt to calyptopis 1 would include both susceptible and robust individuals, whereas the measure of time to molt to calyptopis 2 would have a larger proportion of robust individuals because of the higher mortality among susceptible individuals. There were also statistically significant relationships between the proportion of larvae that reached the calyptopis 1 stage by five days post hatch and the proportion of eggs that hatched in Experiment 1 and 2. However, the sign of this relationship differed between experiments, and visual examination of those data shows that although statistically significant, this relationship is unlikely to be biologically relevant (Figure 2.7).

We observed high variability in all measured parameters (hatching, survival, development) among broods, which may indicate heritable differences among individuals. We left each brood intact and undisturbed before hatching, so experimentally, this variability combines potential differences among individual jars and parental effects, which in turn includes both heritable genetic factors and physical condition based on environmental experience, diet, etc. However, we expect that parental effects primarily drove the variability we observed. This work and other studies of euphausiids (Ross 1981, Kawaguchi et al. 2013) have shown high inter-brood variability in hatching, and we also observed inter-brood variability in later development after larvae from each brood were distributed from their individual jars into multiple petri dishes. Furthermore, similar experiments on copepods in which each female's brood was split into multiple jars showed that the variability among broods was larger than that within broods split across different jars (unpublished data). We cannot determine from our data whether this inter-brood variability is due to heritable factors or environmental experience. If there is a subset of the population that is more resilient to low pH, and this resilience is due to

genetic factors, those individuals may represent the potential for this population to adapt to low pH, as has been observed in other marine invertebrates (Parker et al. 2012, Kelly et al. 2013).

E. pacifica showed negative responses to low pH in the laboratory at levels that occur within their current field distribution—pH levels that are expected to become more common in the future, which may threaten this species through a decline in suitable habitat. These results highlight the need to conduct OA experiments within the context of an organism's habitat to understand responses to both current and future conditions (McElhany & Busch 2012). Although atmospheric CO_2 levels of 950 ppm are not predicted to occur until after 2100, seawater pCO_2 at these and higher levels are currently observed *in situ* within areas of *E. pacifica's* habitat. *E. pacifica* free spawn their eggs at night near the surface where the pH is most often high, but as the eggs and early larvae sink through the water column, they experience decreased pH at intermediate depths until they are strong enough to swim back towards the surface.

Anthropogenic carbon emissions since the pre-industrial era have resulted in pH declines in Puget Sound of up to 0.11 in the surface waters and 0.06 in deep waters (Feely et al. 2010); these changes are small compared the values we observed (pH 7.56-7.48 in deep waters) indicating that low pH habitats existed in Puget Sound before the industrial revolution. Despite this, the *E. pacifica* larvae we reared in the laboratory were sensitive to these pH conditions. Because time series data on euphausiids in Puget Sound are scarce, we are unable to conjecture about how their populations may be currently shaped by pH. In the CCE, krill are concentrated near highly productive upwelling zones that are also places of low pH due to the upwelling of high pCO_2 deep waters to the surface (Santora et al. 2012). This co-occurrence of low pH with high food levels could lead to tradeoffs between food availability and suitable pH conditions, which may become rarer as the pH of upwelled waters declines. In some organisms, abundant

food has been shown to offset the energetic costs of compensating for low pH (Thomsen et al. 2013, Melzner et al. 2011); this has not yet been demonstrated in euphausiids, but could confer some resilience if food levels increase with pCO_2 in the field.

In both our study and the *E. superba* experiments (Kawaguchi et al. 2011, 2013), the females extruded eggs directly into pH-manipulated seawater, but effects of pH on oogenesis and fertilization were not tested. We are unaware of any work that has tested for these effects in krill; however, evidence from copepods suggests that male exposure has further negative effects on offspring compared to when females alone are exposed (Cripps et al. 2014). The effects of parental exposure and acclimation may be important in krill, but cannot easily be tested for in this species because they have not been successfully mated in the laboratory.

In both experiments, the CO_2-equilibrated water for each treatment was generated in a single equilibration container, a pseudoreplication issue recently identified by Cornwall and Hurd (2015) as common among CO_2 manipulation experiments. In this study we have partially accounted for this through replication in time and through statistical techniques. Experiment 1 was partially replicated in time: the 400 vs 3200 μatm pCO_2 and 800 vs 2400 μatm pCO_2 trials were each repeated, allowing for trial to be included in the mixed model. Three separate trials that overlapped in time were conducted in Experiment 2, and trial was included as a random factor in the statistical model. Logistical constraints always influence experimental design, and we attempted to maximize the number of different females we tested because of the known variability among different females' broods. We conclude that the weight of evidence from two completely separate experimental systems is compelling despite the less-than-ideal experimental design.

E. pacifica early life stages show developmental delays and significantly decreased survival in the laboratory under pH conditions that they are currently exposed to in the field. This and other studies continue to demonstrate the importance of OA experiments that are designed in the context of the organisms' habitat, target the most vulnerable life stages, and are long enough to detect carryover effects. This study, along with the other limited OA work on krill, indicates that krill, particularly the early stages, may be more sensitive to OA than other crustaceans, which could have profound implications for the future of their populations and the organisms that prey on them. The negative response of *E. pacifica* larvae to reduced pH in this laboratory study indicates that they may be living at the edge of their current tolerance.

2.6 ACKNOWLEDGEMENTS

We would like to thank Jonathan Lambert, Tiffany Barber, Kelley Bright, Robyn Strenge, Cristina Villalobos, Julia Brueggeman, BethElLee Herrmann, and Lisa Raatikainen for help with the experiments and data collection; Moose O'Donnell, Erin Bohaboy, and Amelia Kolb for chemistry analyses; Captain Lawrence Baum for collection trips and Rachel Wilborn and Chloe Holzinger for help on collections; Captain Ray McQuin of the RV Barnes for field sampling, Loren Tuttle for technical support, and Tricia Thibodeau for help in the field; Jason Miller for help with experiments and statistical advice; Dr. Susan Lubetkin and University of Washington Biostatistics Consulting for statistical help; and NOAA Northwest Fisheries Science Center and Ocean Acidification Program for funding the NOAA OA facilities and personnel. This study was funded in part by grants from the Washington Ocean Acidification Center and Washington Sea Grant.

2.7 SUPPORTING INFORMATION

Table S2.1. Treatment conditions of individual jars during Experiment 1. Measured temperature (˚C), salinity, total alkalinity (μmol/kg), pH (total scale), and calculated pCO_2 (μatm) and DIC (μmol/kg), with the standard deviation of 4 measurements (trial 2 had three measurements).

Trial	Target pCO_2	# Broods	Temp	Salinity	Alkalinity	pH	pCO_2	DIC
1	400	5	12.2	29.1	2030	7.86 ± 0.03	599 ± 40	1941 ± 8
	400		12.2			7.87 ± 0.03	576 ± 50	1936 ± 10
	400		12.2			7.86 ± 0.04	597 ± 58	1941 ± 12
	400		12.2			7.89 ± 0.04	551 ± 52	1931 ± 12
	400		12.2			7.85 ± 0.03	607 ± 41	1943 ± 8
4	400	4	12.3	30.0	2021	7.86 ± 0.04	586 ± 59	1927 ± 13
	400		12.3			7.89 ± 0.04	544 ± 49	1918 ± 12
	400		12.3			7.91 ± 0.05	526 ± 64	1913 ± 16
	400		12.3			7.9 ± 0.03	533 ± 47	1915 ± 10
5	400	10	12.1	29.5	2029	7.9 ± 0.04	533 ± 50	1924 ± 10
	400		12.2			7.88 ± 0.02	567 ± 28	1934 ± 6
	400		12.1			7.87 ± 0.02	571 ± 22	1933 ± 4
	400		12.2			7.86 ± 0.02	587 ± 26	1935 ± 4
	400		12.2			7.9 ± 0.03	542 ± 45	1927 ± 9
	400		12.2			7.88 ± 0.01	558 ± 10	1931 ± 4
	400		12.2			7.89 ± 0.02	555 ± 22	1930 ± 5
	400		12.2			7.86 ± 0.04	595 ± 52	1938 ± 7
	400		12.2			7.89 ± 0.03	556 ± 38	1930 ± 7
	400		12.2			7.89 ± 0.03	549 ± 43	1928 ± 9
2	800	4	12.2	29.2	2022	7.68 ± 0.07	932 ± 177	1988 ± 41
	800		12.1			7.71 ± 0.06	868 ± 128	1980 ± 37

	800		12.2			7.69 ± 0.07	912 ± 178	1985 ± 39
	800		12.3			7.63 ± 0.05	1056 ± 113	2002 ± 10
3	800	10	12.6	29.2	2022	7.66 ± 0.01	982 ± 29	1995 ± 21
	800		12.6			7.62 ± 0.02	1090 ± 55	2006 ± 16
	800		12.5			7.63 ± 0.04	1050 ± 105	2002 ± 23
	800		12.6			7.64 ± 0.02	1036 ± 71	2001 ± 25
	800		12.6			7.6 ± 0.04	1138 ± 115	2011 ± 28
	800		12.6			7.64 ± 0.02	1033 ± 65	2000 ± 23
	800		12.7			7.66 ± 0.02	981 ± 52	1995 ± 21
	800		13.1			7.65 ± 0.03	1003 ± 77	1997 ± 23
	800		12.6			7.64 ± 0.02	1020 ± 43	1999 ± 21
	800		13.2			7.64 ± 0.01	1034 ± 20	2001 ± 16
5	1600	9	12.3	29.5	2029	7.37 ± 0.03	1938 ± 130	2070 ± 6
	1600		12.2			7.38 ± 0.02	1922 ± 69	2069 ± 5
	1600		12.3			7.39 ± 0.03	1889 ± 129	2067 ± 11
	1600		12.3			7.42 ± 0.03	1745 ± 109	2058 ± 7
	1600		12.2			7.4 ± 0.01	1830 ± 36	2063 ± 7
	1600		12.3			7.39 ± 0.01	1861 ± 59	2065 ± 6
	1600		12.3			7.43 ± 0.03	1696 ± 137	2053 ± 8
	1600		12.3			7.41 ± 0.01	1772 ± 55	2059 ± 3
	1600		12.4			7.4 ± 0.02	1845 ± 106	2064 ± 5
2	2400	5	12.2	29.2	2022	7.27 ± 0.04	2469 ± 251	2100 ± 34
	2400		12.2			7.28 ± 0.04	2442 ± 201	2098 ± 24
	2400		12.2			7.28 ± 0.04	2416 ± 253	2097 ± 30
	2400		12.3			7.3 ± 0.02	2297 ± 129	2090 ± 23
	2400		12.2			7.29 ± 0.03	2364 ± 191	2094 ± 30
3	2400	5	12.9	29.2	2022	7.25 ± 0.06	2611 ± 386	2107 ± 25
	2400		13.4			7.28 ± 0.08	2486 ± 469	2100 ± 30
	2400		13.1			7.26 ± 0.1	2597 ± 650	2106 ± 43

	2400		13.2			7.24 ± 0.05	2668 ± 314	2111 ± 33
	2400		12.8			7.24 ± 0.11	2742 ± 740	2113 ± 24
1	3200	1	12.2	29.1	2030	7.08 ± 0.04	3890 ± 358	2173 ± 17
4	3200	4	12.3	30.0	2021	7.1 ± 0.06	3692 ± 543	2153 ± 26
	3200		12.3			7.09 ± 0.04	3760 ± 315	2156 ± 15
	3200		12.3			7.07 ± 0.06	3971 ± 555	2166 ± 26
	3200		12.4			7.09 ± 0.02	3758 ± 217	2156 ± 10

Table S2.2. AICc scores for generalized linear mixed effects models of hatching, development, and survival with $[H^+]$ concentration for Experiment 1. Best model indicated in bold.

Experiment 1	**Hatching**	**Development**	**Survival**
Response= (brood) + intercept	**505**	307	287
Response= (trial) + intercept	2833	1826	551
Response= [H+] + (brood) + intercept	508	291	283
Response= [H+] + (trial) + intercept	2623	588	366
Response= [H+] + (trial) + (brood) + intercept	510	**288**	**280**
Response= [H+] + (trial) + (brood) + [H+]*(brood) + intercept	512	291	282
Response= [H+] + (trial) + (brood) + [H+]*(trial) + intercept	512	291	282
Response= [H+] + (trial) + (brood) + [H+]*(trial)+ [H+]*(brood) + intercept	515	293	285

Table S2.3. Treatment conditions during each trial of Experiment 2. Average conditions grouped by target pCO_2 (µatm) treatment and experimental trial with the standard deviation of (n) measurements. Temperature, salinity, DIC, and pH were measured; alkalinity and pCO_2 were calculated.

	Target pCO_2	Trial	Source water	Egg Jars	Larvae dishes
Temperature	400	1		12.1 ± 0.2 (19)	12.1 ± 0.7 (135)
		2		12.0 ± 0.0 (5)	12.2 ± 0.5 (119)
		3		12.4 ± 0.4 (15)	12.2 ± 0.3 (142)
	800	1		12.2 ± 0.3 (11)	12.2 ± 0.8 (159)
		2		12.0 (1)	12.2 ± 0.4 (26)
		3		12.3 ± 0.4 (28)	12.4 ± 0.4 (266)
	1200	1		11.9 ± 0.2 (19)	12.4 ± 0.9 (142)
		2		12.3 ± 0.3 (13)	12.2 ± 0.5 (177)
		3		12.5 ± 0.4 (10)	12.2 ± 0.5 (69)
Salinity	400	1	30 ± 0.8 (11)	31 ± 1.5 (4)	32 ± 3 (13)
		2	31 ± 1.2 (20)	31 ± 0.7 (2)	34 ± 1.1 (22)
		3	31 ± 1.2 (18)	32 ± 0.6 (4)	34 ± 1.1 (14)
	800	1	30 ± 0.8 (11)	31 ± 1.5 (4)	33 ± 3.3 (13)
		2	31 ± 1.3 (20)	30 ± 0 (2)	33 ± 1.4 (19)
		3	31 ± 1.4 (18)	32 ± 0.5 (6)	33 ± 1.4 (15)
	1200	1	30 ± 0.8 (11)	30 ± 0 (4)	32 ± 2.5 (13)
		2	31 ± 1.0 (20)	31.2 ± 1.1 (5)	34 ± 2.6 (22)
		3	31 ± 1.0 (18)	31 ± 1.4 (2)	35 ± 2.8 (14)
Alkalinity	400	1	2075 ± 33 (11)	2158 ± 61 (4)	2215 ± 111 (13)

		2	2065 ± 65 (20)	2062 ± 6 (2)	2265 ± 90 (22)
		3	2066 ± 68 (18)	2066 ± 28 (4)	2279 ± 111 (14)
	800	1	2075 ± 35 (11)	2205 ± 64 (4)	2240 ± 117 (13)
		2	2050 ± 44 (20)	2064 ± 20 (2)	2215 ± 72 (19)
		3	2050 ± 46 (18)	2055 ± 27 (6)	2187 ± 76 (15)
	1200	1	2062 ± 37 (11)	2216 ± 78 (4)	2190 ± 101 (13)
		2	2042 ± 33 (20)	2077 ± 14 (5)	2305 ± 136 (21)
		3	2044 ± 34 (18)	2045 ± 6 (2)	2354 ± 149 (13)
DIC	400	1	1936 ± 28 (11)	2039 ± 38 (4)	2071 ± 90 (13)
		2	1928 ± 57 (20)	1957 ± 2 (2)	2112 ± 75 (22)
		3	1928 ± 60 (18)	1960 ± 31 (4)	2128 ± 90 (14)
	800	1	2025 ± 24 (11)	2145 ± 57 (4)	2180 ± 103 (13)
		2	1995 ± 39 (20)	2028 ± 1 (2)	2158 ± 65 (19)
		3	1992 ± 41 (18)	2009 ± 28 (6)	2133 ± 66 (15)
	1200	1	2047 ± 31 (11)	2205 ± 76 (4)	2175 ± 89 (13)
		2	2020 ± 32 (20)	2071 ± 13 (5)	2266 ± 130 (22)
		3	2020 ± 34 (18)	2034 ± 1 (2)	2308 ± 142 (14)
pH	400	1	7.99 ± 0.01 (11)	7.92 ± 0.05 (4)	7.96 ± 0.04 (13)
		2	7.98 ± 0.01 (20)	7.89 ± 0.02 (2)	7.96 ± 0.05 (22)
		3	7.98 ± 0.01 (18)	7.88 ± 0.02 (4)	7.95 ± 0.06 (14)
	800	1	7.72 ± 0.04 (11)	7.73 ± 0.02 (4)	7.7 ± 0.02 (13)
		2	7.72 ± 0.03 (20)	7.66 ± 0.07 (2)	7.69 ± 0.03 (19)
		3	7.72 ± 0.02 (18)	7.68 ± 0.02 (6)	7.68 ± 0.03 (15)
	1200	1	7.58 ± 0.03 (11)	7.57 ± 0.01 (4)	7.56 ± 0.04 (13)

		2	7.59 ± 0.04 (20)	7.53 ± 0.05 (5)	7.60 ± 0.04 (21)
		3	7.60 ± 0.03 (18)	7.56 ± 0.01 (2)	7.58 ± 0.05 (13)
pCO_2	400	1	430 ± 11 (11)	540 ± 64 (4)	488 ± 43 (13)
		2	438 ± 18 (20)	554 ± 26 (2)	496 ± 75 (22)
		3	438 ± 18 (18)	565 ± 35 (4)	516 ± 87 (14)
	800	1	871 ± 80 (11)	883 ± 26 (4)	949 ± 39 (13)
		2	842 ± 51 (20)	989 ± 154 (2)	959 ± 47 (19)
		3	831 ± 40 (18)	925 ± 56 (6)	968 ± 66 (15)
	1200	1	1186 ± 77 (11)	1327 ± 24 (4)	1325 ± 126 (13)
		2	1141 ± 100 (20)	1341 ± 166 (5)	1256 ± 137 (21)
		3	1120 ± 79 (18)	1244 ± 52 (2)	1316 ± 130 (13)

Table S2.4. AICc scores for generalized linear mixed effects models of hatching, development, and survival with $[H^+]$ concentration for larvae raised to five days post hatch in Experiment 2. Best model indicated in bold.

Experiment 2 (five days post hatch)	**Hatching**	**Development**	**Survival**
Response= (brood) + intercept	**599**	458	**266**
Response= (trial) + intercept	3207	3187	459
Response= [H+] + (brood) + intercept	**599**	458	268
Response= [H+] + (trial) + intercept	3149	3070	449
Response= [H+] + (trial) + (brood) + intercept	601	**454**	271
Response= [H+] + (trial) + (brood) + [H+]*(brood) + intercept	604	456	273
Response= [H+] + (trial) + (brood) + [H+]*(trial) + intercept	604	456	273
Response= [H+] + (trial) + (brood) + [H+]*(trial)+ [H+]*(brood) + intercept	606	459	276

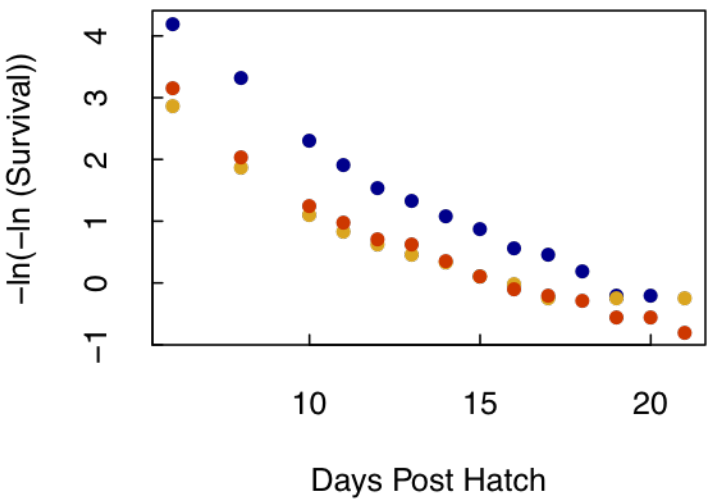

Fig S2.1. Visual examination of proportional hazards assumption in Experiment 2 survival data showing approximately parallel –ln(–ln) survival among treatments until after Day 17, when n becomes very small.

Chapter 3

EARLY LIFE STAGES OF *CALANUS PACIFICUS* ARE NEITHER EXPOSED NOR SENSITIVE TO LOW pH WATERS IN PUGET SOUND, WA

3.1 ABSTRACT

We characterized the vertical distribution of *Calanus pacificus* eggs and larvae and the carbonate chemistry that they are exposed to in Puget Sound, Washington. We found that, under stratified conditions, more than 90% of eggs and naupliar stages 1-4 were distributed above the pycnocline in seawater with pH higher than 7.7. When eggs and larvae from 101 females were reared under a range of pH conditions in the laboratory (pH 7.2-8.0), we observed a small decline in population hatching success at pH 7.3 in one experiment, while in another, inter-individual variability among different females' broods masked this effect. Exposure to pH of 7.3 in one experiment led to a slight increase in survival, but did not influence development rate. These results indicate that *C. pacificus* early life stages are generally tolerant to short-term direct effects of ocean acidification.

3.2 *CALANUS PACIFICUS* pH EXPOSURE AND SENSITIVITY

Calanus pacificus is an abundant, ecologically important copepod found throughout the North Pacific. Copepods display species and stage-specific responses to pH (Wang *et al.* 2018) and early life stages are often more sensitive than adults (Lewis *et al.* 2013; Cripps *et al.* 2014). Research on congeners shows no effects of pH on hatching (Thor *et al.* 2018b) or development (Bailey *et al*. 2016) in *C. glacialis*, or on naupliar survival in *C. finmarchicus* (Pedersen *et al.* 2014b). *C. pacificus* spawns negatively-buoyant eggs at the surface, but how deep they sink, or whether turbulent mixing keeps the eggs suspended, is unknown.

We characterized the vertical distribution and pH exposure of *C. pacificus* eggs and Nauplius 1-6 (N1-6) in Puget Sound, WA (station P15 in Hood Canal; 47.66 ˚N 122.86 ˚W) during the day and night on 15-16 June 2012 as described in McLaskey *et al*. (2016). In brief, we collected environmental data using a conductivity temperature depth (CTD) profiler equipped with a pH sensor (SBE 18, Sea-Bird Electronics) and Niskin bottles, which were used to collect water for spectrophotometric pH, total dissolved inorganic carbon (DIC), and total alkalinity (A_T) analyses. All carbonate chemistry samples in this study were collected and analyzed according to Dickson *et al*. (2007). Zooplankton were collected using depth-stratified tows of a 60-cm diameter, 75-μm mesh, closing ring net and preserved in a 5% buffered formalin and seawater solution. Sampling depths were chosen to characterize the pH profile shape.

Surface pH was 8.26-8.30 (Ω_{ar}=2.24-2.58) and decreased along the pycnocline to ~7.7, below which it declined slowly with depth, reaching a minimum of 7.52-7.56 (Ω_{ar}=0.46-0.49) in bottom waters (Figure 3.1; Table S3.1). The majority of *C. pacificus* early life stages were found in the upper 20 m where seawater pH was >7.7. More than 90% of stages egg through N4, 80% of N5, and 55% of N6 were above the pycnocline.

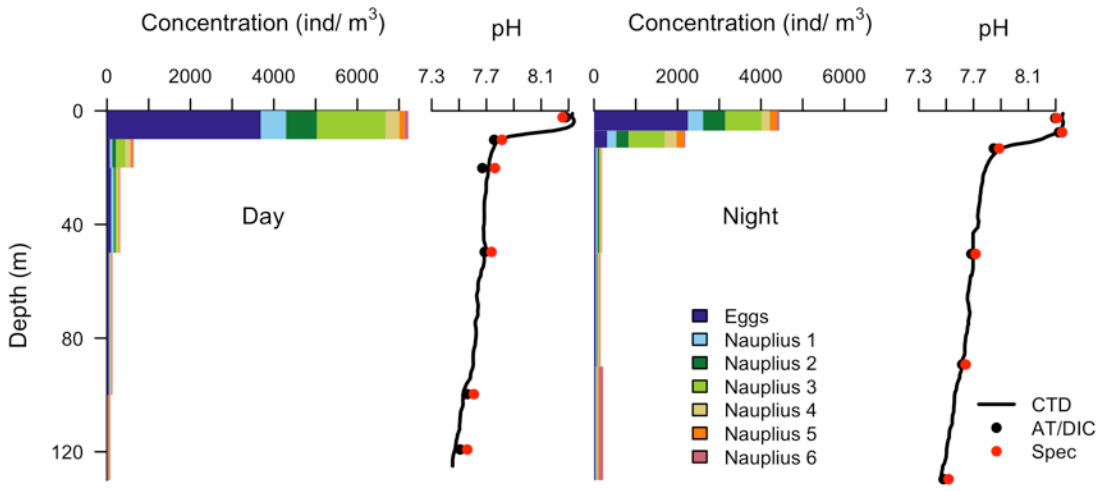

Figure 3.1. Vertical distribution of *Calanus pacificus* early life stages and water column pH at station P15 in Hood Canal, Puget Sound. Depth profiles of pH were calculated from discrete total alkalinity and dissolved inorganic carbon samples (black points), or measured by spectrophotometry from discrete samples (red points). Continuous measurements from the CTD pH probe (black line) were corrected using an average offset from the discrete samples.

We used three types of experiments to investigate the pH sensitivity of *C. pacificus*, each designed to reveal different aspects of inter-individual variability. Two were conducted at Northwest Fisheries Science Center in Seattle. *C. pacificus* were collected during the day in August and September 2012 from the east side of Bainbridge Island (approx. 47.67, -122.49) using a 1-m diameter, 333-µm mesh, ring net with a non-filtering cod end raised from near bottom to the surface. Zooplankton were transported in chilled seawater (~12 ˚C) to the lab where females were sorted and placed individually in 200-mL polystyrene jars of pCO_2-equilibrated seawater then incubated overnight at 12 ˚C on a recirculating seawater system with pH and temperature control described by Miller *et al*. (2016).

The following morning, females were removed and measured. For Individual Brood experiments, eggs spawned from 6-19 females were counted then left undisturbed in the jars to

hatch; for Mixed Brood experiments, eggs from 6-10 females in the same treatment were distributed evenly among ten jars, 30 eggs total per jar, and returned to their treatment conditions. Two trials of each type were run (Table S3.2); in each, eggs and nauplii were left to develop for 5 days, by which time approximately half had reached N3, the first feeding stage. Conditions were verified with spectrophotometric pH samples taken from the jars and recirculating systems; A_T and DIC were sampled from the systems.

A Split Brood experiment was conducted at the Friday Harbor Laboratories (FHL) to characterize pH response within a brood. We used the same jars and water distribution system as above, connected to the FHL seawater control system that is described in O'Donnell *et al*. (2013). Copepods were collected during the day on 16 August 2013 from San Juan Channel (48.60 ˚N 123.09 ˚W) using a 60-cm diameter, 100-µm mesh, closing net with a non-filtering cod end lifted from 110 to 40 m depth. Females were sorted into jars of pCO_2-equilibrated seawater, with ten females in pH 8.0 and ten in 7.3, then incubated overnight at 14 ˚C. The following morning, each brood >30 eggs was gently distributed between a jar of pH 8.0 seawater and one of pH 7.3, then put back on their respective system for three days, at which time approximately half had reached N3. Conditions were verified with spectrophotometric pH and A_T analyses.

In the Individual Brood experiments, hatching, naupliar survival, and the proportion of N3 larvae were highly variable among females. There was a small increase in survival rate at pH 7.3 compared to pH 7.9 (Figure 3.2a, Tables S3.3 and S3.4; GLMM $p=0.02$, marginal $R^2=0.02$, conditional $R^2=0.25$). In the Mixed Brood experiments, we observed a 20% decrease in hatching success between pH 7.7 and 7.3 (Figure 3.2b, Table S3.4; GLMM $p<0.001$; marginal $R^2=0.10$, conditional $R^2=0.12$), but no differences in survival or development to the N3 stage. When variability among females is accounted for, lower pH had a small effect on population hatching

success. In the Split Brood experiment, different females' broods displayed negative, neutral, and positive responses to lower pH; there were no differences in hatching, survival, or development among treatments (Figure 3.2c, Table S3.3). These results suggest that the magnitude and direction of response to pH is variable among different females' broods. All analyses were done using the lme4 and MuMIn packages in R.

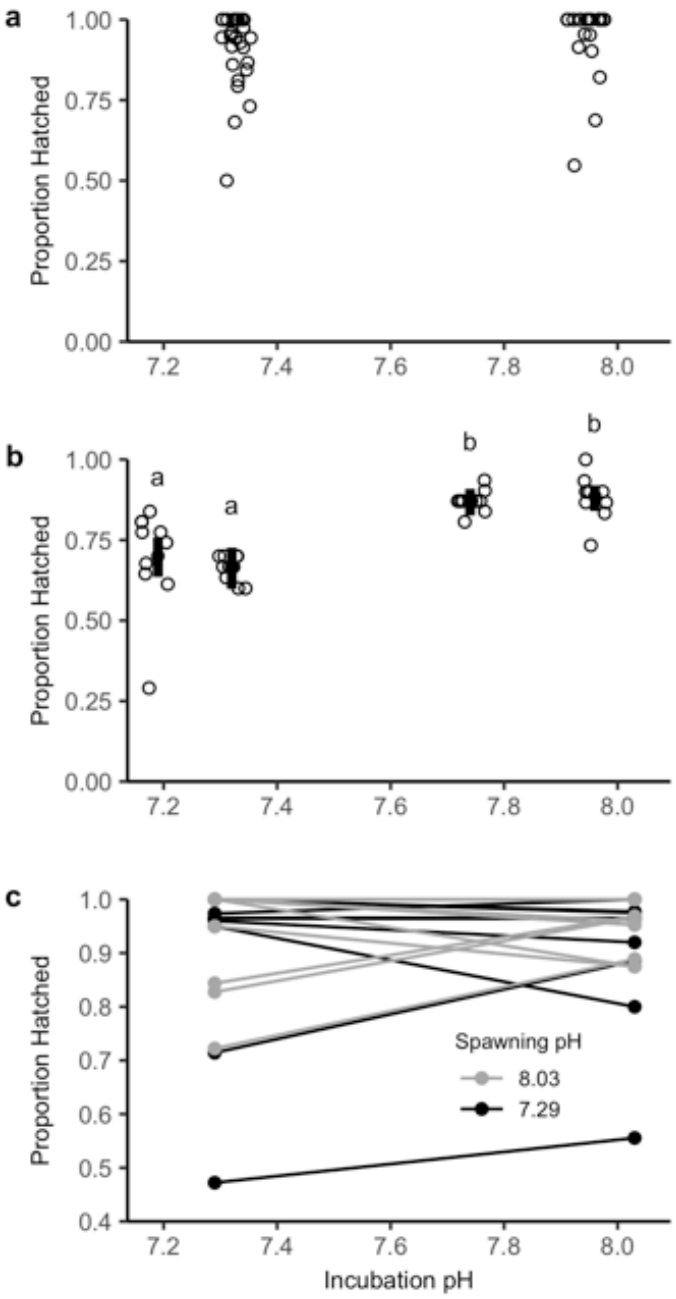

Figure 3.2. Proportion of eggs that hatched in (a) Individual Brood experiments (each point represents an individual female's brood), (b) Mixed Brood experiments (each point represents a jar containing a mixture of eggs from different females), and (c) the Split Brood experiment (each line represents an individual female's brood that was split and reared at two different pH levels). Vertical bars show 95% confidence intervals calculated from the best-fit GLMM; letters indicate statistically significant differences among treatments (Table S3.3); a small random jitter was added to the x-axis value of points in (a) and (b).

In stratified waters, *C. pacificus* early life stages have limited exposure to pH < 7.7. Areas with strong upwelling and periods of low stratification will increase their exposure. Our results show that *C. pacificus* early life stages are relatively robust to low pH, and have highly variable responses among different females' broods. This agrees with research on other *Calanus* species that indicates general tolerance, although sensitivity varies among populations (Thor *et al*. 2018a) and multi-generational exposure can decrease scope for growth (Pedersen *et al*. 2014a). The inter-individual variability we observed suggests either high plasticity or heritable variation, which could make their populations more resilient to ocean acidification. Datasets of paired carbonate chemistry and zooplankton distributions are rare and often have coarse resolution for early life stages (Lewis *et al*. 2013), but provide critical information when evaluating species sensitivity.

3.3 ACKNOWLEDGMENTS

We wish to thank Captain Ray McQuin of the RV Clifford A. Barnes for field sampling; Loren Tuttle for technical support; BethElLee Herrmann for help identifying field samples; Lisa Raatikainen and Jason Miller for help with experiments; Dave Thoreson for collection trips; Moose O'Donnell and Erin Bohaboy for chemistry analyses; Jon Havenhand for help with experimental design; Matt George for general assistance during the FHL experiment; and NOAA Northwest Fisheries Science Center and Ocean Acidification Program for funding the NOAA OA facilities and personnel. This study was funded in part by grants from the Washington Sea Grant, University of Washington, pursuant to National Oceanic and Atmospheric Administration Award No. NA10OAR4170057.

3.4 SUPPORTING INFORMATION

Table S3.1. Full carbonate chemistry conditions from field sampling. Temperature, salinity, A_T, DIC, and pH (total) were measured; pCO_2 and Ω_{ar} were calculated from A_T and DIC using the R package *seacarb* and K_1 and K_2 constants from Lueker *et al.* (2000), $KHSO_4$ constant from Dickson (1990), $[B]_T$ from Uppström (1974), and K_F from Perez and Fraga (1987).

Time	Depth (m)	Temperature (˚C)	Salinity	A_T (µmol kg^{-1})	DIC (µmol kg^{-1})	pH	pCO_2 (µatm)	Ω_{ar}
Day	2	15.9	24.6	1855	1624	8.26	189	2.58
	10	9.7	29.0	2032	1983	7.81	771	0.86
	20	9.3	29.2	2031	2005	7.76	950	0.71
	50	9.1	29.5	2058	2027	7.74	931	0.74
	100	8.5	29.8	2061	2066	7.61	1315	0.54
	119	8.4	29.9	2065	2082	7.56	1480	0.49
Night	3	14.2	25.5	1859	1657	8.31	219	2.24
	8	11.6	28.0	1919	1703	8.35	206	2.32
	13	10.0	28.9	2026	1994	7.89	912	0.75
	50	9.1	29.6	2053	2023	7.72	939	0.73
	89	8.8	29.7	2066	2054	7.64	1130	0.63
	130	8.5	30.0	2079	2103	7.52	1600	0.46

Table S3.2. Carbonate chemistry conditions during the experiments. Spectrophotometric pH (total scale) was measured in the experimental jars and systems; A_T (µmol/kg), salinity, and C_T (µmol/kg) were measured in the systems; pCO_2 was calculated from pH and A_T. When more than one measurement was taken the average is given ± the standard deviation of (n) measurements.

Exp Type	Target pCO_2	# Broods	Sample Type	pH	A_T (µmol/kg)	Salinity	C_T (µmol/kg)	pCO_2 (µatm)
Ind.								
Brood	400	6	System	7.94 ± 0.01 (4)	2045 ± 4 (6)	27.4 ± 0.14 (2)	1918 ± 4 (3)	491 ± 13 (4)
			Jars	7.94 ± 0.01 (6)				494 ± 10 (6)
	800	2	System	7.69 ± 0.01 (2)			1995 ± 1 (2)	928 ± 16 (2)
			Jars	7.68 ± 0.02 (3)				940 ± 50 (3)
	2400	8	System	7.28 ± 0.01 (4)			2101 ± 7 (2)	2470 ± 78 (4)
			Jars	7.32 ± 0.03 (6)				2268 ± 153 (6)
Ind.								
Brood	400	16	System	7.96 ± 0.01 (4)	2076 ± 7 (2)	27.6 ± 0.01 (2)		479 ± 10 (4)
			Jars	7.95 ± 0.01 (6)				486 ± 7 (6)
	2400	19	System	7.31 ± 0.05 (6)				2339 ± 283 (6)
			Jars	7.33 ± 0.03 (8)				2221 ± 149 (8)
Mixed								
Brood	400	10 split	System	7.97 ± 0.01 (6)	2073 ± 4 (2)	27.6 ± 0.05 (3)	1942	470 ± 11 (6)
			Jars	7.96 ± 0.01 (6)				479 ± 9 (6)
	2400	9 split	System	7.31 ± 0.02 (6)			2141	2324 ± 119 (6)
			Jars	7.32 ± 0.02 (6)				2252 ± 114 (6)
Mixed								
Brood	800	6 split	System	7.75 ± 0.01 (6)	2087 ± 2 (2)	28.4 ± 0.09 (3)	2025	811 ± 16 (6)
			Jars	7.74 ± 0.01 (6)				825 ± 17 (6)
	3200	7 split	System	7.17 ± 0.02 (6)			2194	3279 ± 143 (6)
			Jars	7.21 ± 0.01 (6)				2985 ± 91 (6)
Split								
Brood	400		Jars	8.03 ± 0.03 (9)	2111 ± 0 (2)	30.5		398 ± 32 (9)
	2400		Jars	7.23 ± 0.07 (9)	2115 ± 0 (2)			2900 ± 544 (9)

Table S3.3. Summary of *Calanus pacificus* hatching, survival, and development rate in laboratory experiments. Averages ± standard deviation of the proportion of eggs that hatched, the proportion of larvae that survived, and the proportion of larvae that developed to the Nauplius 3 (N3) in experiment jars. Individual Brood jars contained an individual females' brood; Mixed Brood jars contained eggs from 6-10 females; Split Brood jars contained half of an individual females' brood.

Experiment	Target pCO_2	# Jars	Hatching	Survival	Proportion N3
Individual					
Brood	400	6	0.99 ± 0.02	0.64 ± 0.27	0.61 ± 0.21
	2400	8	0.92 ± 0.17	0.88 ± 0.11	0.71 ± 0.28
Individual					
Brood	400	16	0.93 ± 0.13	0.39 ± 0.14	0.57 ± 0.24
	2400	19	0.91 ± 0.1	0.47 ± 0.18	0.44 ± 0.24
Mixed					
Brood	400	10	0.88 ± 0.07	0.53 ± 0.23	0.52 ± 0.15
	2400	10	0.66 ± 0.04	0.57 ± 0.18	0.49 ± 0.25
Mixed					
Brood	800	10	0.7 ± 0.16	0.7 ± 0.11	0.57 ± 0.25
	3200	10	0.87 ± 0.03	0.54 ± 0.3	0.7 ± 0.16
	400 spawn				
Split Brood	400 incubate	10	0.95 ± 0.05	0.71 ± 0.36	0.79 ± 0.25
	400 spawn				
	2400 incubate	10	0.93 ± 0.1	0.83 ± 0.17	0.88 ± 0.2
	2400 spawn				
	400 incubate	10	0.9 ± 0.14	0.77 ± 0.3	0.71 ± 0.36
	2400 spawn				
	2400 incubate	10	0.9 ± 0.17	0.65 ± 0.29	0.65 ± 0.37

Table S3.4. Full model set for proportion hatched, proportion of larvae alive, and proportion of N3 larvae by each experiment type. Binomial GLMMs with logit link (method glmer in lme4 package in R Version 3.5.2) and AICc values shown. In the models, fixed effects are shown without parentheses and random effects with parentheses. Top models, as determined AICc are highlighted in bold; when the difference between lowest AICc < 2, the most parsimonious model was selected**.**

Individual Brood	**Hatching**	**Survival**	**Prop N3**
Response= Treatment + (trial) + (brood) + intercept	200	**290**	320
Response= Treatment + (trial) + intercept	354	365	486
Response= Treatment + (brood) + intercept	198	318	319
Response= (trial) + intercept	353	378	491
Response= (brood) + intercept	**199**	322	**317**
Mixed Brood			
Response= Treatment + (jar) + intercept	**193**	227	222
Response= (jar) + intercept	222	**225**	**220**
Split Brood			
Response= Spawn Treatment* Incubation Treatment + (Female) + intercept	161	205	161
Response= Spawn Treatment + Incubation Treatment + (Female) + intercept	159	208	163
Response= Incubation Treatment + (Female) + intercept	157	206	161
Response= Spawn Treatment + (Female) + intercept	157	206	161
Response= (Female) + intercept	**155**	**204**	**160**

Chapter 4

DIRECT AND INDIRECT EFFECTS OF ELEVATED CO_2 ARE REVEALED THROUGH SHIFTS IN PHYTOPLANKTON, COPEPOD DEVELOPMENT, AND FATTY ACID ACCUMULATION

(This manuscript has been previously published as: McLaskey A.K., Keister J.E., Schoo K.L., Olson M.B., Love B.A. (2019) Direct and indirect effects of elevated CO_2 are revealed through shifts in phytoplankton, copepod development, and fatty acid accumulation. PLoS ONE 14(3): e0213931)

4.1 ABSTRACT

Change in the nutritional quality of phytoplankton is a key mechanism through which ocean acidification can affect the function of marine ecosystems. Copepods play an important role transferring energy from phytoplankton to higher trophic levels, including fatty acids (FA)—essential macronutrients synthesized by primary producers that can limit zooplankton and fisheries production. We investigated the direct effects of pCO_2 on phytoplankton and copepods in the laboratory, as well as the trophic transfer of effects of pCO_2 on food quality. The marine cryptophyte *Rhodomonas salina* was cultured at 400, 800, and 1200 μatm pCO_2 and fed to adult

Acartia hudsonica acclimated to the same pCO_2 levels. We examined changes in phytoplankton growth rate, cell size, carbon content, and FA content, and copepod FA content, grazing, respiration, egg production, hatching, and naupliar development. This single-factor experiment was repeated at 12˚C and at 17˚C. At 17˚C, the FA content of *R. salina* responded non-linearly to elevated pCO_2 with the greatest FA content at intermediate levels, which was mirrored in *A. hudsonica*; however, differences in ingestion rate indicate that copepods accumulated FA less efficiently at elevated pCO_2. *A. hudsonica* nauplii developed faster at elevated pCO_2 at 12˚C in the absence of strong food quality effects, but not at 17˚C when food quality varied among treatments. Our results demonstrate that changes to the nutritional quality of phytoplankton are not directly translated to their grazers, and that studies that include trophic links are key to unraveling how ocean acidification will drive changes in marine food webs.

4.2 INTRODUCTION

Increasing CO_2 concentrations in the atmosphere and ocean due to anthropogenic carbon emissions are causing widespread changes in ocean chemistry that reduce seawater pH and the availability of carbonate ions, a process called ocean acidification (OA). Average surface ocean pH has declined from 8.2 to 8.1 since the industrial revolution, and is expected to decline an additional 0.3-0.4 pH units by 2100 (IPCC 2014). Across a wide range of marine organisms, reduced pH is generally associated with declines in growth, survival, and reproduction with high variability among and within groups (Kroeker et al. 2013; Wittmann and Pörtner 2013). Marine species can also be affected by reduced pH through indirect effects, which require the presence of another species to affect the species of interest (Wootton 1994). Indirect effects such as altered

species interactions (Gaylord et al. 2015) and changes in habitat-forming organisms (Sunday et al. 2016) will likely drive many of the ecosystem changes caused by OA.

One important species interaction is the transfer of energy and nutrients from one trophic level to the next (Gaylord et al. 2015). The phytoplankton-copepod link is a critical trophic link in pelagic ecosystems because copepods are the most abundant mesozooplankton and are an important food source for fish larvae. High pCO_2 affects the growth rate and elemental composition of marine phytoplankton in species-specific ways (King et al. 2015) and therefore can alter the quantity and quality of prey available for zooplankton through changes in total production, morphology, macronutrient, and micronutrient composition. Elevated pCO_2 generally increases the C:N and C:P ratios of phytoplankton (Finkel et al. 2010; Reinfelder 2012) and can also affect their fatty acid content (King et al. 2015). Fatty acids (FA), and in particular polyunsaturated fatty acids (PUFA), are important macronutrients that are predominantly synthesized by primary producers and are necessary for supporting the growth, survival, and reproduction of aquatic organisms (Brett and Müller-Navarra 1997). Laboratory studies on individual phytoplankton species have primarily shown negative effects of increased pCO_2 on PUFAs (Rossoll et al. 2012; Torstensson et al. 2013; Wynn-Edwards et al. 2014; Bermúdez et al. 2015; Meyers 2016; Jacob et al. 2017) or no significant changes in FA (King et al. 2015; Isari et al. 2016; Bi et al. 2017). Mesocosm studies on natural communities have observed a wide range of responses including declines in PUFAs with increased pCO_2 (Bermúdez et al. 2016a), no effect on FA (Bermúdez et al. 2016b) or increased PUFAs (Leu et al. 2013; Wang et al. 2017). Phytoplankton stoichiometry and FA content are also affected by temperature and the interaction between pCO_2 and temperature (Torstensson et al. 2013; Bermúdez et al. 2015; Bi et al. 2017), making the effect of OA on food quality difficult to predict.

Many OA studies have found that copepods are generally robust to pH levels predicted for the end of the century (Kurihara and Ishimatsu 2008; McConville et al. 2013; Hildebrandt et al. 2014; Bailey et al. 2016; Runge et al. 2016), although some species, life stages (Lewis et al. 2013; Cripps et al. 2014b), and populations (Thor and Oliva 2015; Aguilera et al. 2016) are more sensitive. There is also growing evidence of sub-lethal effects such as changes in respiration, ingestion, and reproductive output, that could have important implications for copepod populations (Fitzer et al. 2012; Li and Gao 2012; Thor and Dupont 2015; Thor and Oliva 2015). Changes in the biochemistry of their prey may also influence copepods because their egg production and hatching are dependent on dietary PUFA, particularly eicosapentaenoic acid (EPA; 20:5ω3) and docosahezaenoic acid (DHA; 22:6ω3) (Jónasdóttir et al. 2009), which they cannot produce themselves at ecologically significant rates (Bell et al. 2007; Parrish et al. 2012).

Initial studies that investigated the effects of OA on phytoplankton-copepod linkages concluded that copepod responses corresponded to pCO_2-induced changes in phytoplankton food quality. The copepod *Acartia tonsa* had decreased development rates, growth rates, and egg production when phytoplankton food quality declined with elevated pCO_2 (Rossoll et al. 2012; Schoo et al. 2013; Cripps et al. 2016), but *Acartia grani* were not affected by high pCO_2 when there was no change in phytoplankton food quality (Isari et al. 2016). However, recent mesocosm studies have shown more complex responses. The FA content of copepods declined with increased pCO_2 in mesocosms that had reduced phytoplankton FA at elevated pCO_2 (Bermúdez et al. 2016b) and when there was no change in the phytoplankton community's FA (Garzke et al. 2017). In another mesocosm, PUFA content of the phytoplankton community increased under elevated pCO_2, copepod grazing declined, and copepod FA content was not affected (Wang et al. 2017). In a crossed temperature x CO_2 study, higher temperature was a

much stronger driver than CO_2, causing altered fatty acid composition and declines in copepod abundance, although changes in the phytoplankton were not measured (Garzke et al. 2016). These studies show that the effect on copepods depends on the phytoplankton responses, but that there are also other complicating factors that modulate copepod responses. Carefully controlled laboratory studies are an important tool to illuminate the mechanisms that underlie these community responses.

There are a variety of ways increased pCO_2 can affect the phytoplankton-copepod link including direct effects on copepod metabolic costs or behavior, and on phytoplankton abundance or cell size, which can influence copepod grazing. The balance between quality and quantity of prey ingested and the metabolic costs of the copepods will ultimately determine the growth and reproductive output of the copepods. In this study, we investigated the effects of pCO_2 on copepod populations mediated by changes in their prey quality using the copepod *Acartia hudsonica* and the cryptophyte *Rhodomonas salina* as a model system. *A. hudsonica* is a temperate-boreal coastal calanoid copepod found in the northwest Atlantic, with its congeners found throughout the world's oceans. The effects of elevated pCO_2 on this species have not been investigated, but other *Acartia* species show varied responses including increased egg production and faster naupliar development (Engström-Öst et al. 2014), decreased egg production (Aguilera et al. 2013), and no changes in survival, body size, egg production, hatching, or development rate (Kurihara and Ishimatsu 2008; Zhang et al. 2011). We acclimated phytoplankton and copepods to different pCO_2 levels and characterized a wide range of responses in each. We hypothesized that OA-mediated changes in phytoplankton FA would drive changes in copepod reproductive output, and that this indirect pathway would be the primary mechanism through which OA would affect the copepods.

4.3 METHODS

This study consisted of two separate experiments in which adult *Acartia hudsonica* were maintained at three target pCO_2 levels, 400, 800, 1200 µatm (pH 7.99, 7.75, 7.61), and were fed *Rhodomonas salina* cultured at those same pCO_2 levels. We characterized the physiology and biochemistry of *R. salina* and *A. hudsonica* and assessed the reproductive output and larval development of *A. hudsonica* at each pCO_2 level before and after acclimation to the treatments. In the first experiment (Exp 12C), the temperature was 12˚C; in the second (Exp 17C), it was 17˚C; experiments were run sequentially, not concurrently.

4.3.1 *Atmospheric carbon control simulator (ACCS)*

Experiments were conducted at the Shannon Point Marine Center (SPMC) in Anacortes, Washington. Control of the carbonate chemistry of all cultures and experiments was achieved using an atmospheric carbon control simulator (ACCS) that has been described in detail (Love et al. 2017). In short, the ACCS combines CO_2-free air with pure CO_2 using mass flow controllers to achieve the treatment levels; these air-CO_2 mixtures are then used to bubble reservoirs of 0.2-µm filtered, UV-exposed natural seawater (salinity 28-32) to equilibrate the seawater to target pCO_2 conditions, and distributed to sealed atmospheric simulation chambers where cultures and experimental vessels are maintained. Gas exchange helps maintain target pCO_2 conditions in these chambers. The pCO_2 of inflowing air-CO_2 mixtures and outflowing headspace gasses are verified with a Li-COR Li-820 CO_2 sensor. Equilibration reservoirs were held at experimental temperature in an incubator and atmospheric simulation chambers in a temperature-controlled cold room. Only a single cold room was available so conducting a full temperature x CO_2

factorial experiment was not possible: the two experiments were run sequentially and are treated herein as separate experiments.

The carbonate chemistry of equilibrated seawater and cultures was verified with discrete total inorganic carbon (C_T) and spectrophotometric pH measurements taken in triplicate. *R. salina* cultures and equilibrated seawater used for water changes were sampled daily, *A. hudsonica* cultures were sampled every 1-3 days, and larval development containers were sampled when females were removed and at the end of development tests (described below). C_T was measured using an Apollo SciTech analyzer (AS-C3); spectrophotometric pH (total scale) was measured using an Agilent 8453A UV-VIS diode array spectrophotometer and the m-cresol blue method (Dickson et al. 2007). Full carbonate system parameters were calculated using CO2sys (Lewis and Wallace 2012) using the constants of Mehrbach et al. (Mehrbach et al. 1973) refit by Dickson and Millero (Dickson and Millero 1987) and the total pH scale. Full details on carbonate chemistry methods have been previously described (Love et al. 2017).

4.3.2 *Phytoplankton culturing*

Rhodomonas salina culture was obtained from Biologische Anstalt Helgoland, Alfred Wegener Institute for Polar and Marine Research (M. Boersma). Phytoplankton culturing for this study required a balance between producing enough biomass daily to feed large numbers of copepods and maintaining carbonate chemistry conditions during phytoplankton growth. This tradeoff guided decisions regarding the growth conditions and required preliminary testing of the carbonate system control. Stock cultures of *R. salina* were maintained at experimental temperatures in f/2 enriched seawater following Guillard and Ryther (1962). All seawater for phytoplankton culturing was 0.2-μm sterile filtered, and autoclaved prior to being adjusted to target pCO_2 levels in the equilibration reservoirs. New phytoplankton cultures were inoculated

every day in a f/10 growth medium (nutrient concentrations adjusted from Guillard and Ryther 1962) to ensure constant food quality for the copepods and harvested after a four-day growth period on a 14:10 hr L:D cycle. As testing had revealed differences in the growth rates between the two experimental temperatures, initial cell densities were adjusted to 10000 cells ml^{-1} for Exp 12C and 2500 cells ml^{-1} for Exp 17C; the same initial densities were used for all pCO_2 treatments. The freshly inoculated cultures were maintained in atmospheric simulation chambers and constantly bubbled with air-CO_2 mixtures of the target pCO_2 level. Culture densities and cell sizes were determined daily with a Coulter counter (Beckman Coulter Z2) on five replicate samples, and carbon, nitrogen, and FA content of *R. salina* were measured every few days (described below). Specific growth rate μ (d^{-1}) was calculated from the daily cell counts according to the equation: $\mu = (\ln(D_1)-\ln(D_0)/T$, where D_0 is the starting cell density, D_1 the final density, and T is the growth time (d).

4.3.3 *Copepod culturing and pCO_2 acclimation*

A. hudsonica were obtained from the University of Connecticut (M. Finiguerra, originated from the lab of H.G. Dam). At SPMC, cultures were maintained in water baths at 13-15˚C and ambient CO_2, and fed at surplus from the stock culture of *R. salina*. Mature male and female copepods were sorted from the culture over two days prior to the start of experiments. A subset of females were used to test initial egg production, hatching success, and naupliar development (described below); the rest of the adults were distributed into 500-mL jars of pCO_2-equilibrated seawater at a density of 45 individuals per jar, then held in the atmospheric simulation chambers for an acclimation period. During the acclimation period, jars were given a 75% water change daily and fed pCO_2-acclimated *R. salina* every 12 hours to maintain a cell concentration above

the saturation feeding density of 3000 cells mL^{-1} (~0.2 µgC mL^{-1} (Durbin and Durbin 1992)) while allowing for an estimated maximum ingestion rate of 6000 cells $female^{-1}$ hr^{-1}.

Both experiments had a similar structure that began with a pCO_2 acclimation period starting on day 1; in Exp 12C the acclimation period was six days whereas in Exp 17C, it was reduced to four days due to higher metabolic turnover at higher temperature. *Acartia* sp. are small-bodied, low lipid-storage copepods that have been shown to rapidly respond to food over a period of a few hours (Uye 1981; Kiørboe et al. 1985; Tester and Turner 1990). In Exp 12C, a subset of females was added to jars of males on day 3 at a ratio of 1 female:2 males to ensure the females would be fertilized for egg production, hatching, and development experiments. In Exp 17C, a subset of females was incubated with males for the entire acclimation period at a ratio of 1 female:2 males. At the end of each acclimation period, females that had been incubating with males were used for egg production and subsequent hatching and naupliar development tests. In Exp 12C, two replicate egg production, hatching, and naupliar development trials were run before and after the acclimation period; however, due to logistical constraints, the 800 µatm pCO_2 target treatment was only included in one trial. Respiration and ingestion rate tests took place over two days (days 6 and 7 in Exp 12C and days 4 and 5 in Exp 17C) and consisted of two replicate respiration tests and two separate ingestion rate tests using acclimated and non-acclimated prey (described below). Remaining females were put in food-free water for 24 hrs before being frozen for FA analyses. Females were not reused in any tests except those that were used in ingestion rate tests were also included in elemental and FA analyses.

4.3.4 *Reproductive output and naupliar development*

In all egg production, hatching, and naupliar development tests, females were incubated individually inside mesh-bottom egg production chambers suspended within 250-ml containers

of treatment pCO_2-equilibrated seawater held inside the atmospheric simulation chambers. After 24 h, the females were removed, measured for prosome length (head and thoracic segments), and the containers of undisturbed eggs were placed back into the atmospheric simulation chambers to develop. The duration of the tests differed between Exp 12C and Exp 17C because of faster development rates at the higher temperature: in Exp 12C, eggs and nauplii were allowed to develop for 8 days after spawning and in Exp 17C they developed for 5 days.

After hatching, nauplii were fed *R. salina* once per day at 25% of the density given adults (described above). During tests of the direct effects of pCO_2 on *A. hudsonica* naupliar development, the nauplii were fed stock *R. salina* that had not been pCO_2 acclimated; during tests at the end of the acclimation period, nauplii were fed *R. salina* that had been cultured at the corresponding target pCO_2 treatment. Nauplii were fed starting on day 4 in Exp 12C and day 2 in Exp 17C so that food would be available when they reached the Nauplius II stage, the first feeding stage. At the conclusion of the naupliar development tests, 10% of the jars were checked for naupliar survival and all were preserved in 5% buffered formalin/seawater solution for counting and staging. Hatching success was calculated from the number of hatched nauplii and unhatched eggs found in each container at the end of the experiment; naupliar development was calculated by the proportion of hatched nauplii that reached the Nauplius IV stage (N IV) at the end of the experiment. The number of females included in each trial varied from 20 to 60 females per treatment (actual numbers given in Table 4.)

4.3.5 *Respiration rate*

The effects of pCO_2 concentration on the respiration rate of adult female *A. hudsonica* was measured in two replicate trials for each experiment with oxygen microsensors. 2-ml vials filled with pCO_2-equilibrated seawater from the corresponding pCO_2 treatment and containing 7

females each were monitored with PreSens Oxygen Sensor Spots (Fibox 4 with PST3 sensor spots, PreSens Precision sensing, Germany) under dim light every 15 minutes for 4.4-5.4 hrs. Each respiration test consisted of five replicate vials containing females and five equilibrated seawater blanks per treatment. Copepods were transferred from the acclimation jars into filtered sterilized seawater before they were added to the respiration vials to reduce the transfer of microbes with them; the same volume of this seawater that was added with the copepods was also added to each blank. After each test, female prosome lengths were measured and respiration rate was standardized to dry weight, calculated from prosome length following the equation of Durbin et al. (1992). During Exp 12C, temperature during respiration rate measurements was 13.5 ˚C; during Exp 17C, measurements were made at 16.9 ˚C.

4.3.6 *Ingestion rate*

Ingestion rate of *A. hudsonica* can be affected directly through pCO_2 effects on the copepods as well as indirectly as a response to pCO_2 effects on the phytoplankton. To separate these two processes, the effect of pCO_2 acclimation on female *A. hudsonica* ingestion rate was tested on copepods grazing *R. salina* that had been cultured under ambient (400 µatm) pCO_2 regardless of the copepod pCO_2 acclimation treatment, and again on *R. salina* cultured at the same acclimation pCO_2 level as the copepods. These two tests were each conducted once per experiment using 250-ml bottles containing 15 females per bottle, with four replicates and two control bottles without copepods per treatment. Initial *R. salina* concentrations were ~300 µg C L^{-1} (calculated assuming 75 pg C $cell^{-1}$). Bottles were covered in foil and incubated for 24 hours, after which female copepods were measured; cell concentrations were measured before and after the incubation with a Coulter counter (Beckman Coulter Z2) after being preserved in 5% acid

Lugol's solution. Cell counts were corrected for growth in the control bottles and ingestion rates were calculated according to Frost (1972) and standardized to measured prosome length.

4.3.7 *Elemental and fatty acid composition*

R. salina elemental (C, N) and fatty acid composition were evaluated at several time points throughout the experiments; in Exp 12C, 14 elemental samples and 8-9 fatty acid samples were taken per treatment and in Exp 17C, 7-10 elemental and 3-4 fatty acid samples were taken per treatment (exact numbers given in Table 3 and S4.1 Table). *A. hudsonica* elemental composition was only measured in Exp 17C; fatty acid composition was evaluated on 3-5 samples per treatment at the end of each experiment. For stoichiometric analysis of carbon and nitrogen content, approximately 4 x 10^6 phytoplankton cells were filtered onto a pre-combusted GF/F filter and encapsulated in tin foil; *A. hudsonica* females that had been starved for 24 hrs were collected in tin capsules (30 copepods per sample). Samples were dried in a drying oven at 60˚C for 24 hrs and stored in a desiccator until they were analyzed at the UC Davis Stable Isotope Facility on a PDZ Europa ANCA-GSL elemental analyzer. Phytoplankton samples for FA analysis were filtered as for elemental analysis and stored in Eppendorf tubes layered with N gas and frozen at -80°C until further analysis; copepods for FA analysis were counted into glass test tubes, rinsed with DI water, layered with N gas and frozen at -80 ˚C. Lipids were extracted from the samples using a modification of the methods described by Folch et al. (1957) and Bligh and Dyer (1959) and the FAs were measured as fatty acid methyl esters (FAMEs); detailed methods are described by Malzahn et al. (2010). Samples for FA analyses were extracted in dichloromethane:methanol (2:1 vol:vol) in an ultrasound bath on ice for 10 minutes and then at -80 °C for 24 hours. After centrifugation, the water-soluble fractions were removed by washing with 0.88% KCl buffer. The aqueous phase was discarded and the organic remainder evaporated

using N gas. Esterification was achieved by addition of methanolic-sulphuric acid and incubation at 70 °C for 75 min. The FAMEs were washed from the methanolic-sulphuric acid using n-hexane. Evaporation of the excess n-hexane yielded the final FAMEs, which were analyzed using a Gas Chromatograph Mass Spectrometer (GC/MS; Varian CP3800 GC with Saturn 2000 Ion Trap MS) equipped with a HP-88 column (0.25 mm ID, 30 m length, 0.2 µm film; Agilent Technologies) at Western Washington University. FAs were identified using a NIST 08 MS library and quantified using a known amount of C19:0 added to each sample at the first extraction step.

4.3.8 *Fatty acid accumulation*

We calculated the ratio of *A. hudsonica* total FA content to total ingested FA and compared across pCO_2 treatments. Total ingested FA was calculated by multiplying the average *R. salina* total FA concentration by the average *A. hudsonica* ingestion rate for each treatment and a FA accumulation efficiency was calculated by dividing the average *A. hudsonica* total FA concentration by the total ingested FA.

4.3.9 *Statistical analyses*

Phytoplankton cell size, carbon and nitrogen content, and C:N ratio were analyzed using linear mixed effects models using sampling date as a random factor with post-hoc least-squares means comparisons among treatments using the R packages lme4 and emmeans. Phytoplankton growth rate, copepod carbon and nitrogen carbon content, phytoplankton and copepod fatty acid content, and copepod respiration and ingestion rate were tested for differences among pCO_2 levels within each experiment using an ANOVA and post-hoc Tukey HSD tests. *A. hudsonica* egg production was tested with negative binomial models (glmber.nb) to account for the overdispersion of the

data due to females that did not spawn eggs. Female prosome length was considered as a covariate in the models with treatment as a fixed factor and experimental trial as a random factor. The proportion of eggs that hatched and the proportion of hatched nauplii that developed to the N IV stage were tested using mixed effects logistic regressions on a logit scale with the lme4 R package. Experimental trial and individual female brood were included as random effects.

4.4 RESULTS

4.4.1 *Chemistry*

Chemistry conditions were generally constant over time within each experiment as well as between the two experiments, and pCO_2 treatments were distinct from each other in both experiments (Table 4.1). In general, measured pH was slightly higher and calculated pCO_2 was lower than target levels in algal cultures whereas pH was lower and pCO_2 was higher than target levels in copepod-acclimation and naupliar-development jars.

Table 4.1. Water chemistry summary. Average conditions in each experiment grouped by target pCO_2 treatment, ± 1 standard deviation of (n) measurements. Measurements were taken from pre-equilibrated water, algal cultures, adult copepod acclimation jars, and naupliar development rate jars. Salinity, total inorganic carbon (C_T), and pH were measured; pCO_2 and total alkalinity (A_T) were calculated.

Exp 12C	Target pCO_2	Salinity	C_T (µmol kg^{-1})	pH (total)	pCO_2 (µatm)	A_T (µmol kg^{-1})
Equilibrated water	400	28.7 ± 1.9 (9)	1873 ± 9 (9)	7.99 ± 0.01 (9)	420 ± 8 (9)	2005 ± 8 (9)
	800	28.4 ± 1.5 (9)	1954 ± 14 (9)	7.75 ± 0.02 (9)	776 ± 33 (9)	2012 ± 13 (9)
	1200	29.0 ± 1.5 (13)	1979 ± 19 (13)	7.61 ± 0.02 (13)	1100 ± 52 (13)	2000 ± 17 (13)
Algal cultures	400	30.8 ± 1.2 (23)	1992 ± 18 (23)	8.12 ± 0.05 (23)	327 ± 38 (23)	2194 ± 28 (23)
	800	30.9 ± 1 (23)	2095 ± 16 (23)	7.82 ± 0.03 (23)	693 ± 38 (23)	2186 ± 22 (23)
	1200	31.0 ± 1.1 (23)	2142 ± 24 (23)	7.68 ± 0.04 (23)	994 ± 88 (23)	2190 ± 29 (23)
Acclimation jars	400	30.9 ± 0.8 (8)	1946 ± 18 (8)	7.92 ± 0.03 (8)	516 ± 39 (8)	2064 ± 18 (8)
	800	30.8 ± 0.8 (11)	2016 ± 11 (11)	7.71 ± 0.03 (11)	877 ± 59 (11)	2070 ± 14 (11)
	1200	30.8 ± 0.8 (9)	2038 ± 12 (9)	7.58 ± 0.01 (9)	1193 ± 20 (9)	2057 ± 15 (9)
Development jars	400	30.6 ± 0.5 (9)	1938 ± 14 (9)	7.93 ± 0.02 (9)	501 ± 18 (9)	2069 ± 34 (9)
	800	30.7 ± 0.5 (9)	2020 ± 48 (9)	7.71 ± 0.02 (9)	884 ± 69 (9)	2081 ± 56 (9)
	1200	30.8 ± 0.7 (9)	2044 ± 58 (9)	7.58 ± 0.02 (9)	1215 ± 119 (9)	2069 ± 64 (9)
Exp 17C						
Equilibrated water	400	31.3 ± 0.9 (12)	1919 ± 13 (12)	7.99 ± 0.01 (12)	435 ± 11 (12)	2096 ± 18 (12)
	800	31.3 ± 0.8 (12)	2008 ± 7 (12)	7.75 ± 0.02 (12)	818 ± 39 (12)	2096 ± 8 (12)
	1200	31.3 ± 0.9 (12)	2051 ± 8 (12)	7.60 ± 0.01 (12)	1185 ± 42 (12)	2094 ± 10 (12)
Algal cultures	400	31.9 ± 0.5 (18)	1979 ± 17 (21)	8.11 ± 0.02 (18)	318 ± 40 (21)	2229 ± 13 (18)
	800	31.7 ± 0.5 (18)	2081 ± 29 (21)	7.88 ± 0.06 (18)	623 ± 91 (21)	2224 ± 15 (18)
	1200	31.9 ± 0.5 (18)	2158 ± 15 (21)	7.70 ± 0.03 (18)	972 ± 74 (21)	2237 ± 9 (18)

Acclimation jars	400	31.1 ± 0.7 (12)	1956 ± 10 (15)	7.96 ± 0.01 (12)	458 ± 45 (15)	2123 ± 10 (12)
	800	31.5 ± 0.5 (12)	2034 ± 25 (15)	7.75 ± 0.03 (12)	819 ± 58 (15)	2129 ± 33 (12)
	1200	31.5 ± 0.5 (12)	2077 ± 20 (15)	7.60 ± 0.02 (12)	1137 ± 108 (15)	2131 ± 13 (12)
Development jars	400	31.0 ± 0 (9)	1969 ± 34 (15)	7.98 ± 0.03 (9)	447 ± 70 (15)	2138 ± 33 (9)
	800	31.3 ± 0.5 (9)	2039 ± 32 (15)	7.81 ± 0.05 (9)	748 ± 74 (15)	2142 ± 43 (9)
	1200	31.3 ± 0.5 (9)	2080 ± 33 (15)	7.65 ± 0.06 (9)	1029 ± 120 (15)	2136 ± 35 (9)

4.4.2 *Phytoplankton*

Elevated pCO_2 affected *R. salina* physiology broadly through generally increased growth rate, cell size, and carbon content. Growth rate in Exp 17C was 4 and 8% higher when cultured at 800 and 1200 µatm, respectively ($p<0.0001$; Tukey 400-800 $p=0.013$, 400-1200 $p<0.0001$, 800-1200 $p=0.008$), but differences in growth rate in Exp 12C were not statistically significant ($p=0.25$). *R. salina* cell size was 15 and 14% larger at 800 and 1200 µatm, respectively, than at 400 µatm in Exp 12C and 18 and 16% larger in Exp 17C (Table 4.2, S4.2 Table). Carbon content of *R. salina* was variable over time and sampling date was a significant random factor in the best model for both experiments (S4.1 Table). Carbon content was 8 and 5% higher when cultured at 800 and 1200 µatm, respectively, in Exp 12C, and 9 and 8% higher than at 400 µatm in Exp 17C (Table 4.2, S4.2 Table). C:N molar ratios also increased by 4 and 2% at 800 and 1200 µatm compared to 400 µatm in Exp 12C, and by 8 and 5% in Exp 17C (Table 4.2), with sampling date again a significant random factor (S4.1 Table).

Table 4.2. Phytoplankton growth rate, cell volume, carbon content, and C:N ratio. Average values grouped by target pCO2 treatment, with the standard deviation of (n) measurements. Cell volume was measured via Coulter counter in five replicate samples from each days' feeding cultures, growth rate was calculated from the average cell count of those five replicates; C:N samples were taken opportunistically over the course of the experiment (sampled on 7 days in Exp 12C; 4 days Exp 17C). Superscripts indicate statistically significant differences among pCO2 treatments according to ANOVA and post hoc Tukey test (growth rate) or least-squares means comparisons (cell volume, carbon content, and C:N ratio).

	Target pCO_2	Growth Rate (d^{-1})	Cell Vol (μm^3)	Carbon Content (pg $cell^{-1}$)	C:N
Exp 12C	400	0.60 ± 0.05 (11)	235 ± 10 (35) ^{a}	84 ± 13 (14) ^{a}	5.85 ± 0.46 (14) ^{a}
	800	0.62 ± 0.04 (10)	271 ± 13 (35) ^{b}	91 ± 14 (14) ^{b}	6.10 ± 0.37 (14) ^{b}
	1200	0.64 ± 0.05 (11)	268 ± 12 (35) ^{b}	88 ± 19 (14) ^{ab}	5.99 ± 0.50 (14) ^{b}
Exp 17C	400	0.96 ± 0.02 (9) ^{a}	245 ± 14 (40) ^{a}	75 ± 5 (9) ^{a}	6.04 ± 0.27 (9) ^{a}
	800	1.00 ± 0.03 (9) ^{b}	288 ± 11 (40) ^{b}	82 ± 4 (7) ^{b}	6.52 ± 0.39 (7) ^{b}
	1200	1.04 ± 0.03 (9) ^{c}	285 ± 16 (40) ^{b}	81 ± 7 (10) ^{b}	6.37 ± 0.64 (10) ^{ab}

R. salina FAs responded to increased pCO_2 differently between the two experiments with few observed effects in Exp 12C and strong non-linear effects in Exp 17C (Figure 4.1, S4.1 Fig). In Exp 12C, there were significant shifts in the proportions of several FA classes but no significant differences in the per cell FA content of *R. salina* among pCO_2 treatments (S4.3 Table, S4.4 Table). At elevated pCO_2 the ratio of ω6:ω3 increased, the proportion of MUFA relative to total FA increased, and the proportion of PUFA decreased. In Exp 17C, a wide range of FAs were greatest in cultures acclimated to 800 μatm pCO_2 (Figure 4.1, S4.3 Table). These

differences were significant for total FA, saturated, unsaturated, PUFA, and EPA, but there were no differences in the proportions of each FA type (S4.3 Table, S4.4 Table).

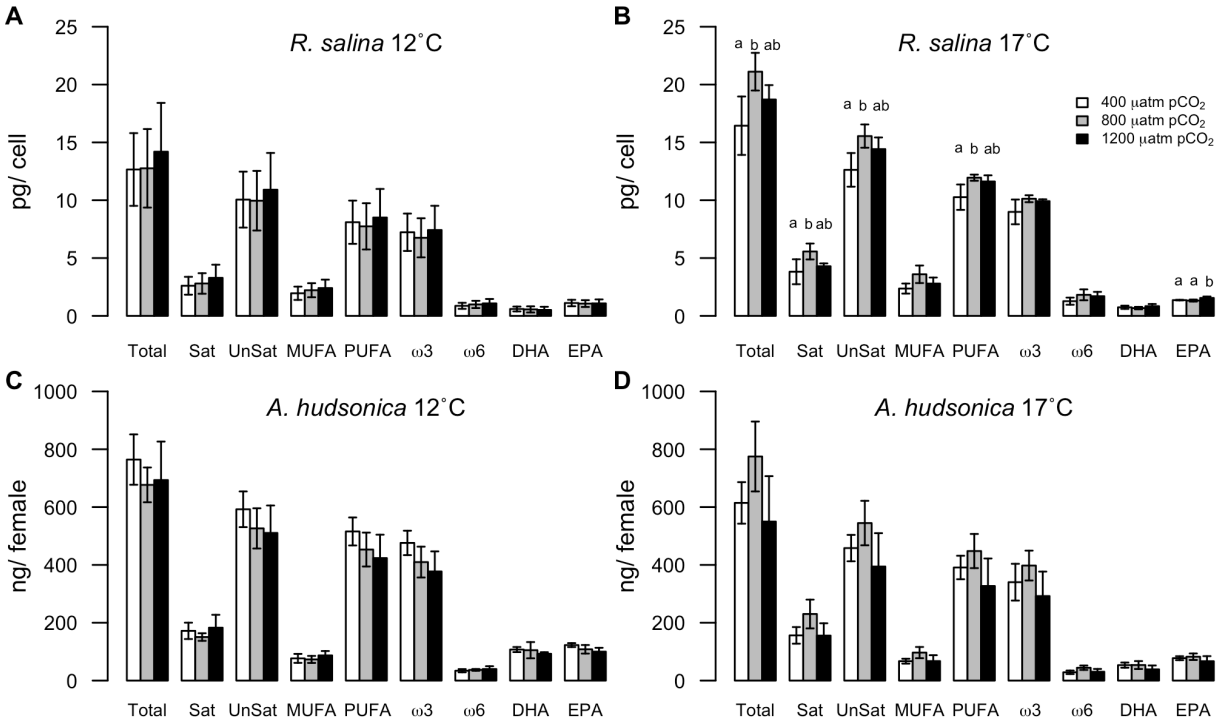

Figure 4.1. Fatty acid content of *R. salina* (A, B; pg cell^{-1}) and *A. hudsonica* (C, D; ng female^{-1}) during Exp 12C and Exp 17C. Error bars show ± 1 standard deviation; letters indicate where significant differences among pCO_2 treatments were detected by Tukey post hoc tests.

4.4.3 *Copepod biochemistry*

There were no significant differences in carbon content (p=0.90), nitrogen content (p=0.89), or C:N (p=0.28) of *A. hudsonica* females raised at different pCO_2 levels in Exp 17C (Table 4.3). These data are not available from Exp 12C. *A. hudsonica* in Exp 12C did not show large differences in FA content with pCO_2 (Figure 4.1, S4.3 Table), but the ratio of ω6:ω3 increased with elevated pCO_2, and the proportion of PUFA declined with elevated pCO_2 (S4.1 Fig, S4.4

Table). Likewise, in Exp 17C, there were no significant differences in *A. hudsonica* FA content with pCO_2 (Figure 4.1, S4.3 Table), but copepods acclimated to 800 µatm pCO_2 had significantly higher proportions of MUFA and lower proportions of PUFA (S4.1 Fig, S4.4 Table).

Table 4.3. Carbon content, nitrogen content, and C:N of female *A. hudsonica* in Exp 17C. Mean and standard deviation of (n) samples containing 30 females each. C and N were not measured in Exp 12C.

Target pCO_2	Carbon Content (µg C copepod^{-1})	Nitrogen Content (µg N copepod^{-1})	C:N
400	3.29 ± 0.22 (5)	0.78 ± 0.03 (5)	4.92 ± 0.17 (5)
800	3.41 ± 0.93 (4)	0.82 ± 0.2 (4)	4.83 ± 0.15 (4)
1200	3.21 ± 0.21 (3)	0.80 ± 0.06 (3)	4.71 ± 0.19 (3)

4.4.4 *Ingestion rate*

There were no differences among copepod pCO_2 acclimation treatments when the copepods grazed *R. salina* that had been cultured under ambient (400 µatm) pCO_2 regardless of the copepod pCO_2 acclimation treatment (Figure 4.2a,c; Exp 12C p=0.811; Exp 17C p=0.105). In Exp 12C, copepod ingestion rate was also not affected when females grazed *R. salina* acclimated to the same pCO_2 level as the copepods (Figure 4.2b; p=0.539). In Exp 17C, *A. hudsonica* females had significantly higher ingestion rates in the 800 and 1200 µatm pCO_2 treatments compared to the 400 µatm treatment when grazing *R. salina* cultured under those same pCO_2 treatments (Figure 4.2d; p=0. 005).

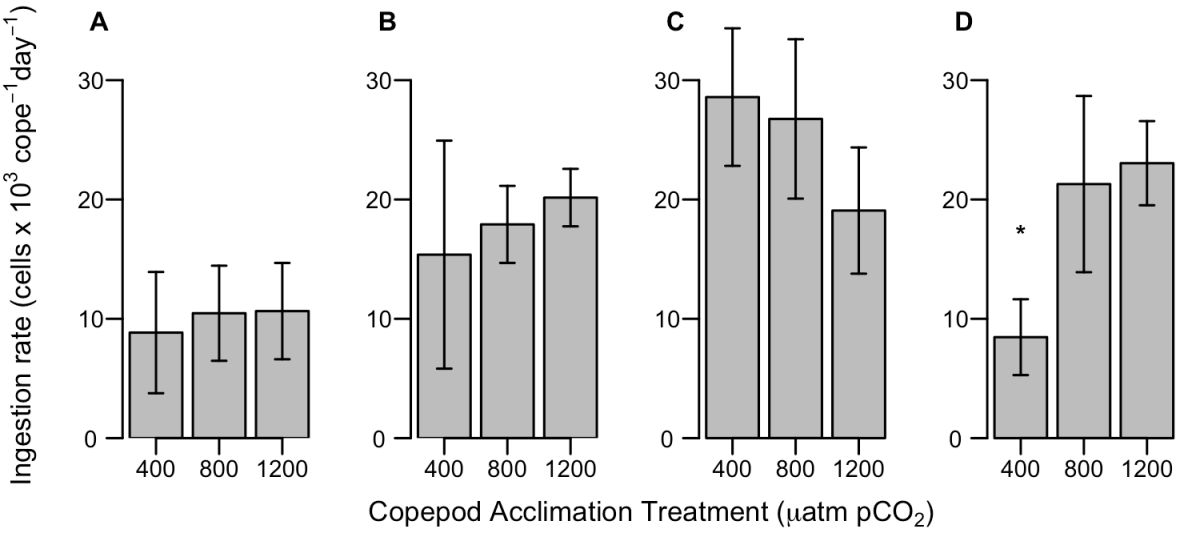

Figure 4.2. Ingestion rate of *A. hudsonica* females on *R. salina* acclimated to 400 μatm pCO_2 (A, C) and on *R. salina* acclimated to the same target pCO_2 as the copepods (B, D) in Exp 12C (A, B) and Exp 17C (C, D). Error bars show ± 1 standard deviation of four replicates; asterisk indicates where a treatment was significantly different from the other two pCO_2 treatments.

4.4.5 *Respiration rate*

There were no clear effects of pCO_2 on female *A. hudsonica* respiration rate in either experiment (Figure 4.3). Respiration rate was similar among treatments in both trials of Exp 12C (Trial 1 p=0.06, Trial 2 p=0.79) and Exp 17C (Trial 1 p=0.70, Trial 2 p=0.24).

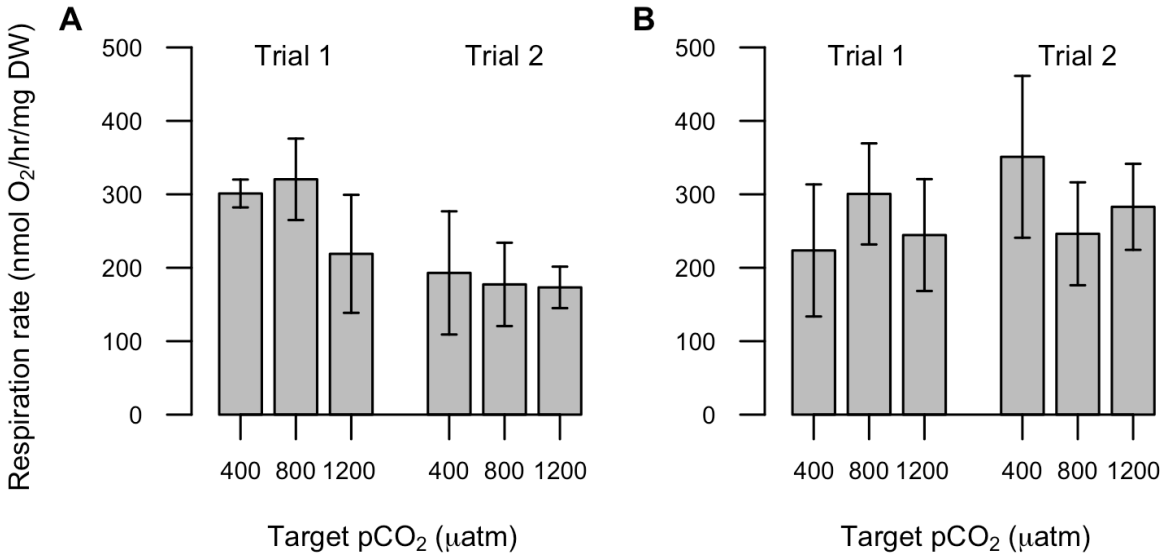

Figure 4.3. Respiration rate of adult female *A. hudsonica* after the pCO_2 acclimation period. The average of five replicates per treatment are plotted for two trials during Exp 12C (A) and Exp 17C (B); error bars show ± 1 standard deviation.

4.4.6 *Reproductive output and naupliar development*

Egg production and hatching success were both highly variable among females within treatments and among experimental trials. We did not detect effects of pCO_2 on hatching before or after the acclimation periods in either experiment (Table 4.4, S4.5 Table). Egg production was only significantly different in Exp 12C pre-acclimation tests, when fewer eggs were produced in the 800 μatm pCO_2 target treatment (Table 4.4, S4.6 Table). Due to logistical constraints, the 800 μatm pCO_2 target treatment was only included in one of the trials (both pre- and post-acclimation) of Exp 12C, which had lower egg production and hatching success across all treatments. This was accounted for in the statistical models; however, the values at 800 μatm given in Table 4.4 are not directly comparable to those in the 400 and 1200 μatm pCO_2 target treatments, which include measurements from both trials.

Table 4.4. Average egg production (egg mm^{-1} female prosome length), proportion hatched, and proportion Nauplius IV (N IV) of individual females' broods in tests pre- and post-acclimation in Exp 12C and Exp 17C. Average responses of broods in each experiment grouped by target pCO_2 treatment, with the standard deviation of (n) measurements (number of females, broods, and broods with hatching for egg production, hatching, and development, respectively). Superscripts indicate where significant differences among pCO_2 treatments were detected by Tukey post hoc tests. Note: in Exp 12C, the 800 µatm pCO_2 target treatment was only included in one of two trials so those values are not directly comparable to those in the 400 and 1200 µatm pCO_2 target treatments, which include measurements from both trials.

	Target pCO_2	**Egg Production (eggs mm^{-1} PL)**	**Prop Hatch**	**Prop N IV Stage**
12˚ C Pre	400	3.4 ± 4.2 (52) [a]	0.46 ± 0.41 (32)	0 ± 0 (18)
	800	0.4 ± 0.8 (32) [b]	0.21 ± 0.39 (7)	0 ± 0 (2)
	1200	2.3 ± 3.8 (52) [a]	0.42 ± 0.42 (26)	0.01 ± 0.02 (15)
12˚C Post	400	13.8 ± 8.0 (49)	0.50 ± 0.47 (54)	0.20 ± 0.29 (34) [a]
	800	10.7 ± 5.7 (22)	0.18 ± 0.34 (24)	0.21 ± 0.38 (8) [ab]
	1200	14.2 ± 7.4 (56)	0.59 ± 0.46 (60)	0.38 ± 0.31 (40) [b]
17˚ C Pre	400	10.6 ± 7.9 (48)	0.79 ± 0.30 (45)	0.02 ± 0.05 (42)
	800	7.6 ± 6.0 (44)	0.87 ± 0.19 (44)	0.01 ± 0.04 (43)
	1200	9.8 ± 8.8 (47)	0.80 ± 0.28 (39)	0 ± 0.01 (37)
17˚ C Post	400	18.3 ± 12.3 (85)	0.22 ± 0.31 (85)	0.30 ± 0.33 (46)
	800	15.6 ± 11.1 (68)	0.20 ± 0.30 (72)	0.27 ± 0.35 (38)
	1200	17.2 ± 12.9 (83)	0.20 ± 0.31 (80)	0.33 ± 0.38 (36)

Higher proportions of nauplii reached the N IV stage in the 1200 µatm pCO_2 treatment compared to 400 µatm in Exp 12C (Figure 4.4a, S4.5 Table). In Exp 17C, there were no significant differences in final naupliar proportions among pCO_2 acclimation treatments (Figure 4.4b, S4.5 Table). There were no differences in naupliar development with pCO_2 level in pre-acclimation tests (testing the short-term direct effects of pCO_2 only) in either experiment. Naupliar mortality was low (0-2%) in all development tests except for one trial after the acclimation period in Exp 12C that had 15% mortality.

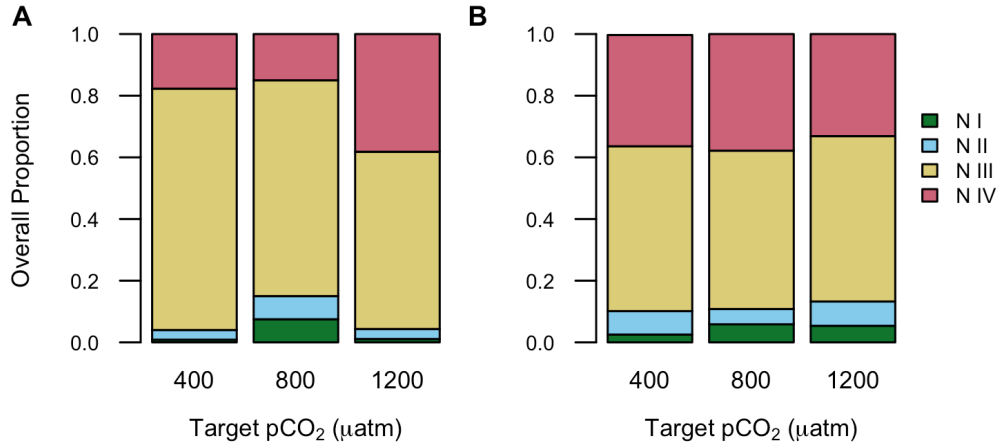

Figure 4.4. Final proportions (all broods combined) of naupliar stages Nauplius I (N I), Nauplius II (N II), Nauplius III (N III), and Nauplius IV (N IV) following development tests of eggs spawned from pCO_2-acclimated *A. hudsonica* females in Exp 12C (A) and Exp 17C (B).

4.4.7 *Fatty acid accumulation*

Differences in total FA content of *R. salina* among pCO_2 treatments, combined with different ingestion rates, led to even great differences in the total FA ingested by copepods among pCO_2 treatments. In both experiments, more FA was ingested at elevated pCO_2 and FA accumulation efficiency decreased with increasing pCO_2 level (Table 4.5).

Table 4.5. Total fatty acids (FA) ingested by *A. hudsonica* and FA accumulation efficiency ratios. Total FA ingested was calculated from *R. salina* total FA concentrations and *A. hudsonica* ingestion rates. FAA is the ratio of *A. hudsonica* total FA to total FA ingested.

	Target pCO_2 (µatm)	Total FA ingested (pg day^{-1})	FA Accumulation Efficiency
Exp 12C	400	195,276	3.91
	800	229,265	2.95
	1200	286,245	2.42
Exp 17C	400	138,758	4.42
	800	449,237	1.73
	1200	430,889	1.28

4.5 DISCUSSION

This study set out to determine how copepods are affected by pCO_2-driven changes in phytoplankton food quality. We hypothesized that changes to the trophic pathway would be the primary mechanism by which OA affected copepod reproductive output, but contrary to our expectations, we found that copepod responses were the result of both direct pCO_2 effects and indirect food quality effects. The responses of phytoplankton FA to elevated pCO_2 differed between the two experiments, while the FA patterns of *A. hudsonica* generally followed those of their prey. However, pCO_2 also affected naupliar development independent of food quality and elevated pCO_2 caused a shift in how copepods accumulated FA. Our results indicate that both direct and indirect effects of elevated pCO_2 will ultimately determine the outcome for copepod populations.

Phytoplankton are affected by pCO_2 in species-specific ways that can alter the quantity and quality of food available for grazers (Finkel et al. 2010; Reinfelder 2012; King et al. 2015). We attribute differences in the effect of pCO_2 on *R. salina* fatty acids between experiments to the different temperatures. Although methodological constraints precluded a single temperature by pCO_2 factorial experiment here, other studies that have directly addressed temperature and pCO_2 as multiple stressors have shown both individual and interactive effects on phytoplankton stoichiometry and FA content (Torstensson et al. 2013; Bermúdez et al. 2015; Bi et al. 2017; Garzke et al. 2017). Phytoplankton fatty acids are also affected by other growth conditions such as nutrient supply ratios (Bi et al. 2017), phytoplankton growth phase (Wang et al. 2017), and growth rate (Bi et al. 2014); although in general, taxonomic differences among groups far outweigh growth conditions in determining phytoplankton FA profiles (Galloway and Winder 2015). Unraveling the responses of phytoplankton to pCO_2 has been a research focus because their differential responses are assumed to be the primary drivers of pCO_2 impacts on the phytoplankton-copepod linkage.

Phytoplankton food quality is an important driver of copepod population dynamics, but is difficult to define and can be characterized in many ways (e.g., macronutrient, lipid, protein, carbohydrate, fatty acid, amino acid, or cholesterol content), with different compounds likely limiting grazer production at different times and under different growth conditions (Anderson and Pond 2000). Elemental stoichiometry is often used as a first approximation of food quality, but can change independently of FA depending on multiple environmental drivers (Bi et al. 2017), and should not be considered in isolation when evaluating possible effects on grazers. FAs are consistently reported as important indications of energy transfer to higher trophic levels and better determinants of egg production than C:N in the laboratory (Jónasdóttir 1994) and field

(Jónasdóttir et al. 1995; Pond et al. 1996). Many studies interpret pCO_2 effects on phytoplankton as changes in food quality without testing the effect on consumers, so characterizing the relative importance of different measures of food quality is essential for understanding the overall effect of pCO_2 on grazers.

The response of copepods to our pCO_2 acclimation treatments may have been decoupled from responses to changes in phytoplankton food quality due to unmeasured direct effects of pCO_2 on their metabolism and physiology, such as decreased digestion efficiency (Stumpp et al. 2013) or increased protein synthesis and ion transport (Pan et al. 2015). OA increases maintenance metabolic costs for some copepods (Pedersen et al. 2014a) but this effect may vary between sexes. Respiration rate of male *Acartia tonsa* increases under elevated pCO_2 but is not affected in females (Cripps et al. 2016). We did not observe an effect of pCO_2 on copepod respiration rate; however, shifts in energy allocation under elevated pCO_2 could change how copepods respond to different nutritional components of their diet. This hypothesis is supported by the decline we observed in FA accumulation efficiency with increased pCO_2. A stable metabolic rate in response to changing pCO_2 concentrations does not mean that pCO_2 has no direct impact on an organism, as OA can cause substantial shifts in energy allocation (Pan et al. 2015); these shifts can maintain performance in the short term but may have long-term consequences for the population and can modulate the influence of changing food quality.

Copepods at elevated pCO_2 in both experiments accumulated FA less efficiently than those at ambient pCO_2, which has important implications for the transfer of FA to higher trophic levels. Although this decline in FA accumulation efficiency indicates metabolic shifts in *A. hudsonica*, we would have expected to see the same response in both ingestion rate tests in Exp17C if direct effects on the copepods were driving the responses. It is important to note that

the low ingestion rates at 400 µatm were only observed in the first ingestion rate trial, despite them feeding on the same food source (400 µatm *R. salina*) in each. Copepod ingestion rate can be influenced by many prey characteristics including cell size (Frost 1972) and food quality (Cowles et al. 1988). We observed increased cell size at elevated pCO_2 in both experiments but increased FA only at 17˚C, so it is possible that different FA content drove the observed differences in ingestion although the ability of copepods to detect and respond to nutritional changes in their prey is not universal or well understood (Isari et al. 2013).

The most unexpected result in this study was that nauplii developed faster, as indicated by higher proportions of late stage nauplii, at elevated pCO_2 in the 12˚C experiment relative to ambient pCO_2, despite a small decline in food quality. Development rate is a complex measure that integrates many physiological processes that could decouple naupliar development rate from food quality. One potential mechanism is maternal provisioning. Exposure of female copepods to elevated pCO_2 conditions can improve the performance of their offspring reared in those conditions (Vehmaa et al. 2012) and non-linear effects of pCO_2 on reproductive output suggest that under pH stress copepods may reallocate energy from somatic growth towards reproduction (Fitzer et al. 2012). The first naupliar stage of *A. hudsonica* is non-feeding and therefore depends entirely on endogenous energy reserves provided by the mother, a process we were unable to measure due to the low biomass of their eggs. Although unexpected, it is also possible that the faster naupliar development rate at elevated pCO_2 was a direct effect of the pCO_2 treatment. A study of *Acartia bifilosa* found the distribution of naupliar stages was older when cultured at reduced pH after 3 days post-spawning, although there were no differences after 4 days (Engström-Öst et al. 2014). Increased growth rate at low pH has also been observed in sea star larvae and juveniles (Dupont et al. 2010a). Unfortunately, our tests on the effect of pCO_2 on

naupliar development prior to the acclimation period failed to capture a distribution of stages (very few nauplii reached the N IV stage), making it difficult to evaluate whether pCO_2 in isolation caused the change in development rate. We cannot identify the mechanism driving increased development rate, but our results indicate that there are important uncharacterized effects of pCO_2 that modulate the influence of food quality on copepod development.

The non-linear changes in phytoplankton FA content that we observed in the 17˚C experiment may help explain variable results among previous studies: if only two pCO_2 treatments are compared, the observed effect of pCO_2 (positive, negative, or none) will depend on which part of the organism's response curve the chosen treatments lie on. Non-linear responses to pCO_2 are likely common and have been observed, e.g., in calcification rates of diverse taxa (Ries et al. 2009), phytoplankton DMSP concentration (Olson et al. 2017), phytoplankton carbon content and growth rate (Langer et al. 2009). Approximately half of the published studies investigating the effects of pCO_2 on phytoplankton FA to date have used only two pCO_2 treatments and therefore could not have detected non-linear responses. Because of these considerations, more than two pCO_2 treatments should be used, and other growth conditions should be chosen carefully either for environmental realism or to elucidate the interactions among different factors.

4.6 CONCLUSIONS

We found that phytoplankton biochemical responses to increased pCO_2 differed between our two experimental temperatures and that copepod responses were a result of both direct pCO_2 effects and indirect food quality effects. At 12˚C there was little change in food quality but naupliar development was faster at high pCO_2, while at 17˚C phytoplankton food quality increased at

moderate pCO_2 but did not translate to benefits for the copepods, demonstrating that organism responses ultimately arise from a combination of both direct and nutritional effects of pCO_2. This hypothesis is also supported by the decline in the ratio of copepod FA stores to ingested FA with elevated pCO_2. This study shows the importance of testing food quality effects on grazers and cautions against a simple extrapolation of phytoplankton biochemistry to higher trophic levels. Carefully designed experimental systems are needed to properly separate direct effects on grazers from the influence of food quality, which has important implications for design and interpretation of many OA experiments.

4.7 ACKNOWLEDGEMENTS

Thank you to Kelley Bright, Amanda Echevarria, Aigbe Woghiren, Miranda Winningham for help running experiments; Michael Brett for helpful discussions about the fatty acid data; Michael Finiguerra for the *A. hudsonica* culture; Stuart Wakeham for project development and fatty acid expertise.

4.8 SUPPORTING INFORMATION

S4.1 Table. Statistical models and AIC scores for generalized linear mixed effects models of *Rhodomonas salina* cell volume, carbon content, nitrogen content, and C:N ratio. In the models, fixed effects are shown without parentheses and random effects with parentheses. Best model's AIC score is highlighted in bold.

Experiment 1 (12 ˚C)	**Cell Volume**	**Carbon Content**	**Nitrogen Content**	**C:N**
Response=Treatment*(Date)	801	304.21	263.61	-4.88
Response=Treatment+(Date)	**801**	**304.21**	263.61	**-4.88**
Response=(Date)	931.55	308	**261.9**	7.63
Experiment 2 (17 ˚C)				
Response=Treatment*(Date)	920.57	169.94	139.85	27.99
Response=Treatment+(Date)	**920.57**	**169.94**	139.85	**27.99**
Response=(Date)	1103.98	175.02	**137.73**	36.12

S4.2 Table. P-values for post-hoc least-squares means comparisons among treatments for *R. salina* cell volume, carbon content, and C:N.

Contrast	**Exp 12C Cell Vol**	**Exp 12C Carbon**	**Exp 12C C:N**	**Exp 17C Cell Vol**	**Exp 17C Carbon**	**Exp 17C C:N**
400-800	<0.0001	0.021	0.0003	<0.0001	0.024	0.0028
400-1200	<0.0001	0.18	0.038	<0.0001	0.031	0.0638
800-1200	0.47	0.57	0.16	0.31	0.92	0.23

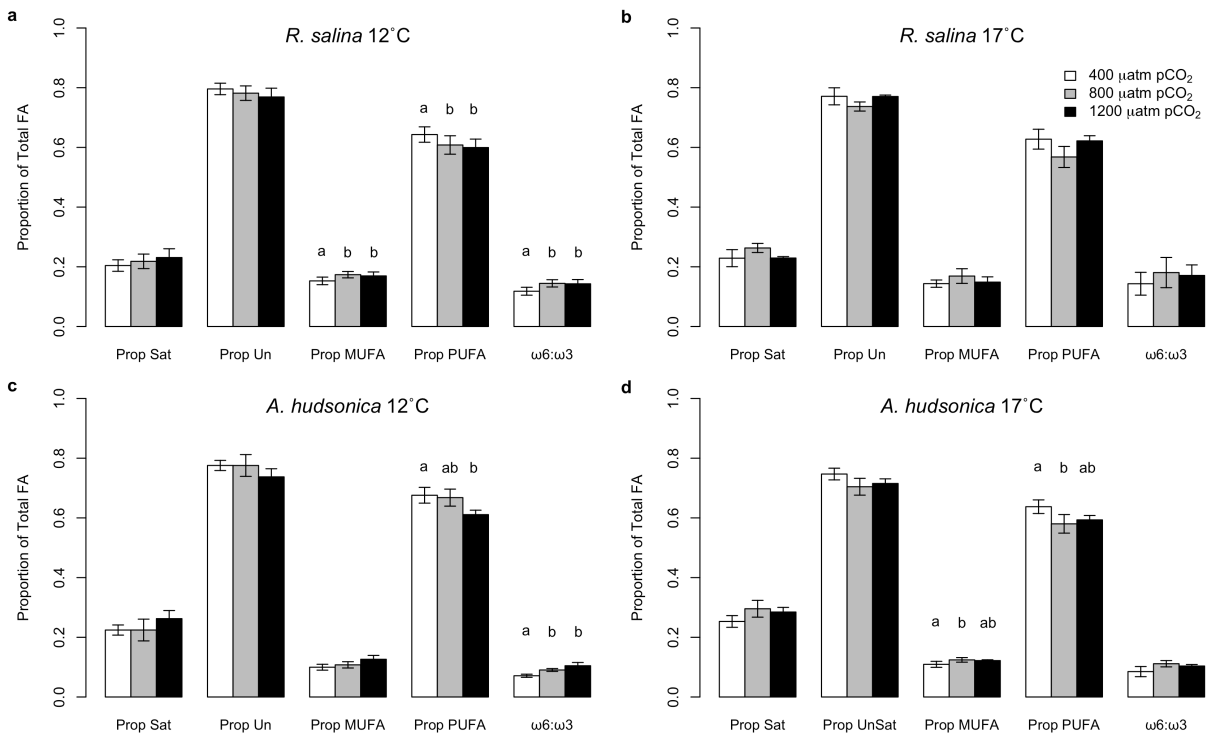

S4.1 Figure. Fatty acid proportions of *R. salina* (a, b) and *A. hudsonica* (c, d) during Exp 1 (12˚ C; a, c) and Exp 2 (17˚ C; b, d). Error bars show ± 1 standard deviation; letters indicate where significant differences among pCO_2 treatments were detected by Tukey post hoc test

S4.3 Table. Quantity of fatty acids in *Rhodomonas salina* (pg cell^{-1}) and *Acartia hudsonica* (ng female^{-1}) during Exp 1 (12 ˚C) and Exp 2 (17 ˚C).

	12C Rhodomonas (pg/cell)			17C Rhodomonas (pg/cell)			12C Acartia (ng/female)			17C Acartia (ng/female)		
Fatty Acid	**400 (n=9)**	**800 (n=9)**	**1200 (n=8)**	**400 (n=4)**	**800 (n=4)**	**1200 (n=3)**	**400 (n=3)**	**800 (n=3)**	**1200 (n=3)**	**400 (n=4)**	**800 (n=4)**	**1200 (n=3)**
C14:0	0.53 ± 0.19	0.55 ± 0.21	0.66 ± 0.27	0.81 ± 0.23	1.27 ± 0.2	0.96 ± 0.08	24.5 ± 7.7	20.3 ± 1.8	21.5 ± 5.6	16.4 ± 3.5	26.5 ± 6	14.5 ± 5
C15:0	0.03 ± 0.02	0.03 ± 0.02	0.04 ± 0.02	0.05 ± 0.01	0.07 ± 0.01	0.06 ± 0.04	1.9 ± 0.5	1 ± 0.9	2 ± 0.9	2.3 ± 0.5	3.9 ± 1.3	2.1 ± 1
C16:0	1.7 ± 0.5	1.9 ± 0.6	2.3 ± 0.8	2.5 ± 0.7	3.6 ± 0.5	2.8 ± 0.1	114 ± 18	100 ± 12	118 ± 24	103 ± 22	154 ± 31	108 ± 27
C16:1n9	0.42 ± 0.14	0.32 ± 0.2	0.45 ± 0.24	0.36 ± 0.3	0.42 ± 0.34	0.48 ± 0.17	0 ± 0	0.9 ± 1.6	2.8 ± 2.7	7 ± 5	12.4 ± 4.6	8 ± 4.6
C16:1n7	0 ± 0	0.1 ± 0.2	0.04 ± 0.12	0.21 ± 0.32	0.56 ± 0.23	0.09 ± 0.15	15.1 ± 6.1	9.4 ± 4.3	11.4 ± 2.9	5.4 ± 4.1	8.6 ± 1.9	6.1 ± 2.6
C17:0	0.16 ± 0.07	0.18 ± 0.05	0.18 ± 0.09	0.25 ± 0.06	0.29 ± 0.02	0.23 ± 0.01	9.5 ± 1.1	8.4 ± 0.2	8.8 ± 1.2	8.6 ± 1.2	10.7 ± 1.7	7.2 ± 3.5
C17:1n7	0.01 ± 0.02	0.01 ± 0.02	0.01 ± 0.02	0 ± 0	0.03 ± 0.03	0 ± 0	7.4 ± 1.7	5.5 ± 4.9	7 ± 0.8	3.9 ± 2.8	6.9 ± 1.3	5.8 ± 0.7
C18:0	0.12 ± 0.06	0.12 ± 0.03	0.13 ± 0.03	0.2 ± 0.05	0.25 ± 0.05	0.23 ± 0.03	22.4 ± 1.6	20.6 ± 1.3	32.5 ± 16.6	26.4 ± 3.1	34.1 ± 11.6	24.1 ± 2.1
C18:1n9 t	0.07 ± 0.05	0.11 ± 0.04	0.12 ± 0.06	0.12 ± 0.02	0.12 ± 0	0.11 ± 0.01	2.1 ± 0.9	2.3 ± 0.9	4.6 ± 2	4.3 ± 0.5	5.8 ± 1.6	3.6 ± 0.5
C18:1n9 c	0.83 ± 0.25	1.09 ± 0.27	1.11 ± 0.35	0.93 ± 0.31	1.59 ± 0.49	1.4 ± 0.59	10.4 ± 1.7	14.6 ± 1.8	16.4 ± 4.2	17.2 ± 7.3	29.7 ± 7.9	17.1 ± 6
C18:1n7	0.62 ± 0.17	0.6 ± 0.17	0.68 ± 0.22	0.75 ± 0.13	0.88 ± 0.05	0.73 ± 0.05	40.2 ± 5.6	37.4 ± 1.7	43.5 ± 17.4	28.8 ± 4.6	33.3 ± 4.2	26.8 ± 8.2
C18:2n6	0.66 ± 0.2	0.75 ± 0.23	0.83 ± 0.3	1 ± 0.2	1.5 ± 0.3	1.5 ± 0.2	22.3 ± 4.1	23.6 ± 0.7	27.1 ± 7.9	19.4 ± 4.6	32.1 ± 4.9	21.7 ± 7.3
C18:3n6	0.14 ± 0.04	0.16 ± 0.05	0.17 ± 0.06	0.13 ± 0.09	0.2 ± 0.13	0.09 ± 0.16	5.6 ± 1	6.2 ± 0.4	6.1 ± 1.3	21.8 ± 34.6	6.9 ± 1.6	4.7 ± 1.2
C18:3n3	2.1 ± 0.4	2.1 ± 0.5	2.4 ± 0.6	2.9 ± 0.4	3.5 ± 0.1	3.3 ± 0.2	97.6 ± 10.7	87 ± 7.2	80.9 ± 20.5	72.3 ± 46.7	110.1 ± 14.3	81.3 ± 23.4
C18:4n3	3.4 ± 0.8	3 ± 0.8	3.5 ± 1	4 ± 0.8	4.6 ± 0.3	4.2 ± 0.2	148 ± 19	110 ± 12	104 ± 32	137 ± 22	151 ± 17	105 ± 32
C20:2	--	--	--	--	--	--	5.6 ± 0.6	6.4 ± 2.3	6.5 ± 2.5	4.8 ± 1	5.8 ± 1.7	4.1 ± 1.4
C20:4n6	0.07 ± 0.03	0.08 ± 0.04	0.08 ± 0.04	0.11 ± 0.02	0.13 ± 0.02	0.14 ± 0.02	6.1 ± 1	7.2 ± 2.2	6.6 ± 1	4.8 ± 0.9	5.4 ± 1.5	4.2 ± 1.2
C20:5n3	1.1 ± 0.3	1.1 ± 0.3	1.1 ± 0.3	1.4 ± 0	1.3 ± 0.1	1.6 ± 0.1	123 ± 7	108 ± 15	100 ± 13	77.4 ± 6.9	82.5 ± 11.3	66.9 ± 20.9
C22:6n3	0.6 ± 0.21	0.56 ± 0.27	0.51 ± 0.28	0.74 ± 0.14	0.67 ± 0.11	0.84 ± 0.19	107 ± 9	105 ± 28	93 ± 5	53.4 ± 9	53.7 ± 13.6	38.8 ± 16.4
C23:0	0.02 ± 0.02	0.01 ± 0.01	0 ± 0	0 ± 0	0.1 ± 0	0 ± 0	--	--	--	0 ± 0	0.6 ± 1.2	0 ± 0
C22:1n9	--	--	--	--	--	--	1.5 ± 1.4	3 ± 2.1	1.3 ± 1.2	0.4 ± 0.8	0 ± 0	0 ± 0
Total	12.7 ± 3.1	12.8 ± 3.4	14.2 ± 4.2	16.4 ± 2.5	21.1 ± 1.6	18.7 ± 1.2	764 ± 87	677 ± 60	694 ± 133	614 ± 72	775 ± 121	550 ± 163
Saturated	2.6 ± 0.8	2.8 ± 0.9	3.3 ± 1.1	3.8 ± 1.1	5.6 ± 0.7	4.3 ± 0.2	172 ± 28	150 ± 13	183 ± 45	156 ± 29	230 ± 50	156 ± 38
Unsaturated	10.1 ± 2.4	10 ± 2.6	10.9 ± 3.2	12.6 ± 1.5	15.5 ± 1	14.4 ± 1	592 ± 62	526 ± 70	511 ± 95	458 ± 46	545 ± 77	394 ± 124
ω3	7.2 ± 1.6	6.8 ± 1.7	7.4 ± 2.1	9 ± 1.1	10.1 ± 0.3	9.9 ± 0.2	476 ± 42	410 ± 53	377 ± 70	340 ± 64	398 ± 52	292 ± 93
ω6	0.87 ± 0.26	0.99 ± 0.31	1.08 ± 0.38	1.3 ± 0.3	1.8 ± 0.5	1.7 ± 0.4	34 ± 5.6	36.9 ± 3.1	39.8 ± 9.9	46 ± 33.9	44.4 ± 7.6	30.6 ± 9.8
MUFA	2 ± 0.6	2.2 ± 0.6	2.4 ± 0.7	2.4 ± 0.4	3.6 ± 0.8	2.8 ± 0.5	76.7 ± 15.5	73.1 ± 12.1	87.1 ± 15.1	67.1 ± 8.5	96.8 ± 19.4	67.4 ± 20.8
PUFA	8.1 ± 1.9	7.7 ± 2	8.5 ± 2.5	10.3 ± 1.1	11.9 ± 0.3	11.6 ± 0.5	516 ± 48	453 ± 59	424 ± 81	391 ± 41	448 ± 59	327 ± 104
DHA/EPA	0.52 ± 0.09	0.5 ± 0.13	0.44 ± 0.14	0.54 ± 0.1	0.51 ± 0.05	0.54 ± 0.1	0.87 ± 0.05	0.96 ± 0.13	0.93 ± 0.09	0.69 ± 0.13	0.65 ± 0.11	0.57 ± 0.08
Sat/Unsat	0.26 ± 0.03	0.28 ± 0.04	0.3 ± 0.05	0.3 ± 0	0.4 ± 0	0.3 ± 0	0.29 ± 0.03	0.29 ± 0.06	0.36 ± 0.05	0.34 ± 0.04	0.42 ± 0.06	0.4 ± 0.03
n6/n3	0.12 ± 0.01	0.14 ± 0.01	0.14 ± 0.01	0.14 ± 0.04	0.18 ± 0.05	0.17 ± 0.04	0.07 ± 0.01	0.09 ± 0	0.1 ± 0.01	0.15 ± 0.15	0.11 ± 0.01	0.1 ± 0
Prop Saturated	0.2 ± 0.02	0.22 ± 0.02	0.23 ± 0.03	0.23 ± 0.03	0.26 ± 0.02	0.23 ± 0	0.22 ± 0.02	0.22 ± 0.04	0.26 ± 0.03	0.25 ± 0.02	0.3 ± 0.03	0.28 ± 0.02
Prop Unsaturated	0.8 ± 0.02	0.78 ± 0.02	0.77 ± 0.03	0.77 ± 0.03	0.74 ± 0.02	0.77 ± 0	0.78 ± 0.02	0.78 ± 0.04	0.74 ± 0.03	0.75 ± 0.02	0.7 ± 0.03	0.72 ± 0.02
Prop MUFA	0.15 ± 0.01	0.17 ± 0.01	0.17 ± 0.01	0.14 ± 0.01	0.17 ± 0.02	0.15 ± 0.02	0.1 ± 0.01	0.11 ± 0.01	0.13 ± 0.01	0.11 ± 0.01	0.12 ± 0.01	0.12 ± 0
Prop PUFA	0.64 ± 0.03	0.61 ± 0.03	0.6 ± 0.03	0.63 ± 0.03	0.57 ± 0.04	0.62 ± 0.02	0.68 ± 0.03	0.67 ± 0.03	0.61 ± 0.01	0.64 ± 0.02	0.58 ± 0.03	0.59 ± 0.01

S4.4 Table. P values for ANOVA and post-hoc Tukey test for fatty acids. Only those with significant ANOVA p values are shown.

	Rhodomonas Exp 12C				Rhodomonas Exp 17C			
Fatty Acid	**ANOVA**	**400-800**	**400-1200**	**800-1200**	**ANOVA**	**400-800**	**400-1200**	**800-1200**
C20:5n3					0.018	0.81	0.044	0.019
Total					0.028	0.023	0.33	0.29
Saturated					0.036	0.034	0.72	0.15
Unsaturated					0.025	0.021	0.18	0.47
PUFA					0.029	0.029	0.098	0.84
ω6/ω3	0.0004	0.0009	0.002	0.97				
Prop MUFA	0.004	0.004	0.026	0.76				
Prop PUFA	0.01	0.04	0.012	0.81				
	Acartia Exp 12C				Acartia Exp 17C			
ω6/ω3	0.0045	0.045	0.0037	0.13				
Prop MUFA					0.042	0.048	0.095	0.9
Prop PUFA	0.032	0.91	0.037	0.062	0.019	0.019	0.066	0.72

S4.5 Table. Statistical models and AIC scores for generalized linear and mixed effects models of *A. hudsonica* hatching proportions and proportion of nauplii to develop to the Nauplius IV (N IV) stage. In the models, fixed effects are shown without parentheses and random effects with parentheses. Best model's AIC score is highlighted in bold.

	12C Pre-acclimation		**12C Post-acclimation**		**17C Post-acclimation**	
	Prop Hatch	**Prop N IV**	**Prop Hatch**	**Prop N IV**	**Prop Hatch**	**Prop N IV**
Response=(Experiment) + (Brood) + Treatment	185.71	22.392	329.58	323.73	892.01	375.61
Response=(Experiment) + Treatment	232.06	20.392	656.36	428.74	2302.53	440.04
Response=(Brood) + Treatment	192.11	20.392	453.82	**321.73**	890.01	373.84
Response=(Brood)	189.85	**16.497**	473.28	325.95	**887.29**	**370.16**
Response=(Experiment)	228.94	**16.497**	656.14	470.76	2300.28	437.78
Response=(Experiment) + (Brood)	**181.71**	18.497	**326.21**	327.95	889.29	371.86

	17C Pre-acclimation	
	Prop Hatch	Prop N IV
Response=(Brood) * Treatment	386.2	73.78
Response=(Brood) + Treatment	386.2	73.78
Response=(Brood)	**384.21**	**72.96**

S4.6 Table. Statistical models and AIC scores for mixed-effects negative binomial models of *A. hudsonica* egg production. In the models, fixed effects are shown without parentheses and random effects with parentheses. Best model's AIC score is highlighted in bold.

	12C Pre-acclimation	**12C Post-acclimation**	**17C Post-acclimation**
Response=(Experiment) + Treatment + ProsomeLength	**439.19**	829.2	1694.49
Response=(Experiment) + Treatment	463.76	913.43	1761.14
Response=(Experiment) + ProsomeLength	451.13	**828.25**	**1691.31**
Response=(Experiment)	472.22	912.66	1758.72

	17C Pre-acclimation
Response=Treatment + ProsomeLength	850.07
Response=Treatment	885.83
Response=ProsomeLength	**850.16**

Chapter 5

ENZYME ACTIVITIES OF KRILL (*EUPHAUSIA PACIFICA*) IN RESPONSE TO PH AND OXYGEN EXPOSURE: A COUPLED FIELD-LABORATORY APPROACH TO STUDYING OCEAN CHANGE

5.1 ABSTRACT

Krill are abundant and ecologically important zooplankton that inhabit dynamic environments characterized by strong natural variability; however, global ocean change is shifting the range of conditions these animals experience as seawater pH and oxygen concentrations decline and temperatures increase. In this study, we combined field and laboratory approaches to investigate the effects of ocean change on North Pacific krill, *Euphausia pacifica*, using enzyme activities as physiological indicators. Electron Transport System (ETS) and aminoacyl-tRNA synthetases (AARS) activity are two enzyme activities that are used in zooplankton research as proxies for respiration rate and protein synthesis, respectively. We measured ETS and AARS activity in adult female *E. pacifica* across a strong natural gradient of pH and oxygen conditions found in Puget Sound, WA. In addition, we investigated the effect of pH and oxygen on krill in the laboratory. Acclimation to different pH and oxygen conditions in the laboratory did not reveal any effects on respiration rate, ETS activity, or AARS activity of krill. However, individuals

collected from the field had lower ETS activity where oxygen concentrations were lower, which would depress their metabolic potential. AARS activity had a weak positive relationship with pH but high variability among sampling sites, which may be a result of the sensitivity of this enzyme activity to short-term physiological changes. Although differences in age structure suggest different patterns of recruitment between *E. pacifica* populations in areas with potentially stressful conditions and those without, populations persist at stressful sites, potentially due to the high food concentrations available in this productive system. Importantly, we were able to detect responses in the field that we did not detect in the lab, showing the importance of factors present only in the field (e.g., co-occurring stressors, diel variability in exposure, and realistic food conditions) for determining their responses to individual drivers.

5.2 INTRODUCTION

Krill are a key component of many marine ecosystems as important prey species that link primary production to higher trophic levels. They are very successful in dynamic environments characterized by strong variability such as the Southern Ocean and Eastern Boundary Upwelling Systems, and they often display high variability in life traits and behaviors. *Euphausia pacifica* is the dominant krill species in the California Current Ecosystem (CCE) and inhabits a wide range from Baja California through the Gulf of Alaska and across the North Pacific to Japan. In the CCE, *E. pacifica* populations inhabit regions of seasonal upwelling, which brings cold waters that are rich in CO_2 and low in oxygen onto the continental shelf (Feely et al. 2008), resulting in strong spatial and temporal variations in ocean conditions. *E. pacifica* also undergo large vertical migrations over the course of their development and, once they are more mature, on diel cycles.

Therefore, krill living in the CCE are often exposed to a wide range of pCO_2, pO_2, and temperature conditions on daily and seasonal time scales.

Increased carbon dioxide concentrations in the atmosphere have resulted in increased ocean temperatures, declining dissolved oxygen (DO) concentrations, and decreased pH (IPCC 2014). These long-term trends are shifting the environmental variability experienced by marine organisms out of the range they are accustomed to; seawater pH in the CCE has already shifted significantly from its pre-industrial range of variability (Hauri et al. 2013), while DO concentrations are declining in the CCE (Chan et al. 2008; Ren et al. 2018) and its coastal estuaries (Lowe et al. 2019). These broad changes are expected to impact marine organisms in complex and potentially interactive ways (Ekau et al. 2010; Hofmann et al. 2010; Kroeker et al. 2013). Ocean change is a complex phenomenon: global and local drivers cause multiple physical and chemical changes that interactively affect closely-connected biological systems. Studying such complex processes requires a varied tool kit, diverse research approaches, and integrative thinking.

Krill are large zooplankton that are patchy in space and time, making them challenging to study both in the laboratory and *in situ*, but previous studies have broadly characterized their responses to DO and pH. *E. pacifica* can withstand mildly hypoxic conditions (Li et al. 2019) but avoids anoxic waters in the field (Jaffe et al. 1999), while laboratory studies indicate that *E. pacifica* is sensitive to reduced pH conditions (Cooper et al. 2016a; b; McLaskey et al. 2016). *E. pacifica* also display a high degree of individual variability in many different physiological and life traits (Gomez-Gutierrez 2002; Feinberg et al. 2007; McLaskey et al. 2016), which may be an important strategy for success of their populations. This variability is important to consider when

investigating ocean change in these organisms but also contributes to the difficulty of studying them.

Physiological indices are useful tools to characterize the state of zooplankton *in situ*. They avoid many of the pitfalls of laboratory experiments and shipboard incubations by providing a measure of an organisms' physiological state based on their experience prior to being caught, and are less labor intensive than incubation methods, allowing greater sampling coverage. Two physiological rates of krill that can be estimated via enzyme activity proxies are respiration rate and growth rate. The Electron Transport System (ETS) is the physical basis for respiration; its activity provides a measure of maximum metabolic activity, and is used as a proxy for respiration rate (Harris et al. 2000). Aminoacyl-tRNA synthetases (AARS) are a group of enzymes that catalyze the first step of protein synthesis and AARS activity has been used as a proxy for growth rate in zooplankton (Yebra et al. 2017). These indices are usually employed to characterize differences across broad scales in populations or communities pooled prior to measurement. To our knowledge, this is the first time they have been applied to investigate variation in individuals within a population.

We investigated the effects of oxygen and pH on krill in the context of global ocean change using a coupled field-laboratory approach. Puget Sound is a large fjord-like estuary in Washington State, U.S.A. comprised of several interconnected basins separated by shallow sills. Its complex bathymetry and circulation patterns give rise to very different environmental characteristics within close proximity (Feely et al. 2010; Pelletier et al. 2018). In some areas, pH as low as 7.32 has been observed in deep waters (Feely et al. 2010), while low oxygen conditions regularly develop over the course of the summer, leading to seasonal hypoxia (Newton et al. 2002). We characterized ETS and AARS activities as *in situ* indicators of individual adult female

E. pacifica across an environmental gradient of oxygen and pH. In addition, we conducted shipboard respirometry experiments to establish a relationship between respiration rate and ETS activity in this species. Finally, we conducted two separate laboratory experiments to investigate the effect of acclimation to different pH and oxygen conditions on the two enzyme activities in adult female *E. pacifica.* By pairing shipboard observations and laboratory experiments, this study sought to leverage multiple methodologies to understand how a complex pelagic species is affected by changing ocean conditions.

5.3 METHODS

5.3.1 *Field observations*

Our sampling locations in Puget Sound were chosen to capture a broad range of environmental conditions, from Hood Canal, which has restricted circulation and develops low oxygen and pH conditions over the summer, through the well-mixed Main Basin, to South Sound, which maintains relatively high oxygen and pH levels.

We conducted two cruises, 23-30 June and 25 Aug-1 Sept 2018, aboard the R/V Clifford A. Barnes. We sampled water chemistry and zooplankton at six established stations: P11, P12, P15, P8, P28, and P38 (Figure 5.1). At each station, we collected physical and chemical data using a CTD profiler equipped with a pH sensor (SBE 18), oxygen sensor (SBE 43), and Niskin bottles, which were used to collect water at discrete depths for total inorganic carbon (C_T), total alkalinity (A_T), oxygen, and chlorophyll-a. Depths for discrete samples were chosen to characterize the shape of the vertical profile at each station, as determined by the CTD. Oxygen from discrete depths was measured by the modified Winkler titration method (Carpenter 1965). The CTD oxygen sensor calibration was confirmed with these Winkler titrations, so profile

readings were not modified. Water samples from the surface and depth of the fluorescence maximum were filtered on to Whatman GF/F filter, wrapped in foil, and frozen. In the laboratory 4-16 days after samples were filtered, chl-*a* was extracted in 90 % acetone with sonication, and measured via fluorescence on a Turner Designs fluorometer (TD700). The CTD fluorescence sensor calibration was confirmed with these samples.

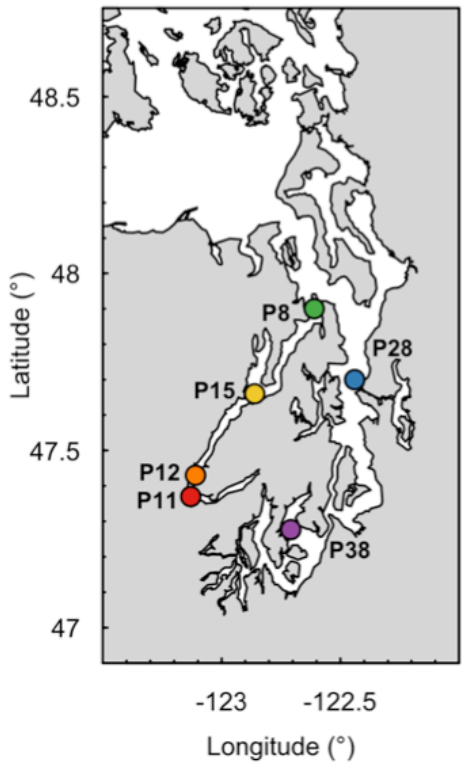

Figure 5.1. Sampling locations in Puget Sound, WA.

All carbonate chemistry samples were collected and analyzed according to Dickson et al., (2007). A_T was measured by open-cell potentiometric titration and C_T was measured by acidification and quantification using a CO_2 coulometer (UIC model CM5015) at the University of Washington's School of Oceanography. Certified Reference Materials were analyzed as an

independent verification of instrument calibrations (Dickson et al. 2007). We calculated full carbonate parameters from A_T and C_T using the R package *seacarb* and constants from Lueker et al. (2000) and the total pH scale. The pH profile for each CTD cast was corrected using an average offset to pH calculated from the discrete A_T and C_T samples.

5.3.2 *Zooplankton sampling*

We collected live adult female *E. pacifica* from surface waters (upper 50 m) at each sampling station during the nighttime using a 60-cm diameter Bongo frame equipped with black 335-µm mesh nets and non-filtering cod ends towed for <10 min at 2-3 kts. The contents of each cod end were diluted in coolers of seawater and immediately sorted to remove healthy euphausiids. Adult euphausiids were identified under a microscope and healthy adult females (obvious ovary) were separated for enzyme activity assays and respirometry experiments (described below). At all times, krill were kept chilled (10-14 ˚C) and were gently transferred using broad spoons to prevent damage. Krill preserved for enzyme analyses were measured for total length (from behind the eye to the end of the telson) at 6X using a calibrated eyepiece reticle then flash frozen individually in liquid nitrogen.

We characterized the nighttime density (# m^{-3}) and vertical distribution of adult euphausiids at stations P12 and P38 with oblique tows of a 5-net, 335-µm mesh, 0.25-m^2 Hydro-Bios Multinet sampler. We sampled the density of early life stages at the same stations with a 60-cm diameter, 200-µm mesh ring net lifted vertically from 10 m off the bottom to the surface during the dusk period (within an hour of sunset). Flowmeters were used to monitor the volume of water filtered for all collections and samples were preserved in a 5% buffered formalin and seawater solution. In the laboratory, euphausiids larger than 10 mm total length in the oblique tows were speciated, sexed, and measured. Samples that contained >30 large euphausiids were

split prior to analysis. The samples from vertical tows were quantitatively diluted to 4-10 times their settled volume and 2-3 subsamples were taken with a 1-mL Stempel pipette. In addition, one 10-mL Stempel pipette subsample was evaluated for any stages not found in the smaller subsamples. *E. pacifica* early life stages were identified and stages were classified as nauplius, calyptopis, or furcilia.

5.3.3 *Enzyme analyses*

Individual *E. pacifica* for enzyme analyses were stored at -70 ˚C until they were processed (max. 9 months). Samples were ground in a Teflon glass grinder at 2 ˚C for 90 sec in 20 mM Tris Buffer (pH 7.8) then centrifuged at 4000 rpm for 10 min at 2 ˚C. We then used aliquots of the supernatant to assay ETS, AARS, and protein content.

ETS was assayed using the method of Owens and King (1975), as modified by Gómez et al. (Gómez et al. 1996), and adapted for a 96-well plate. ETS activity was measured via INT (2-(*p*-iodophenyl)-3-(*p*-nitrophenyl)-5-phenyl tetrazolium chloride) reduction to formazan by the change in absorbance, measured kinetically at 490 nm with a spectrophotometer (SpectraMax M2, Molecular Devices). For each assay, 30 µL of sample supernatant were added to 90 µL substrate solution (1.7 mM NADH and 0.25 mM NADPH dissolved in phosphate buffer) and 30 µL INT (0.2 %, pH 8.5). Blank measurements were taken using phosphate buffer (0.1M phosphate buffer pH 8.5, 0.2 % v/v triton x-100, 0.15 % w/v polyvinylpyrrolidone, 75 µm MgSO4) without added substrates. Assays and blanks were measured in triplicate at 25˚C and corrected to *in situ* temperatures (depth integrated, described in Statistical Methods) using the Arrhenius equation with an activation energy of 15 kcal mol^{-1} (Packard et al. 1975) and potential respiration was calculated according to Packard and Christensen (2004).

AARS was measured following the method of Yebra and Hernadez-León (2004), modified by Yebra et al. (2011), and adapted for a 96-well plate (Yebra et al. 2017). Assays contained 60 µL of water, 40 µL of Pyrophosphate Reagent (Sigma P7275), and 50 µL of sample supernatant. Assays were measured in triplicate and for each kinetic run, triplicate background blanks were run containing 60 µL of water, 40 µL of Pyrophosphate Reagent (Sigma P7275), and 50 µL of 20 mM Tris Buffer (pH 7.8). Oxidation of NADH was monitored for 15 min at 25 ˚C by the change in absorbance, measured kinetically at 340 nm with a spectrophotometer (SpectraMax M2, Molecular Devices). AARS activities were calculated as in Herrera (Herrera 2014) and corrected to *in situ* temperatures with the Arrhenius equation using an activation energy of 8.57 kcal mol^{-1} (Yebra et al. 2005).

Protein content was determined according to the bicinchoninic acid (BCA) method (Smith et al. 1985) using a Pierce BCA Protein Assay Kit (Thermo Scientific). Sample supernatant was diluted to 1/16 concentration with Tris buffer to target a protein concentration of 25-250 mg mL^{-1}, within the linear range of this assay. Bovine serum albumin was used as a standard and dilutions were prepared using Tris buffer. Triplicate assays were run for each sample.

5.3.4 *Respiration rate experiments*

The relationship between respiration rate and ETS activity in *E. pacifica* was characterized by paired respirometry experiments conducted on cruises and enzyme analyses. Oxygen consumption of individual krill was measured by closed-cell respirometry in nominally 20-mL vials containing optical oxygen sensors (PSt7 PreSens) and a 12 mm magnetic stir bar separated from the animal by 200 µm mesh. Prior to experiment set up, all respirometry chambers were

assembled, filled with filtered seawater so that no air bubbles were present, and stored in a water bath inside an incubator at 12 ˚C.

Adult female *E. pacifica* approximately 15-19 mm in total length were placed in a tub of filtered seawater until the experiment was set up. To transfer krill to vials, they were again carefully caught with broad spoons then slid into the vial adding ~3 mL seawater with them; in each trial, a similar volume was also added to 2-3 control vials that did not contain krill.

Experiments lasted for 2 hours (oxygen drawn down 14-40 %) with measurements taken every 15 minutes. When measurements were taken, each vial was carefully lifted out of the water bath and placed directly onto a magnetic stir plate for ~15 sec while at least three measurements were taken with the oxygen meter and logger (PreSens Microx 4), and any unusual activity was noted. At the culmination of the experiment, each individual was removed, measured for total length, and frozen in liquid nitrogen. All handling of krill, experimental set up, and measurement were done under red light.

5.3.5 *Laboratory Experiments*

To help interpret field observations, laboratory experiments were conducted to determine the direction and relative effects of pH and oxygen acclimation on ETS and AARS activity in *E. pacifica*. In two separate experiments, we acclimated adult female *E. pacifica* to three different pH or oxygen levels for 10 days, after which we measured their respiration rate and froze them in liquid nitrogen for enzyme analyses.

Experimental organisms were collected on 23 July 2017 between 23:00-00:30 for the pH acclimation experiment and on 20 Sept 2017 between 20:00 and 21:15 for the oxygen acclimation experiment. Krill were collected in Possession Sound, WA using a 60-cm diameter Bongo frame equipped with black 335-µm mesh nets and non-filtering cod ends towed for <10

min. The contents of each cod end were immediately diluted in coolers of seawater and sorted to remove healthy euphausiids. For pH acclimation, euphausiids were stored in 1-4 L containers at a concentration of 5 ind L^{-1}, sealed with all air removed to eliminate splashing, and transported in coolers to the Friday Harbor Laboratories (FHL). Healthy adult females (obvious ovaries) were identified under the microscope and put in experimental chambers (described below) between 06:00-08:00 on 24 July 2017. For oxygen acclimation, krill were transported in coolers to the NOAA Mukilteo Research Station within an hour, and healthy adult female *E. pacifica* were identified under the microscope and put in experimental chambers.

5.3.6 *pH experiment*

Experimental acclimation to pH in the laboratory was conducted at the FHL Ocean Acidification Environmental Laboratory (OAEL), using a flow-through system with pH controlled through CO_2 bubbling that is described in O'Donnell et al. (2013). Target pH levels were 8.0, 7.5, and 7.2: three flow-through systems were used, one per pH treatment. Within each system, conditioned seawater was delivered to eight flow-through boxes that each contained two 500-mL mesh-sided experimental chambers with one individual krill per chamber, for a total of 16 individuals per system. Experimental systems were kept covered in black plastic to reduce light. Temperature and pH were monitored and logged every 10 min with a Honeywell Durafet III electrode and salinity was measured daily using a YSI EC300 conductivity meter. Carbonate chemistry conditions were verified with discrete total alkalinity (one per treatment) and spectrophotometric pH (three per treatment) samples taken on day 1, 7, and 10. Durafet pH measurements were also taken daily inside individual experimental chambers to characterize the variability among chambers within each treatment.

Krill were fed Shellfish Diet 1800 (Reed Mariculture) twice per day and newly hatched *Artemia salina* (San Francisco Bay Brand) nauplii once per day. On days 1-4 they were fed 40 uL of Shellfish Diet at each feeding and 375 *A. salina* nauplii per day; on days 5-10 they were fed 60 uL of Shellfish Diet at each feeding and 500 *A. salina* nauplii. On days 2, 5, and 8, each individual was carefully transferred to a clean jar and the presence of eggs or molts were recorded. On day 10, respiration rates of individual krill (9 in pH 7.2 treatment; 10 in pH 7.5 and 7.9 treatments) were measured via respirometry (same methods as shipboard respiration rate experiments described above), and each individual was measured for total length and then flash frozen in liquid nitrogen, transported on dry ice back to the University of Washington, and stored at -70 C until assayed for enzyme activities.

5.3.7 *Oxygen experiment*

Acclimation of krill to different oxygen levels in the laboratory was done at the NOAA Mukilteo Research Station in experimental systems with independent temperature, pH, and oxygen control. Natural seawater was filtered to one micron, exposed to UV light, and degassed prior to entering a mixing reservoir on each system, where nitrogen, oxygen, and carbon dioxide gasses were injected to maintain target conditions. Temperature, pH, and dissolved oxygen were monitored continuously using Omega thermistors, Honeywell Durafet III probes, and Vernier optical dissolved oxygen probes, respectively, and chemistry parameters were automatically maintained through a data-driven feedback system. From the mixing reservoir, treatment seawater was delivered to 10-12 experimental containers per system. Krill were kept one individual per container, and a mix of both 250- and 500-mL containers were used. Nine systems were used, with three at each target oxygen level of 3, 5, and 9 mg DO L^{-1}. Temperature, pH, and

oxygen concentration were recorded in each system every six seconds, but were binned into 10 minute averages prior to summarizing and visualizing.

Oxygen probes in each system were verified with periodic independent oxygen measurements (PreSens OXY-10 mini with PSt3 probes). Carbonate chemistry conditions were verified with A_T and C_T samples collected from one system of each treatment at the end of the experiment, and each Durafet probe was checked with duplicate samples from each system for spectrophotometric pH measurements using an Ocean Optics USB 230 2000+ Fiber Optic Spectrometer with SpectraSuite software and a 5mM solution of Sigma Aldrich m-cresol purple indicator dye.

Krill were fed Shellfish Diet 1800 (Reed Mariculture) twice per day (60 uL in 250-mL jars, 120 in 500-mL jars at each feeding) and newly hatched *A. salina* nauplii at a concentration of 1 nauplii mL^{-1} once per day. On days 2, 5, and 8, each individual was carefully transferred to a clean jar and the presence of eggs or molts were recorded. On day 10, respiration rates of 10 individuals per treatment were measured via respirometry (same methods as shipboard respiration rate experiments described above), and each individual was measured for total length and then flash frozen in liquid nitrogen and stored at -70 ˚C until assayed for enzyme activities.

5.3.8 *Statistical analyses*

We used linear mixed models (LMMs) to evaluate the influence of environmental drivers on ETS and AARS activity in the field. Adult krill migrate over the entire water column on diel cycles, so to characterize their environmental exposure, temperature, pH, and oxygen were integrated over the entire water column at each station using measurements from the CTD probes. pH was converted to $[H^+]$ to remove the effect of the log scale. Krill ascend to the surface at night to feed so we integrated chlorophyll *a* concentrations, calculated from CTD

fluorescence, in the upper 30 m of the water column at each station, a measure that has been used before to characterize the food environment of krill (Ross et al. 2000). We checked for correlation and multicollinearity among predictor variables with variance inflation factors (R package *car*) and predictor variables that were significantly correlated at the alpha=0.05 level were not considered in the same model. Interactions among predictor variables were not considered due to the limited sample size. All predictor variables were scaled to $(x-\mu)/SD$.

Protein-specific ETS (spETS) and AARS (spAARS) activities were log transformed to satisfy model assumptions and visual inspection of residual plots did not reveal any deviations from normality or homoscedasticity. For random effects, we considered Station (6 levels) and Station&Cruise (12 levels) separately, and their inclusion was based on likelihood ratio tests (method exactLRT in R package RLRsim) using alpha=0.01 to avoid over-parameterization. AICc and Akaike weight were calculated for each model and the set of best models included those with Akaike weight ≥0.05. Model-averaged parameter estimates were computed by the zero method, i.e., models that did not include a variable assumed a parameter estimate of zero for that variable (Burnham and Anderson 2002).

We conducted a scaled principal component analysis (PCA) of the environmental parameters included in the LMMs (method prcomp) and compared average enzyme activities with each principal component using linear regressions.

Differences in length distributions of adult *E. pacifica* between stations P12 and P38 were tested with non-parametric Kruskal-Wallis tests.

For each laboratory experiment, differences in spETS, spAARS activity, and respiration rate among treatments were tested with non-parametric Kruskal-Wallis and post-hoc Dunn's tests. All analyses were performed in R (V 3.5.2).

5.4 RESULTS

5.4.1 *Field observations*

We observed a range of environmental conditions among our six stations and between the two cruises (Figure 5.2). The stations in Hood Canal (P11, P12, P15) were characterized by the lowest sub-pycnocline pH and oxygen levels, as well as lower temperatures. There were also large phytoplankton blooms in Hood Canal during the cruises. Stations P8 and P28 were both well-mixed stations with weaker stratification and generally high pH and oxygen, while station P38 in South Sound had generally warmer waters, particularly in August, with high oxygen and pH. The lowest oxygen levels we observed were in the bottom waters at station P12 in August (Winkler titration 1.93 mg DO L^{-1}), but all other measurements were above hypoxic levels (S5.1 Table). The lowest pH values we observed were also at station P12 where bottom waters were pH 7.32 and pH 7.30 (calculated from A_T and C_T) in June and August, respectively (S5.2 Table).

Temperature, pH, and oxygen integrated over the entire water column displayed similar patterns, with the lowest average pH and oxygen concentrations at the Hood Canal stations, higher average temperatures at station P38. Chlorophyll *a* concentrations in the upper 30 m were generally higher at the Hood Canal stations but the greatest concentration was observed at P8 in June (Table 5.1), which had a moderately intense but vertically dispersed bloom.

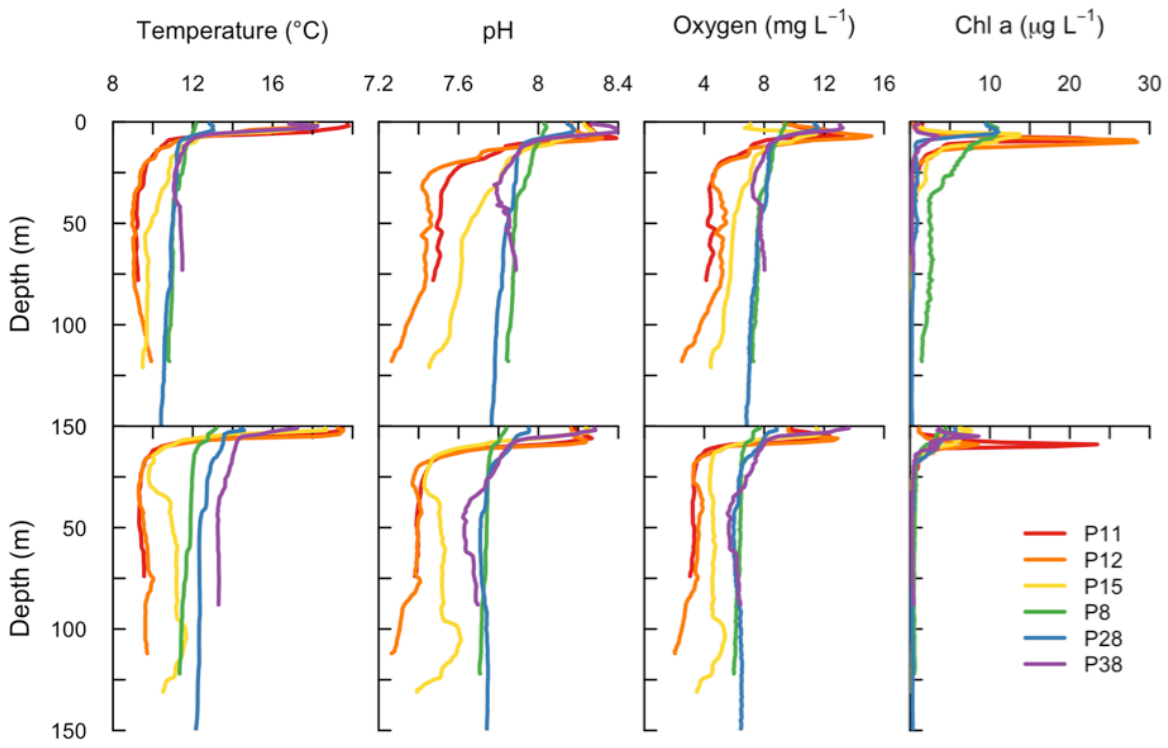

Figure 5.2. Seawater chemistry at sampling stations in Puget Sound. Depth profiles of temperature (˚C), pH, oxygen (mg L^{-1}), and chlorophyll *a* (µg L^{-1}) at each station during the June cruise (top row) and August cruise (bottom row). All parameters were measured continuously with a CTD; pH was corrected based on an offset from pH calculated from discrete A_T and C_T samples.

Table 5.1. Summary of environmental parameters used in linear models for each station.

Cruise	Station	Mean Temp	Mean pH	Mean O_2 (mg L^{-1})	Mean Chl 30 m (ug L^{-1})
June	P11	10.20	7.64	5.46	3.65
June	P12	9.78	7.50	5.41	5.08
June	P15	10.42	7.70	6.21	4.27
June	P8	11.14	7.90	7.81	7.37
June	P28	10.91	7.84	7.64	3.04
June	P38	11.76	7.90	8.18	0.97
August	P11	10.15	7.52	4.19	3.16
August	P12	10.18	7.45	3.89	1.91
August	P15	11.15	7.55	4.96	2.45
August	P8	11.79	7.74	6.36	1.68
August	P28	12.49	7.75	6.46	2.22
August	P38	13.62	7.73	6.71	1.90

5.4.2 *Linear mixed models*

Integrated oxygen and pH were significantly correlated with each other (Pearson's r= 0.97; $p<0.001$). Variance inflation factors were all less than 2.1 when oxygen and pH were not included together, indicating that multicollinearity was low. Therefore the final model set did not include any models that contained both oxygen and pH (Table 5.2; S5.3 Table).

A likelihood ratio test supported including either Station (simulated p= 0.002) or Station&Cruise (simulated p= 0.005) as random effects in the model for log(spETS). Because the random effect with the fewest levels, Station, had a greater estimated random effects variance (0.006 with 0.062 residual) than Station&Cruise (0.005 with 0.062 residual), we used Station as

a random effect. The set of best models contained three models: their weighted average parameter estimates were greatest for oxygen, followed by pH (Table 5.2).

Table 5.2. Top set of linear mixed models for log(spETS) using Station as a random effect. ΔAICc scores, Akaike weight (wi), and parameter estimates given for each model (when parameter estimate is missing, that factor was not included in the model); weight-averaged parameter estimates across the top model set.

Δ AICc	wi	Oxygen	[H+]	Temp	Chl
0	0.42				
0.2	0.38	0.076			
2.2	0.14		-0.075		
Weighted average		**0.029**	**-0.010**	**0**	**0**

The likelihood ratio test indicated that including Station&Cruise as a random effect improved the model fit for log(spAARS) (simulated $p<0.0001$; estimated variance 0.03 with 0.15 residual), but Station did not (simulated $p= 0.021$; estimated variance 0.007 with 0.17 residual). The top model set contained five models: their weighted average parameter estimate for hydrogen ion concentration was moderately higher than the others (Table 5.3 and S5.3 Table).

Table 5.3. Top set of linear mixed models for log(spAARS) using Station&Cruise as a random effect. ΔAICc scores, Akaike weight (wi), and parameter estimates given for each model (when parameter estimate is missing, that factor was not included in the model); weight-averaged parameter estimates across the top model set.

Δ AICc	**wi**	**Oxygen**	**$[H^+]$**	**Temp**	**Chl**
0	0.61				
3.2	0.12		-0.11		
4.0	0.08			0.09	
4.0	0.08	0.09			
5.0	0.05				-0.05
Weighted average		**0.007**	**-0.013**	**0.008**	**0.007**

5.4.3 *Principal component analysis*

The PCA on station environmental parameters explained 59 % of the total observed variance with principal component axis 1 (PC1), and 32 % with PC2. PC1 was primarily determined by DO, pH, and temperature, while PC2 was determined by Chl and temperature. The PCA biplot shows that sampling points separated by cruise and basin (Figure 5.3). spETS activity was correlated with PC2 (Figure 5.3; p=0.005, R2=0.51); spAARS activity was not correlated with any PC.

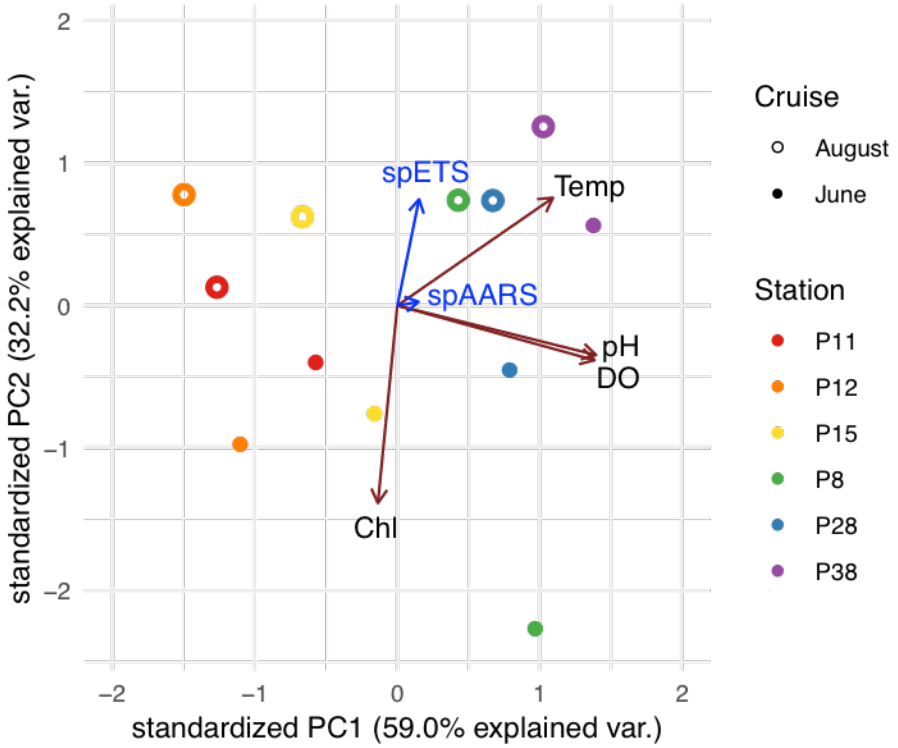

Figure 5.3. Principal component analysis (PCA) biplot of the environmental variables used in LMs with the correlations of spETS and spAARS activities with PC1 and PC2 plotted in blue. Color indicates station with warm colors (red, orange, yellow) showing stations located in Hood Canal. Filled points are stations sampled during June; open circles were sampled during August.

5.4.4 *Respirometry experiments*

Seven respirometry trials were run with 15-18 individuals each for a total of 93 paired respiration rate and ETS activity measurements (Figure 5.4). Respiration rate and ETS activity were significantly correlated with each other (Figure 5.4a; $p<0.0001$, $R^2=0.18$) but there was a stronger correlation between respiration rate and dry weight (Figure 5.4b; $p<0.0001$, $R^2=0.35$), as well as between ETS activity and dry weight ($p<0.0001$, $R^2=0.26$).

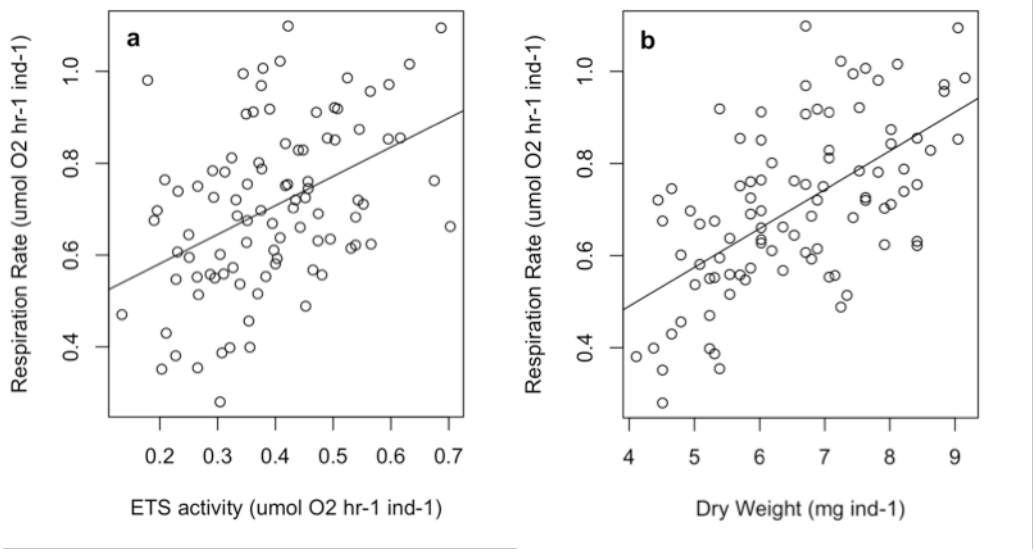

Figure 5.4. Respiration rate measured via respirometry correlates with (a) ETS activity ($p<0.0001$, $R^2=0.18$), and (b) dry weight ($p<0.0001$, $R^2=0.35$).

5.4.5 *Population distributions*

More adult krill were caught in August than in June at both P12 and P38. In both months, there was a higher density of adults at P12 in Hood Canal than at P38 in South Sound; however, there were higher densities of larval stages at P38 during both cruises (Figure 5.5). The length frequency distributions of adults were also significantly different, with larger adults found at P38 than P12 during both cruises (Figure 5.6; Kruskal-Wallis p=<0.0001 June, p<0.0001 August).

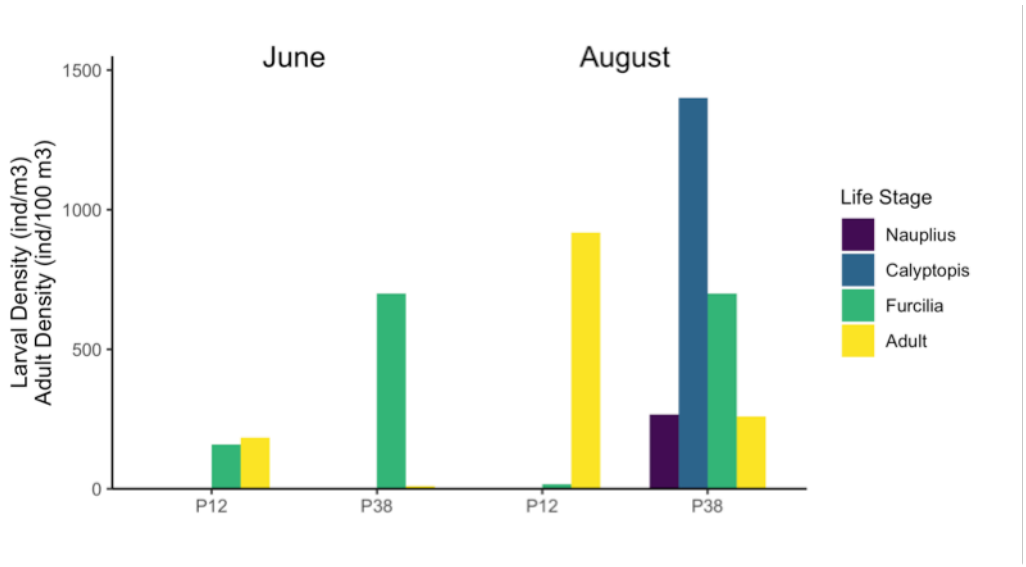

Figure 5.5. Densities of krill by life stage at stations P12 (Hood Canal) and P38 (South Sound) in June and August. Density of larval stages (nauplius, calyptopis, furcilia) in number of individuals m^{-3}; density of adults in individuals 100 m^{-3}.

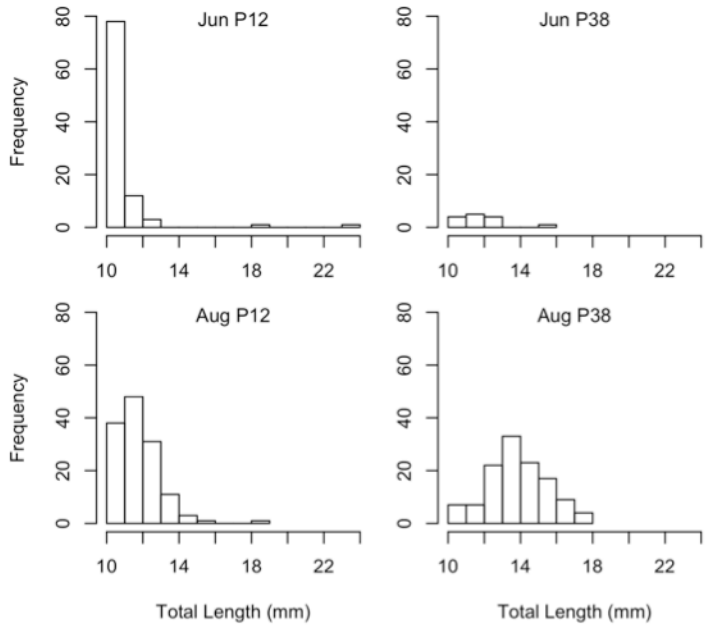

Figure 5.6. Length frequency distributions of adult (>10 mm total length) female *E. pacifica* caught during June and August at station P12 in Hood Canal and at station P38 in South Sound.

5.4.6 *pH Experiment*

Temperature over the pH experiment averaged 12.2 ˚C (Table 5.4; S5.1 Figure). Temperature did not record in the pH 7.5 target treatment but this treatment shared the same cooling system as the pH 7.9 target treatment so likely maintained a similar temperature range. Average salinity, measured daily, was 28.61 and ranged between 26.80-30.30 over the course of the experiment.

The Durafet probe recorded average pH of 7.97, 7.50, and 7.21 in the three treatments (Table 5.4; S5.1 Figure). Spectrophotometric pH analyses largely validated these results with the high treatment ranging from 7.87-7.98, moderate from 7.51-7.54, and low from 7.07-7.23 (Table 5.4). Total alkalinity varied slightly over the course of the experiment and was 2070, 1921, and 2005 μmol kg^{-1} on days 1, 7, and 10, respectively.

Table 5.4. Average temperature and pH recorded every ten minutes by the experimental control system, average salinity measured daily in the jars, and spectrophotometric pH (Spec pH) measurements taken from the jars on days 1, 7, and 10. Averages ± one standard deviation of (n) measurements given.

Target pH	Temperature (n=1960)	pH (n=1960)	Salinity measured in the jars	Spec pH Day 1	Spec pH Day 7	Spec pH Day 10
pH 7.9	12.27 ± 0.51	7.97 ± 0.04	28.53 ± 1.26 (21)	7.87 ± 0.02 (3)	7.98 ± 0.01 (3)	7.96 ± 0.02 (3)
pH 7.5		7.50 ± 0.02	28.43 ± 1.30 (21)	7.53 ± 0.01 (3)	7.51 ± 0.03 (3)	7.54 ± 0.01 (3)
pH 7.2	12.11 ± 0.58	7.21 ± 0.06	28.64 ± 1.35 (26)	7.07 ± 0.04 (3)	7.15 ± 0.00 (3)	7.23 ± 0.02 (3)

Overall survival of females for the ten-day experiment was 67 %. All individuals molted at least once during the experiment and of the 31 individuals that remained at the end, 20 had molted twice and one had molted three times. As a metric of how well females were feeding, eggs and nauplii were found in the jars throughout the experiment. Oxygen consumption

measured via respirometry at the end of the experiment was variable among individuals and differed between the two trials (Table 5.5). There were no significant differences among treatments in either trial (Kruskal-Wallis p=0.37 Trial 1, p=0.15 Trial 2).

Table 5.5. Respiration rate of *E. pacifica* after ten day acclimation period at different pH and oxygen levels. Two replicate trials were conducted in each experiment; average measurements (μmol O_2 hr^{-1} mg DW^{-1}) grouped by trial and treatment conditions ± standard deviation of (n) measurements.

Treatment Condition	**Trial 1**	**Trial 2**
pH 7.9	0.110 ± 0.023 (5)	0.124 ± 0.039 (5)
pH 7.5	0.126 ± 0.020 (5)	0.102 ± 0.019 (5)
pH 7.2	0.113 ± 0.028 (5)	0.129 ± 0.026 (4)
9 mg DO L^{-1}	0.085 ± 0.019 (5)	0.089 ± 0.018 (5)
5 mg DO L^{-1}	0.077 ± 0.024 (5)	0.079 ± 0.017 (5)
3 mg DO L^{-1}	0.073 ± 0.014 (5)	0.085 ± 0.020 (5)

There were no significant differences among treatments in spETS activity (Figure 5.7a; Kruskal-Walis p=0.10) or in spAARS activity (Figure 5.7b; Kruskal-Walis p=0.65).

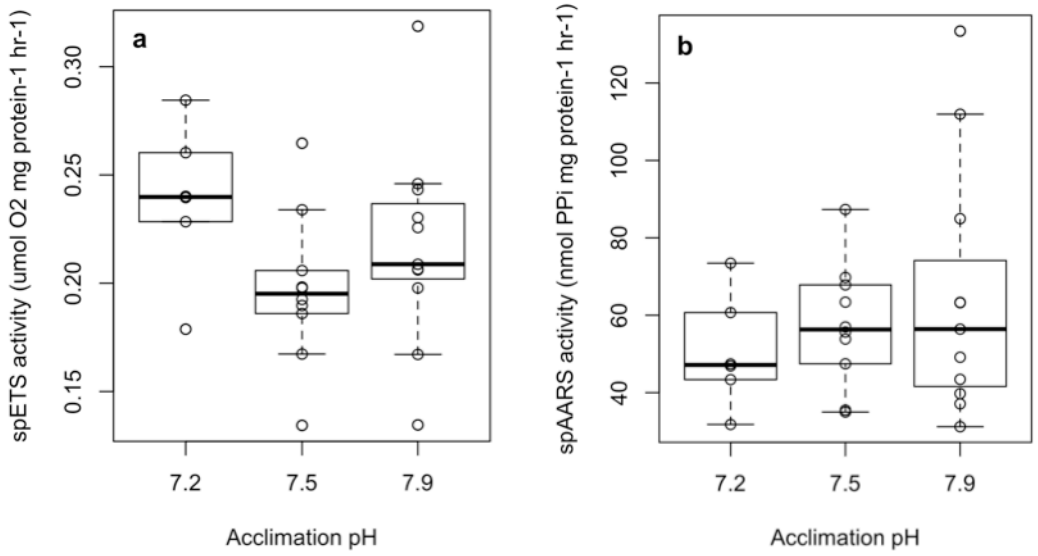

Figure 5.7. Protein specific ETS activity (a) and spAARS activity (b) in individual krill after acclimation to different pH treatments. Bold line indicates the median, box shows the interquartile range, dashed line shows the range of the data excluding outliers, and points represent each individual measurement.

5.4.7 *Oxygen Experiment*

Oxygen concentrations among the different treatments were distinct from each other over the experiment, with some variability among and within systems (Table 5.6; S5.1 Figure). Average oxygen conditions ranged from 3-3.6 mg L^{-1} in the three low concentration systems, 5-5.1 mg L^{-1} in the moderate systems, and 9.1-9.4 mg L^{-1} in the high oxygen systems (Table 5.6). The discrete independent oxygen measurements verified the continuously-measured oxygen probe values. Average temperatures among all nine systems ranged from 11.5-12.2 ˚C and pH ranged from 7.77-7.93. A_T measured in the three systems at the end of the experiment ranged from 2059-2071 µmol kg^{-1} and C_T ranged from 1982-2001 µmol kg^{-1} (S5.4 Table). Spectrophotometric pH

samples from each system showed that pH varied by 0.05 pH units among all nine and that Durafet measurements were within 0.01-0.05 pH units of the spectrophotometric samples.

Table 5.6. Average temperature, pH, and dissolved oxygen in each experimental system. Mean values ± one standard deviation of n measurements.

System	Temp (˚C)	pH	Oxygen (mg L^{-1})	n measurements
M2	12.2 ± 0.37	7.85 ± 0.01	3.57 ± 0.55	3290
M5	11.9 ± 0.04	7.84 ± 0.02	3.00 ± 0.1	3300
M9	11.5 ± 1.06	7.93 ± 0.67	3.06 ± 0.36	3300
M1	11.9 ± 0.52	7.82 ± 0.02	5.00 ± 0.16	3302
M4	11.9 ± 0.07	7.84 ± 0.01	5.00 ± 0.15	3290
M10	12.0 ± 0.07	7.81 ± 0.02	5.12 ± 0.41	3292
M3	11.9 ± 0.12	7.82 ± 0.02	9.43 ± 0.11	3300
M11	11.9 ± 0.4	7.82 ± 0.22	9.13 ± 0.17	3300
M12	12.0 ± 0.1	7.77 ± 0.03	9.11 ± 0.16	3136

Overall survival for the ten-day experiment was 57 %. Of the 55 individuals that remained at the end of 10 days, 87 % had molted at least once during the experiment and 11 % had molted twice; eggs were observed in a few of the jars. Respiration rates measured at the end of the experiment were variable among individuals and there were no significant differences among treatments in either trial (Table 5.5; Kruskal-Wallis Trial 1 $p=0.51$, Trial 2 $p=0.51$). There were also no significant differences in spETS activity (Figure 5.8a; Kruskal-Walis $p=0.86$) or spAARS activity (Figure 5.8b; Kruskal-Walis $p=0.22$).

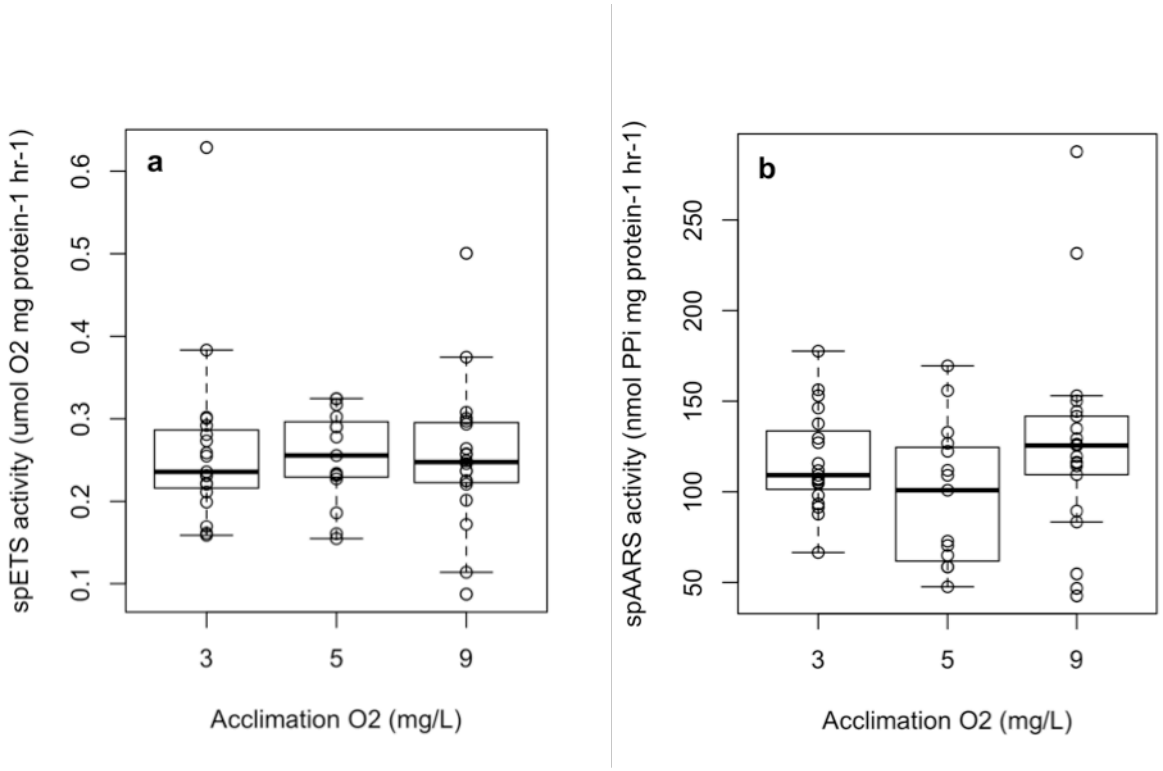

Figure 5.8. Protein specific ETS activity (a) and spAARS activity (b) in individual krill after acclimation to different oxygen treatments. Bold line indicates the median of the data, box shows the interquartile range, dashed line shows the range of the data excluding outliers, and points represent each individual measurement.

5.5 Discussion

In this study, we characterized the response of ETS and AARS activity in individual *E. pacifica* across a broad range of environmental conditions in the field, as well as after short-term acclimations to a range of pH and O_2 conditions in the laboratory. Both approaches revealed a picture of a generally tolerant species that is characterized by a high degree of inter-individual variability. In the field we detected an effect of DO on ETS activity, with lower metabolic activity in areas with low oxygen. That this correlation was not observed in the laboratory may

indicate the importance of additional factors encountered in the field that mediate their response to oxygen concentrations.

There are many potential processes that could influence responses in the field including additional unmeasured factors, interactions among drivers, and variable exposures. Krill in the laboratory were exposed to constant conditions but krill in the field have variable exposure as they undergo diel vertical migration, which could reduce or impose additional stress. Fluctuating conditions likely elicit different responses than static conditions but their effect is not well characterized. Living in fluctuating pH conditions is more energetically costly than static conditions for mussels (Mangan et al. 2017) and bivalves are more vulnerable to concurrent diurnal fluctuations in DO and pH than to fluctuating pH with constant DO (Gobler et al. 2017). All depth-averaged oxygen values at our sampled stations were above those used in the experiment but some stations had lower oxygen levels in the deeper waters that krill occupy during the day. *E. pacifica* is an oxyregulator down to 8.4 kPa (~3.6 mg L^{-1}) at 10 ˚C, below which it displays an increase in respiration rate until reaching its critical point of 6 kPa (~2.5 mg L^{-1}) (Tremblay and Abele 2016), conditions which were present at one of our stations. The *in situ* responses could also be due to interactive effects. Although AICc scores indicate that variations in oxygen best explain the data, the close correlation between pH and oxygen in field means that their effects cannot be decoupled, and the response observed *in situ* may be the result of multiple stressors.

Few ocean acidification studies have focused on krill, and none to date have examined multiple stressors. Although technically and logistically challenging, such studies should be a priority because of the strong correlation of stressors in the environment and other known interactions e.g., between temperature and hypoxia tolerance (Tremblay and Abele 2016). Our

results show that lower oxygen concentrations decrease the maximum respiratory capacity of krill (as estimated by ETS activity), which could limit their ability to cope with increased maintenance costs like acid-base regulation, or with low food conditions, e.g, during seasons with low primary productivity or while overwintering. Adult *E. superba* actively maintain their extracellular pH but exhibit declining haemolymph pH with increasing pCO_2, indicating that there is a limit to this energetically-costly process (Ericson et al. 2018). Similarly, growth of *E. pacifica* is reduced at elevated pCO_2, likely due to energy being diverted to other processes (Cooper et al. 2016a). We did not observe an effect of pH acclimation on respiration rate or ETS activity in the laboratory, but in another study, *E. pacifica* had reduced respiration rate after 21 days acclimation to 1200 μatm pCO_2 as compared to 400 μatm, which may indicate that it cannot completely regulate its acid-base balance (Cooper et al. 2016b). In the LMM analysis of ETS activity, temperature and chlorophyll were not important factors, but ETS activity was significantly correlated with PC2, which was primarily determined by chlorophyll a and temperature, and was the axis along which the two cruises separated. This indicates that although oxygen was the single main driver of ETS activity, there were also likely seasonal effects and important interactions**,** for example the relationship between temperature and oxygen shifted over the course of the season so that waters with similar oxygen levels were warmer in August than in June, reducing the physiological respite that low temperatures provide in deep waters where stressful low pH and DO conditions occur.

Variability among sampling locations had a greater influence on AARS activity of krill than the environmental parameters we investigated. This again suggests that other factors were important to their physiology, such as unconsidered parameters, e.g., food quality, or interactive effects. Interactions are likely to be important (as discussed above), however, detecting

interactions in the field typically requires a high degree of power, particularly with naturally co-varying drivers. Also, the timescales over which each of these enzyme activities respond to environmental conditions is not well defined. AARS activity in copepods changes within 48 hours (Holmborn et al. 2009), whereas ETS activity in mysids is stable over 74 hours of starvation (Herrera et al. 2011), while *E. distingenuda* populations show diel variability in ETS activity (Herrera et al. 2019). AARS activity may be a sensitive marker that responds to fine-scale variability that the field metrics we measured did not capture. AARS activity measured in individual krill incubated for 12-48 hrs under low-food conditions was different than individuals collected from the same location but not incubated (Chapter 6). The environmental parameter with the strongest support for determining AARS activity was pH, with lower activities associated with low pH habitats. Similarly, although there were no differences among pH treatments in the lab experiment, the highest AARS activities were only observed in the highest pH treatment. This is consistent with decreased growth rate of *E. pacifica* at elevated pCO_2 (Cooper et al. 2016a).

The size structure of adult krill differed between South Sound and Hood Canal, with generally larger individuals observed in South Sound. This could be the result of differential predation pressure, as Pacific hake, which prey heavily on krill, are absent from South Sound because of its shallow depth (T. Essington, pers. comm.). Comparisons across spatio-temporal gradients incorporate important factors that are not possible to replicate in the lab or easily measure in the field such as predation and food competition. The age structure of the populations also differed, with few larval stages found in Hood Canal in August. This could potentially be due to greater sensitivities of early life stages to low pH (McLaskey et al. 2016) and DO (Li et al. 2019). Despite this, a large krill population persists in Hood Canal that is unlikely to be sustained

by outside sources. This study represents a limited sampling, but the low density of larval stages in Hood Canal in August could indicate that that population is sustained by early reproduction before the most stressful conditions develop later in the season. During 2012-2013, monthly sampling in Hood Canal showed similar densities of eggs, nauplii, and adults over the whole season, but sharp declines in calyptopes and furcilia in September and October, which could indicate mortality of sensitive calyptopis stages when low pH and DO conditions occur. It is important to note that high productivity coupled with strong stratification and weak mixing is one of the primary factors driving low oxygen/pH environments in Hood Canal (Newton et al. 2002; Feely et al. 2010), but also may provide a nutritional environment favorable enough to mitigate these stressors.

We observed a high degree of inter-individual variability in enzyme activities in our experimental treatments and sampling locations. This is a common characteristic of krill, e.g., *E. pacifica* displays high variability in brood size and timing (Feinberg et al. 2007, 2013), hatching rate (McLaskey et al. 2016), development rate and the number of larval stages (Feinberg et al. 2006), and alternate hatching mechanisms (Gomez-Gutierrez 2002). This variability represents a methodological challenge to researchers, as it necessitates a high degree of replication to detect effects. However, this may also be an important strategy underlying the success of krill in highly dynamic environments. Mature *E. pacifica* are capable of producing 50-300 eggs every 5 days under good conditions and therefore can capitalize on favorable conditions for large recruitment events, allowing their populations to persist in highly variable environments. High variability in individual responses is likely due to both phenotypic plasticity and heritable variation. Plasticity allows organisms to persist under changing conditions in the short term, but genetic variation is required for populations to adapt to long-term changes that are outside their current tolerances.

The role of food in mediating krill responses is unknown and difficult to disentangle in the current study, but is likely to be very important (Pedersen et al. 2014a; Ramajo et al. 2016; Osma et al. 2016). The LMM results indicate that chlorophyll was not an important determinant of ETS or AARS activity; however, Puget Sound is a highly productive system and krill are strong swimmers capable of finding phytoplankton layers so may have been able to meet their nutritional needs at all locations. The condition of animals cultured in the laboratory is always an important consideration when extrapolating lab results to the field, and can both exacerbate and ameliorate environmental factors. Nutritional state is another characteristic that could have driven different responses in the laboratory experiments and field observations, but it is more likely that the diet provided in the lab would be lower quality, and we saw no evidence of diminished physiological state or increased sensitivity to stressors in the lab.

The paired respiration rate and ETS activity measurements of individuals displayed a positive correlation as expected, but each was more closely correlated with the dry weight of individual krill. Although ETS is the physical basis of respiration, over the small scale we investigated body size is a better predictor of respiration. We also observed a respiration rate to ETS activity ratio (R:ETS) that was greater than one. Recent studies have increased our understanding of the ETS activity assay and revealed processes that underestimate respiration in zooplankton measured via this method. *In vivo* respiration rate measurements include oxygen consumption that is stimulated when ADP is converted to ATP using the proton gradient set up by the ETS, which creates a positive feedback on ETS activity that is not present in the *in vitro* ETS assay when membranes are disrupted during homogenization (Osma et al. 2016). In addition, during beta-oxidation of fatty acids, oxygen is consumed by other enzymes such as oxidases. We intentionally focused our comparison on differences in ETS activities rather than

absolute values because our focus was on shifts in activity in response to environmental conditions.

5.6 CONCLUSIONS

Field observations across natural gradients of physical and chemical characteristics can be used to understand how species respond to environmental fluctuations and allow inferences about how organisms will respond to environmental changes in the future. Respiration rate, ETS activity, and AARS activity of *E. pacifica* were unaffected after ten-day acclimation to different pH and oxygen conditions in the laboratory, but enzyme activity measurements of individuals collected from the field reveal that krill physiology responds to the environmental conditions they experience. Oxygen levels primarily determined ETS activity of krill, with low oxygen environments acting to depress their metabolic capacity. AARS activity had a weak positive relationship with pH, but high variability among sampling sites, which may be a result of the short-term sensitivity of this enzyme activity to small environmental fluctuations. *E. pacifica* populations persist in areas of Puget Sound that seasonally develop conditions that are harmful to their early life stages, but we found differences in age structure that suggest these areas may be dependent on early recruitment before harmful conditions develop. Notably, we did not detect an effect of chlorophyll on enzyme activities, indicating that in this highly productive system, high food concentrations in all areas may also support the tolerance of this species to chemical stressors.

5.7 Acknowledgements

I wish to thank Lidia Yebra, Ted Packard, and May Gómez for guiding me in the enzyme activity methods and for very helpful conversations about the data; Captain Ken Pinnell, Brian Bare, and Jen Nomura of the R/V Clifford A. Barnes for field sampling; Amanda Winans, Katie Keil, Anna Boyar, Anita Montero, and Morgan Beste for help in the field; Shelly Carpenter and Rachel Lundeen for advice on running assays; Shallin Busch, Paul McElhany, Mike Maher, Shelly Trigg, and Lindsay Alma for assistance with the oxygen experiment; Thank you to the Patricia L. Dudley Endowment from FHL for making those experiments possible, Sasha Seroy and Becca Guenther for help during the pH experiment. This material is based upon work partially supported by the Washington Ocean Acidification Center and University of Washington School of Oceanography student ship time.

5.8 Supporting Information

S5.1 Table. Winkler's titrations for dissolved oxygen. Average ± standard deviation of (n) titrations.

Station	Depth (m)	Oxygen (mg L^{-1})
Jun P11	2	9.3 (1)
Jun P11	8	14.37 ± 0.3 (2)
Jun P11	11	7.32 ± 0.08 (2)
Jun P11	28	4.33 ± 0.05 (2)
Jun P11	78	3.5 ± 0.61 (2)
Jun P12	2	9.23 ± 0.09 (2)
Jun P12	10	10.93 ± 0 (2)
Jun P12	15	5.69 ± 0.09 (2)
Jun P12	26	4.39 ± 0.03 (2)
Jun P12	83	4.43 ± 0.05 (2)

Jun P12	118	2.46 ± 0 (2)
Jun P15	2	9.73 ± 0.07 (2)
Jun P15	6	9.23 ± 0.06 (2)
Jun P15	18	7.14 ± 0.02 (2)
Jun P15	56	5.43 ± 0.05 (3)
Jun P15	120	4.27 ± 0.02 (2)
Jun P8	2	8.75 ± 0.02 (3)
Jun P8	40	7.2 ± 0.02 (3)
Jun P8	118	6.76 ± 0.06 (3)
Jun P28	2	11 ± 0.08 (2)
Jun P28	4	10.08 ± 0.16 (2)
Jun P28	12	8.01 ± 0.02 (2)
Jun P28	80	6.95 ± 0.03 (2)
Jun P28	151	6.29 ± 0.13 (2)
Jun P38	2	11.6 ± 0.04 (2)
Jun P38	6	9.32 ± 0.07 (2)
Jun P38	9	7.95 ± 0.02 (2)
Jun P38	34	6.78 (1)
Jun P38	74	7.54 ± 0.08 (2)
Aug P11	2	9.59 ± 0.01 (2)
Aug P11	7	10.3 ± 0.18 (2)
Aug P11	10	5.53 ± 0.26 (2)
Aug P11	12	4.29 ± 0.01 (2)
Aug P11	74	2.86 ± 0.06 (2)
Aug P12	2	9.45 ± 0.2 (2)
Aug P12	9	12.38 ± 0.01 (2)
Aug P12	20	3.16 ± 0.17 (2)
Aug P12	77	3.19 ± 0.04 (2)
Aug P12	112	1.93 ± 0.07 (2)
Aug P15	4	8.48 ± 0.02 (2)
Aug P15	10	5.67 ± 0.05 (2)
Aug P15	16	4.15 ± 0 (2)

Aug P15	106	5.13 ± 0.04 (2)
Aug P15	131	3.35 ± 0 (2)
Aug P8	2	7.04 ± 0.33 (2)
Aug P8	12	6.07 ± 0.05 (2)
Aug P8	122	5.49 ± 0.07 (2)
Aug P28	2	8.43 ± 0.03 (2)
Aug P28	20	6.03 ± 0.01 (2)
Aug P28	58	5.57 ± 0.01 (2)
Aug P28	91	5.94 ± 0.11 (2)
Aug P28	161	6.04 ± 0.03 (2)
Aug P38	2	9.8 ± 0.08 (2)
Aug P38	7	7.34 ± 0.09 (2)
Aug P38	45	5.25 ± 0.02 (2)
Aug P38	63	5.62 ± 0.03 (2)
Aug P38	88	5.86 ± 0.03 (2)

S5.2 Table. Full carbonate chemistry data from discrete samples. Temperature, salinity, total inorganic carbon (C_T), and total alkalinity (A_T) were measured; pH and pCO_2 were calculated. Duplicate C_T analyses were run on some samples, in which case average ± standard deviation of two analyses are shown.

Station	Depth (m)	Temp (˚C)	Salinity	C_T (µmol kg^{-1})	A_T (µmol kg^{-1})	pH	pCO_2 (µatm)
Jun P11	2	19.73	20.82	1497 ± 4.63	1636	8.08	301
Jun P11	8	11.11	28.08	1717 ± 0.11	1993	8.37	154
Jun P11	11	10.58	28.30	1929 ± 0.06	2000	7.83	627
Jun P11	28	9.51	28.92	2028 ± 1.32	2023	7.55	1281
Jun P11	78	9.25	29.38	2061 ± 1.58	2033	7.46	1615
Jun P12	10	11.17	28.10	1850	1979	8.02	390
Jun P12	15	10.16	28.56	1989	1994	7.58	1158
Jun P12	83	9.17	29.42	2046 ± 4.36	2035	7.52	1398
Jun P12	118	9.92	29.90	2127 ± 0.20	2064	7.32	2306
Jun P15	2	17.94	23.03	1575 ± 4.47	1757	8.18	244
Jun P15	6	12.50	28.12	1834 ± 4.81	1975	8.03	377
Jun P15	18	11.19	28.84	1927 ± 0.30	2014	7.87	577
Jun P15	56	9.97	29.37	2002 ± 0.66	2034	7.68	938
Jun P15	120	9.49	29.69	2062 ± 3.99	2058	7.54	1354
Jun P8	2	12.10	28.94	1869 ± 0.72	2017	8.04	372
Jun P8	40	11.04	29.49	1951 ± 2.21	2047	7.89	562
Jun P8	118	10.81	29.66	1968 ± 1.07	2054	7.85	636
Jun P28	2	12.96	28.34	1790 ± 1.01	1991	8.17	259
Jun P28	12	11.28	28.74	1906	2003	7.90	529
Jun P28	151	10.41	29.55	1979 ± 0.06	2042	7.78	764
Jun P38	2	18.38	27.93	1735 ± 0.34	1983	8.20	241
Jun P38	4	12.92	28.19	1734 ± 0.81	1986	8.29	189
Jun P38	9	11.55	28.28	1896 ± 1.04	1995	7.92	510
Jun P38	34	11.09	28.37	1923 ± 1.13	2002	7.85	607
Jun P38	74	11.48	28.61	1912 ± 2.11	2007	7.89	559
Aug P11	6	11.24	28.61	1856	2010	8.08	338

Aug P11	10	10.41	28.78	2021	2009	7.51	1386
Aug P11	18	9.63	29.08	2062	2030	7.44	1645
Aug P11	74	9.55	29.51	2089 ± 0.08	2037	7.37	2007
Aug P12	8	11.88	28.50	1804	1999	8.17	261
Aug P12	20	9.52	29.08	2083	2018	7.33	2147
Aug P12	77	9.95	29.61	2077	2047	7.44	1704
Aug P12	112	9.72	29.72	2135	2063	7.30	2435
Aug P15	3	17.79	27.34	1684	1916	8.20	237
Aug P15	16	9.86	29.27	2040	2020	7.48	1485
Aug P15	30	9.99	29.40	2044 ± 0.28	2029	7.50	1446
Aug P15	106	11.66	30.06	2046	2068	7.61	1168
Aug P15	131	10.48	29.90	2100 ± 1.83	2069	7.42	1827
Aug P8	12	12.16	30.31	2013	2083	7.78	751
Aug P8	122	11.36	30.98	2068 ± 0.67	2117	7.70	961
Aug P28	2	14.16	29.50	1914	2039	7.94	494
Aug P28	20	12.83	29.69	1990	2049	7.74	824
Aug P28	44	12.44	29.90	1998	2060	7.75	810
Aug P28	161	12.16	30.36	2011	2075	7.75	850
Aug P38	2	15.88	28.98	1849	2027	8.06	358
Aug P38	9	14.12	29.26	1934	2029	7.85	618
Aug P38	63	13.30	29.46	1993 ± 1.76	2040	7.69	940
Aug P38	88	13.29	29.51	1981	2046	7.75	822

S5.3 Table. Full model set with AICc values, Δ AICc, and Akaike weights (wi)calculated for each model. In the models, fixed effects are shown without parentheses and random effects with parentheses. Top models, as determined by wi ≥ 0.05 are highlighted in bold.

lmer models of log(spETS)	**AICc**	**Δ AICc**	**wi**
Response= [H+] + temperature + chl + (Station) + intercept	48.3	16.3	0.00
Response= [H+] + temperature + (Station) + intercept	41.1	9.1	0.00
Response= [H+] + chl + (Station) + intercept	41.4	9.4	0.00
Response= [H+] + (Station) + intercept	**34.2**	**2.2**	**0.14**
Response= oxygen + temperature + chl + (Station) + intercept	46.8	14.8	0.00
Response= oxygen + temperature + (Station) + intercept	39.4	7.4	0.01
Response= oxygen + chl + (Station) + intercept	39.8	7.8	0.01
Response= oxygen + (Station) + intercept	**32.2**	**0**	**0.38**
Response= temperature + chl + (Station) + intercept	44.4	12.4	0.00
Response= chl + (Station) + intercept	37.6	5.6	0.03
Response= temperature + (Station) + intercept	38.9	6.9	0.01
Response= (Station) + intercept	**32.0**	**0.0**	**0.42**

lmer models of log(spAARS)	**AICc**	**Δ AICc**	**wi**
Response= [H+] + temperature + chl + (Station&Cruise) + intercept	188.2	12.9	0.00
Response= [H+] + temperature + (Station&Cruise) + intercept	183.5	8.2	0.01
Response= [H+] + chl + (Station&Cruise) + intercept	183.3	8.0	0.01
Response= [H+] + (Station&Cruise) + intercept	**178.5**	**3.2**	**0.12**
Response= oxygen + temperature + chl + (Station&Cruise) + intercept	188.8	13.6	0.00
Response= oxygen + temperature + (Station&Cruise) + intercept	184.0	8.7	0.01
Response= oxygen + chl + (Station&Cruise) + intercept	184.1	8.8	0.01
Response= oxygen + (Station&Cruise) + intercept	**179.3**	**4.0**	**0.08**
Response= temperature + chl + (Station&Cruise) + intercept	184.6	9.3	0.01
Response= chl + (Station&Cruise) + intercept	**180.3**	**5.0**	**0.05**
Response= temperature + (Station&Cruise) + intercept	**179.2**	**4.0**	**0.08**
Response= (Station&Cruise) + intercept	**175.3**	**0**	**0.61**

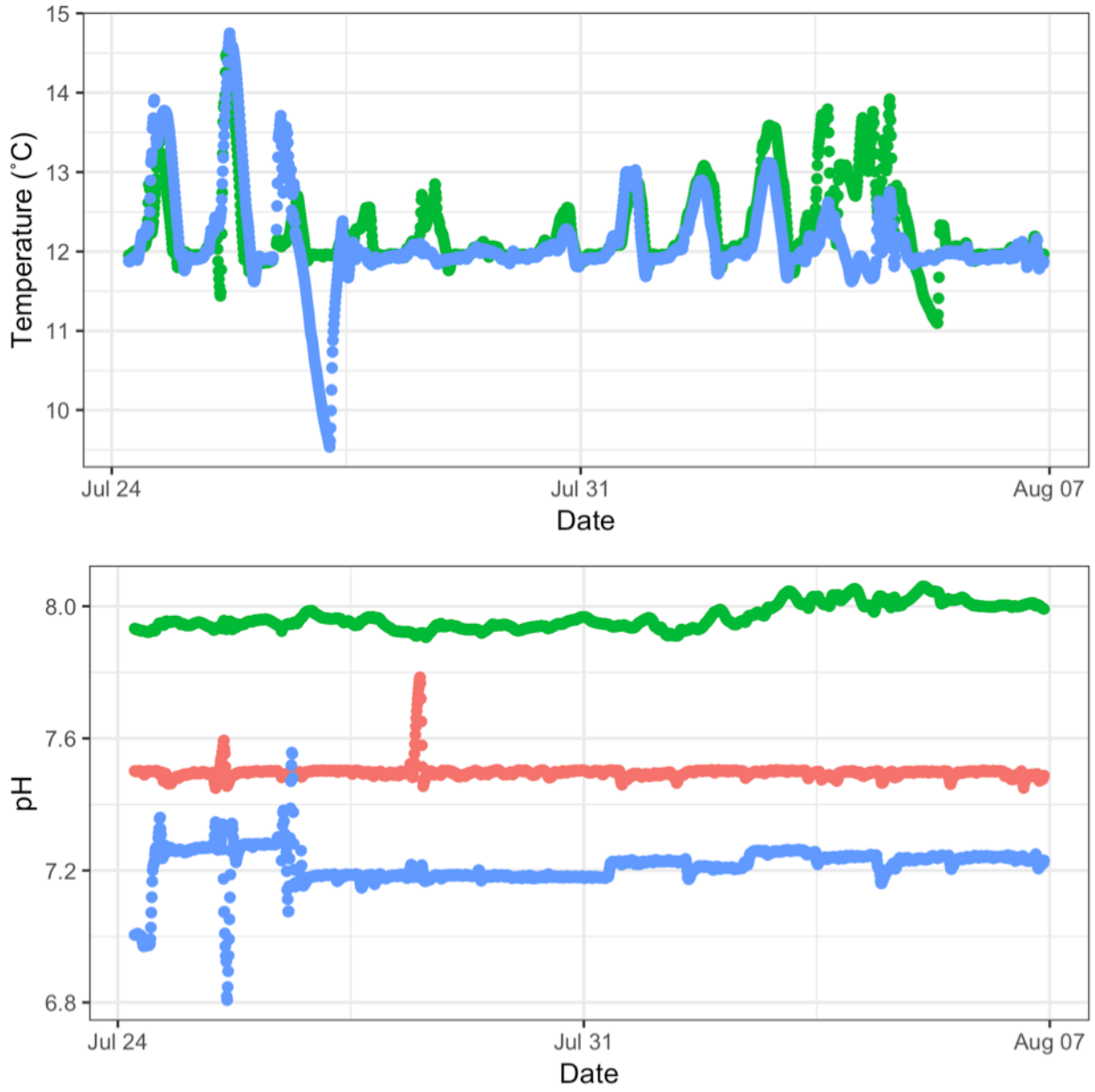

S5.1 Figure. Temperature (˚C) and pH recorded in experimental systems at the FHL OAEL. Temperature in the pH 7.5 target treatment did not record but this experimental system shared the same cooling system as the pH 7.9 target treatment so likely maintained a similar temperature range.

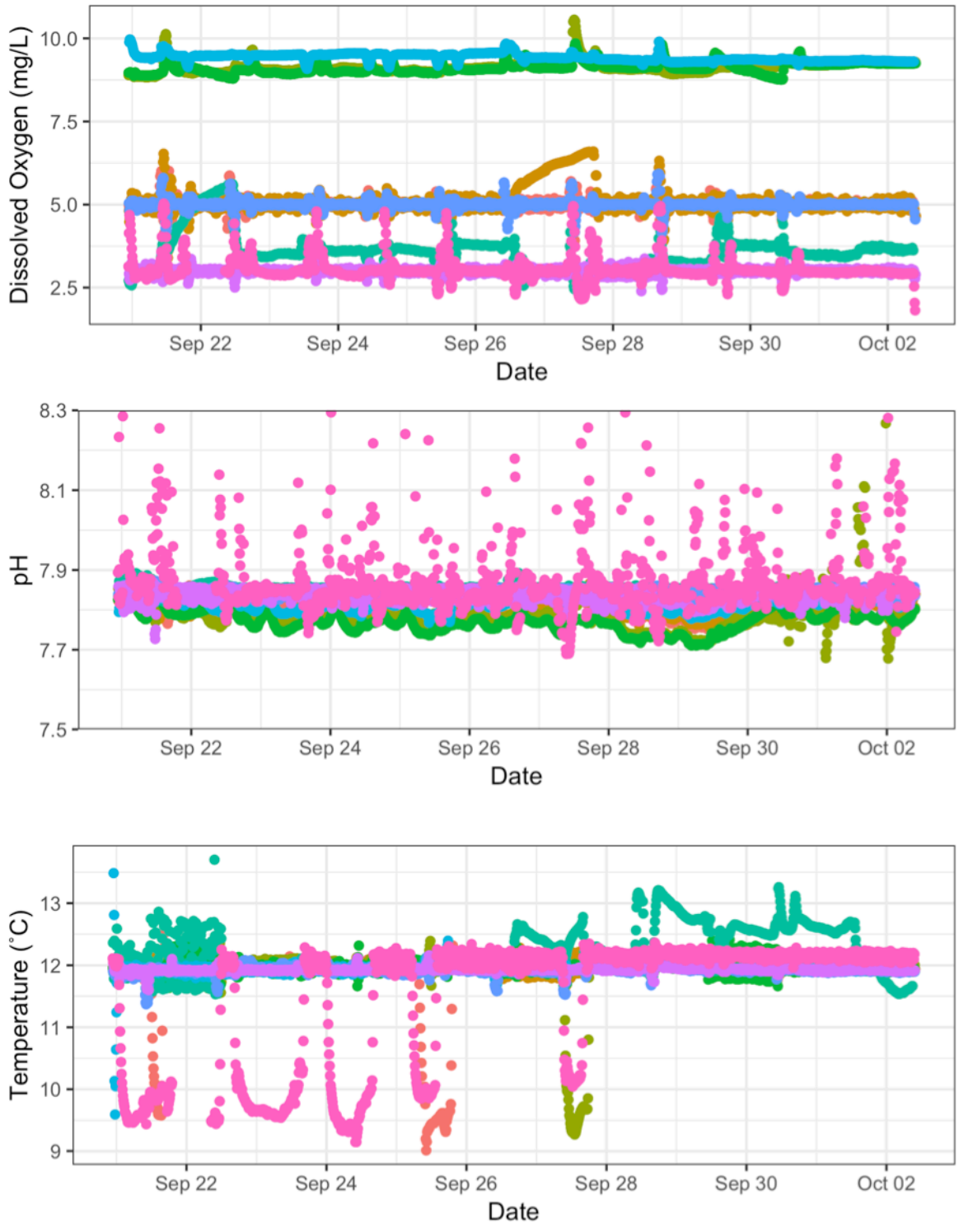

S5.2 Figure. Experimental conditions monitored and recorded for each system during the oxygen acclimation experiment.

S5.4 Table. Carbonate chemistry conditions at the end of the oxygen acclimation period. Total inorganic carbon (C_T) and total alkalinity (A_T) measured, pH calculated.

	C_T (µmol/kg)	A_T (µmol/kg)	pH (total)
MOAT 1	2001	2071	7.79
MOAT 12	2013	2061	7.71
MOAT 2	1982	2059	7.81

Chapter 6

INDIVIDUAL GROWTH RATE (IGR) AND AMINOACYL-tRNA SYNTHETASE (AARS) ACTIVITY AS INDIVIDUAL-BASED INDICATORS OF GROWTH RATE OF NORTH PACIFIC KRILL, *EUPHAUSIA PACIFICA*

6.1 ABSTRACT

We investigated aminoacyl-tRNA synthetases (AARS) activity and individual growth rate (IGR) as individual-based *in situ* indicators of growth in adult krill, *Euphausia pacifica*. Growth rates of field-collected krill were measured via the IGR method and individuals were subsequently preserved for AARS analysis to yield paired measurements. Our results show that conditions during the IGR incubation period influenced AARS activity in these individuals precluding a direct comparison but revealing the different timescales across which these two measures integrate. Importantly, they show that AARS activity changes over time scales of less than 48 hours and provides a measure of fine-scale influences, while IGR of krill is thought to integrate their environmental experience over several days. Each method would require many measurements to estimate population growth rates integrated over seasonal or generational time scales. As part of this project, we investigated how specific the AARS assay is to protein

synthesis by testing a modified protocol that includes an additional blank and found evidence that the current assay may be measuring other cellular processes in addition to its intended signal. Our results suggest that a new blank could be optimized to improve the specificity of the assay.

6.2 Introduction

The growth rate of zooplankton is an important parameter for understanding their role in marine ecosystems, e.g., in determining secondary production and biogeochemical cycling, but is extremely difficult to estimate *in situ*. Methods to estimate zooplankton growth rates include cohort analysis methods, incubation techniques, models, and biochemical indices of, e.g., nucleic acid, protein, and chitin production. Each of these methods includes assumptions and drawbacks, and may be useful in some situations but not others. Of these options, biochemical methods tend to be simple and quick, allowing for greater sampling, and therefore are becoming more widely used (Yebra et al. 2017).

Krill are key components of many marine ecosystems, linking primary production to higher trophic levels. Measurements of their growth rate are critical to estimating secondary production in these systems and for understanding their population dynamics and responses to environmental conditions. The individual growth rate (IGR) method was developed specifically for krill as an alternative to the natural cohort technique and estimates growth rate by incubating individuals for a few days then measuring the change between the length of any shed exoskeletons and the length of the animal after molting. Combined with a population estimate of molting rate, this growth increment can be used to estimate growth rate. This method assumes that the growth increment reflects *in situ* conditions experienced by the individual during the

inter-molt period, and that the number of individuals that molt is relatively constant over time and not affected by incubation conditions. The approach has been used in studies of the Antarctic krill, *Euphausia superba* (e.g., Ross et al. 2000; Nicol 2000; Atkinson et al. 2006; Tarling et al. 2006), and Pacific krill, *E. pacifica* (Pinchuk and Hopcroft 2007; Shaw et al. 2010).

Aminoacyl-tRNA synthetases (AARS) are a group of enzymes that catalyze the aminoacylation of tRNA, the first step of protein synthesis. Their activity is directly related to protein synthesis and has been developed as a proxy for growth rate in zooplankton (Yebra and Hernández-León 2004; Yebra et al. 2011, 2017). Methods for measuring the activity of individual AARS enzymes, or multiple AARS enzymes, often use radio-labeled ATP (Boniecki et al. 2008) or amino acids (Awai et al. 2015) to measure activity. These assays are complicated and require the addition of tRNA for each AARS enzyme, as well as its corresponding amino acid. A continuous colorimetric assay has also been developed to measure AARS activity based on the release of pyrophosphate (PPi) during the aminoacylation of tRNA (Chang et al. 1984). This initial method included the addition of substrates (tRNA and amino acids) providing a measure of the substrate-saturated AARS activity, Vmax. Since then a simplified version of the assay has been developed without the addition of substrates (Yebra and Hernández-León 2004). This method uses a commercial PPi detection kit (Sigma P7275) that contains a pyrophosphate-dependent fructose-6-phosphate kinase, which catalyzes the first of four coupled reactions that ultimately result in oxidation of β-Nicotinamide adenine dinucleotide (NADH). The oxidation of NADH is then measured as the change in absorbance at 340 nm over time, and is converted to the rate of PPi released.

AARS activity is a broadly applied method that has been measured in several crustacean zooplankton taxa and calibrated to other estimates of growth from length increments,

accumulation of protein, egg production rate, RNA:DNA, and empirical models. Seven of those studies either manipulated growth through wide variations in food concentration (Yebra and Hernández-León 2004; Yebra et al. 2006, 2011; Holmborn et al. 2009; Herrera et al. 2012) or in temperature (Yebra et al. 2011; Herrera et al. 2012). In addition, two studies examined differences among copepodite stages of *Calanus helgolandicus* (Yebra et al. 2005) and larval stages of *E. superba* (Guerra 2006), and two studies compared field collected copepods (Yebra et al. 2005, 2006). Each of these studies grouped individuals prior to measurement. To our knowledge, variation in growth rate of individuals within a population has not been investigated.

The commercial PPi detection kit used for the AARS assay contains a PPi-dependent enzyme to couple PPi to NADH oxidation, but there are other compounds present in a homogenized zooplankton sample that can also oxidize NADH. The commercial Pyrophosphate Reagent also includes a high concentration of NADH, which will cause a large change in redox state and likely stimulate many reactions in the sample homogenate. The current methodology uses a blank that contains the Pyrophosphate Reagent and water without the addition of sample homogenate, and therefore measures NADH oxidation due to the non-enzymatic background oxidation associated with the reagent mixture. Potential NADH oxidation due to other compounds in the zooplankton sample cannot be separated with the current methodology. In this study we sought to investigate AARS activity and IGR in adult *E. pacifica* and to explore methodological advantages and constraints of each. Another goal was to assess how specific the AARS assay is to protein synthesis by testing a modified protocol with an additional blank. This study was part of a larger project that performed AARS activity and NADH oxidation tests in more individuals than IGR; electron transport system (ETS) activity was also measured, providing additional physiological information.

6.3 METHODS

We conducted two cruises, 23-30 June and 25 Aug-1 Sept 2018, aboard the R/V Clifford A. Barnes in Puget Sound, WA. Live adult female *E. pacifica* were collected from surface waters (upper 50 m) at each of four sampling stations (Figure 6.1) during the nighttime using a 60-cm diameter Bongo frame equipped with black 335-µm mesh nets and non-filtering cod ends towed for less than 10 min. The contents of each cod end were diluted in coolers of seawater and immediately sorted for healthy euphausiids. Adult euphausiids were identified under a microscope and healthy adult females (obvious ovaries) were separated to use in IGR experiments at a subset of stations (Table 2). From three stations, additional individuals were also frozen on liquid nitrogen for enzymatic analyses (described below) immediately after sorting.

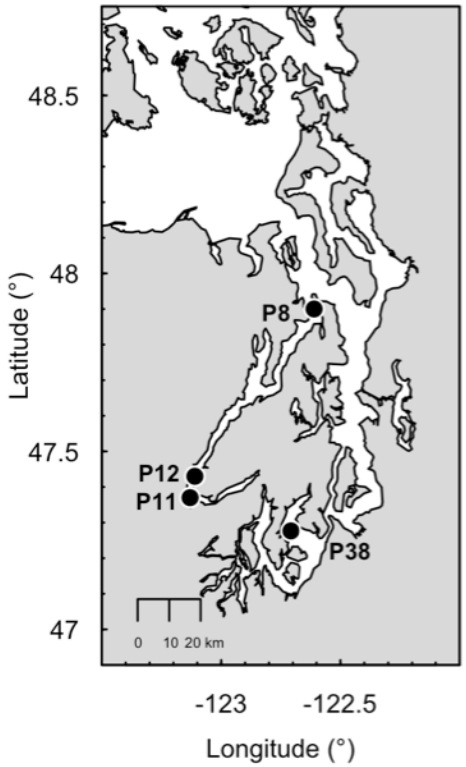

Figure 6.1. Sampling locations in Puget Sound, WA.

6.3.1 *Individual growth rate experiments*

In each individual growth rate (IGR) experiment, adult female *E. pacifica* were added one per 500-mL jar of 200-µm filtered seawater then incubated at 12 ˚C in the dark for 48 hours following the methods of Shaw et al. (2010). Five experiments were run with 30-50 individuals each. Jars were checked for molts under red light every 12 hours and individuals that had molted were removed along with their shed exoskeleton. We measured telson length of both the exoskeleton and the animal, as well as total length of the animal; all measurements were conducted by the same person at 6X magnification for total length and 25X for telson lengths using a calibrated eyepiece reticle. After measurement, krill were flash frozen individually in liquid nitrogen for enzyme analyses (described below) and stored at -70 ˚C until they were processed (max. 9 months).

Telson lengths were converted to total length (TL) according to the equation TL (mm) = 4.937*telson length (mm) – 0.4142 (Shaw et al. 2010). The growth increment was defined as the difference between the total length calculated from the animal's telson length and total length calculated from the exoskeleton telson length.

Inter-molt period (IMP) was calculated after Tarling et al. (2006) according to the equation IMP=N*d/m where N is the number alive at the end of the experiment plus the number that had molted and been removed during the experiment, m is the number that molted, and d is the length of the incubation in days.

Growth rate (g) of each individual was calculated by dividing the growth increment by the inter-molt period; weight specific growth rates were calculated by converting TL to dry weight then assuming carbon weight (W) was 40% of dry weight (Feinberg et al. 2007).

$g=\ln(W_{postmolt}/W_{premolt})/IMP$

6.3.2 *Enzyme Analyses*

Samples were removed from the -70 ˚C freezer, immediately ground with a Teflon glass grinder at 2 ˚C for 1.5 min in 20-mM Tris Buffer (pH 7.8), then centrifuged at 4000 rpm for 10 min at 2 ˚C. We then used aliquots of the supernatant to assay AARS activity, protein concentration, and electron transport system (ETS) activity. The AARS activity assay was run on a total of 112 individual adult female *E. pacifica*; an NADH blank (described below) was also run on each.

To test whether a significant component of the NADH oxidation detected by the AARS assay is due to redox reactions stimulated by the large change in redox state rather than by protein synthesis, we measured the activity in cell homogenate two ways: 1) with the addition of the full Pyrophosphate Reagent and 2) with the addition of 0.8 mM NADH in 45 mM Imidazole buffer (pH 7.4), a simplified version of the Pyrophosphate Reagent (Table 1), which hereafter we will call an NADH blank. Although a full mixture containing all the components of the Sigma® Pyrophosphate Reagent except the PPi-dependent PFK would be the ideal blank to test, it is a complex proprietary mixture, and we assume most of the stimulated NADH oxidation is due to the addition of NADH alone.

Table 6.1. Components and final concentrations of Sigma P7275 Pyrophosphate Reagent

Component	**Concentration**
Imidazole * HCl, pH 7.4	45 mM
Citrate	5 mM
EDTA	0.10 mM
Mg2+, Mn2+, Co2+	2 mM, 0.2 mM, 0.02 mM
β-NADH	0.8 mM
D-Fructose-6-phosphate	12 mM
Bovine Serum Albumin	5 mg/ml
Sugar Stabilizer	5 mg/ml
Fructose-6-phosphate kinase, pyrophosphate dependent	0.5 units/ml
Aldolase	7.5 units/ml

Glycerophosphate dehydrogenase	5 units/ml
Triosephosphate isomerase	50 units/ml

AARS was measured following the method of Yebra and Hernadez-León (2004), modified by Yebra et al. (2011), and adapted for a 96-well plate (Yebra et al. 2017). Assays contained 60 µL of water, 40 µL of Pyrophosphate Reagent (Sigma P7275), and were initiated with the addition of 50 µL of sample homogenate. NADH Blanks contained 60 µL of water, 40 µL of 0.8-mM NADH in 45-mM Imidazole buffer (pH 7.4), and 50 µL of sample supernatant. For each sample, assays and NADH Blanks were measured in triplicate. In addition, during each run two types of background blanks were run in triplicate: one containing 60 µL of water, 40 µL of Pyrophosphate Reagent (Sigma P7275), and 50 µL of 20mM Tris Buffer (pH 7.8); and one containing 60 µL of water, 40 µL of 0.8 mM NADH in 45mM Imidazole buffer (pH 7.4), and 50 µL of 20mM Tris Buffer (pH 7.8).

Oxidation of NADH was monitored for 15 min at 25 ˚C by the change in absorbance, measured kinetically at 340 nm with a spectrophotometer (SpectraMax M2, Molecular Devices). AARS activities were calculated as in Herrera et al. (2014) and corrected to *in situ* temperatures with the Arrhenius equation using an activation energy of 8.57 kcal mol^{-1} (Yebra et al. 2005). In addition, we calculated AARS activity using the NADH blank to correct the assay activity following a similar protocol as the ETS assay (Packard and Williams 1981). The Pyrophosphate Reagent background blank (60 µL of water, µL uL of Pyrophosphate Reagent, and 50 µL of Tris Buffer) is subtracted from the assay signal (60 µL of water, 40 µL of Pyrophosphate Reagent, 50 µL of sample homogenate) and the NADH background blank (60 µL of water, 40 µL of 0.8 mM NADH, and 50 µL of 20mM Tris Buffer) was subtracted from the NADH Blank (60 µL of water, 40 µL of 0.8 mM NADH, and 50 µL of sample homogenate). After the background blanks are

accounted for, the NADH blank is subtracted from the assay signal. (Assay - PPi reagent background) - (NADH Blank - NADH background)

Protein content was determined according to the bicinchoninic acid (BCA) method (Smith et al. 1985) using a Pierce BCA Protein Assay Kit (Thermo Scientific). Sample supernatant was diluted to 1/16 concentration with Tris buffer to target a protein concentration of 25-250 mg/mL, within the linear range of this assay. Bovine serum albumin was used as a standard and dilutions were prepared using Tris buffer. Triplicate assays were run for each sample.

As part of a larger project, electron transport system (ETS) activity was also measured in the individual krill. ETS was assayed using the method of Owens and King (1975), as modified by Gómez et al. (1996), and adapted for a 96-well plate. ETS activity was measured via INT (2-(*p*-iodophenyl)-3-(*p*-nitrophenyl)-5-phenyl tetrazolium chloride) reduction to formazan by the change in absorbance, measured kinetically at 490 nm with a spectrophotometer (SpectraMax M2, Molecular Devices). For each assay, 30 µL of sample supernatant were added to 90 µL substrate solution (1.7 mM NADH and 0.25 mM NADPH dissolved in phosphate buffer) and the reaction was initiated by adding 30 µL INT (0.2%, pH 8.5). Blank measurements were taken using phosphate buffer (0.1M phosphate buffer pH 8.5, 0.2% v/v triton x-100, 0.15% w/v polyvinylpyrrolidone, 75 µm $MgSO_4$) without added substrates. Assays and blanks were measured in triplicate at 24 ˚C and corrected to *in situ* temperatures using the Arrhenius equation with an activation energy of 15 kcal mol^{-1} (Packard et al. 1975) and potential respiration was calculated according to Packard and Christensen (2004).

6.3.3 *Statistical analyses*

IGR-estimated growth rate and spAARS activity among individual krill were investigated using linear models in R (V. 3.5.2) with the best model determined based on AICc using the package *AICcmodavg*. Dry weight and experiment were included as fixed effects, with experiment accounting for exposure to different environmental conditions prior to collection. We checked residual plots for homoscedasticity and normality; spAARS was log transformed to meet model assumptions. The relationship between weight specific growth rate and spAARS activity was tested with a linear model. Differences in spETS and log(spAARS) activity among individuals immediately frozen in the field and those used in IGR experiments were tested with linear mixed models (*lme4* package) that included the collection location as a random effect.

The change in absorbance in the NADH blank was log transformed and treated as the response variable; the raw change in absorbance in the assay was also log transformed and considered as fixed effect along with dry weight, ETS activity (uMol O_2 hr^{-1}), and collection station. One process that could potentially contribute to the oxidation of NADH separate from protein synthesis is the electron transport system; because ETS activity was also assayed on the same individual krill in this project, it was included in the analysis as an explanatory variable.

6.4 RESULTS

6.4.1 *IGR-estimated growth rate and AARS activity*

The five IGR experiments resulted in 47 individuals that molted and provided good measurements of both the molt and the post-molt individual (Table 2). Their sizes ranged from 13.7-21.5 mm total length with a mean of 16.8 mm. Inter-molt period (IMP) among the five experiments ranged from 4.8-14 days and averaged 8.6 days. Growth increments ranged from

-0.296 to 0.69 mm, growth rates from -0.038 to 0.134 mm d^{-1}, or -0.0035 to 0.0107 d^{-1}.

The best model describing weight specific growth rate measured via IGR only included dry weight as a predictor (S6.1 Table). Weight specific growth rate decreased with increasing dry weight (Figure 6.2; p=0.0005, R^2=0.22) and similar relationships were observed for growth rate (mm day^{-1}), weight specific growth rate (day^{-1}), and growth increment (mm), as compared to measured total length, calculated dry weight, and assayed protein concentration.

Table 6.2. Summary of IGR experiments. Cruise and station of krill collection, protein specific AARS activity (spAARS; nmol PPi mg $protein^{-1}$ hr^{-1}), weight specific growth rate (Wt sp GR; d^{-1}), Growth rate (mm d^{-1}), inter-molt period (IMP; d), number of individuals (n Ind.), total length (TL; mm), depth integrated temperature (Temp; ˚C) and pH at collection station. Average values and standard error given for individual-based measurements.

Cruise	Station	spAARS ±1 S.E.	Wt sp GR ±1 S.E.	Growth rate ±1 S.E.	IMP	n Ind.	TL ±1 S.E.	Temp (˚C)	pH
June	P12	103 ± 18	0.0048 ± 0.0012	0.064 ± 0.02	4.8	11	15.7 ± 0.8	9.8	7.50
August	P11	66 ± 11	0.0025 ± 0.0017	0.013 ± 0.01	14	6	16.2 ± 0.4	10.2	7.52
August	P12	61 ± 3	0.0047 ± 0.0008	0.041 ± 0.01	8.4	11	15.8 ± 0.3	10.2	7.45
August	P8	113 ± 17	0.0011 ± 0.0009	0.012 ± 0.01	8.2	9	18.7 ± 0.3	11.8	7.74
August	P38	65 ± 5	0.0029 ± 0.0007	0.03 ± 0.01	7.7	10	17.9 ± 0.3	13.6	7.73

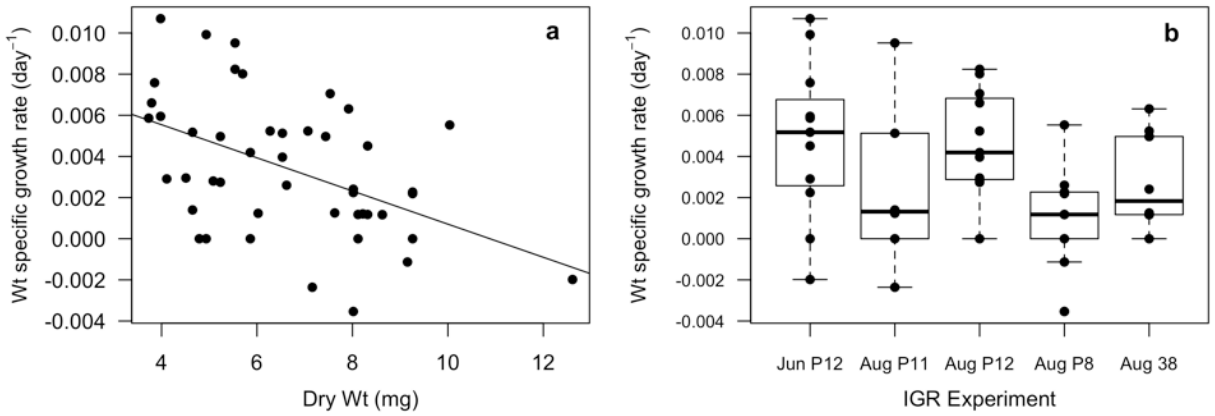

Figure 6.2. (a) Weight specific growth rate (d^{-1}) measured by the individual growth rate method compared to individual dry weight (mg) with solid line showing the model estimate. (b) Weight specific growth rate among the five different IGR experiments; bold line indicates the median, boxes show the inter-quartile range, dashed lines show the range of data excluding any outliers, and points show the measurements from each individual.

AARS assay activity in these 47 individuals ranged from 45 to 529 nmol PPi hr^{-1} and spAARS activity ranged from 35 to 228 nmol PPi mg $protein^{-1}$ hr^{-1}. The top two models had AICc scores within 2 of each other; the best included experiment and dry weight as predictor variables and the second included experiment only (S6.1 Table). Log transformed spAARS activity had weak but significant positive relationship with increasing dry weight (Figure 6.3; $p=0.015$, $R^2=0.11$). Weight specific growth rate (d^{-1}) was weakly negatively correlated with spAARS activity (Figure 6.4; $p=0.019$, $R^2=0.096$); growth increment was also negative correlated (Fig S6.1; $p=0.02$, $R^2=0.088$).

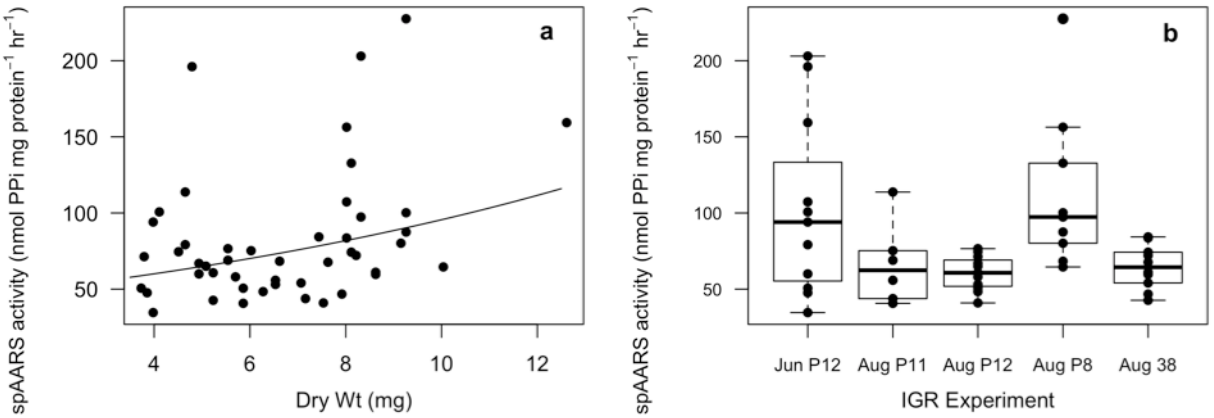

Figure 6.3. (a) spAARS (nmol PPi mg protein -1 hr-1) activity versus individual dry weight (mg) with solid line showing the log(spAARS) model estimate. (b) spAARS activity among the five different IGR experiments; bold line indicates the median, boxes show the inter-quartile range, dashed lines show the range of data excluding any outliers, and points show the measurements from each individual.

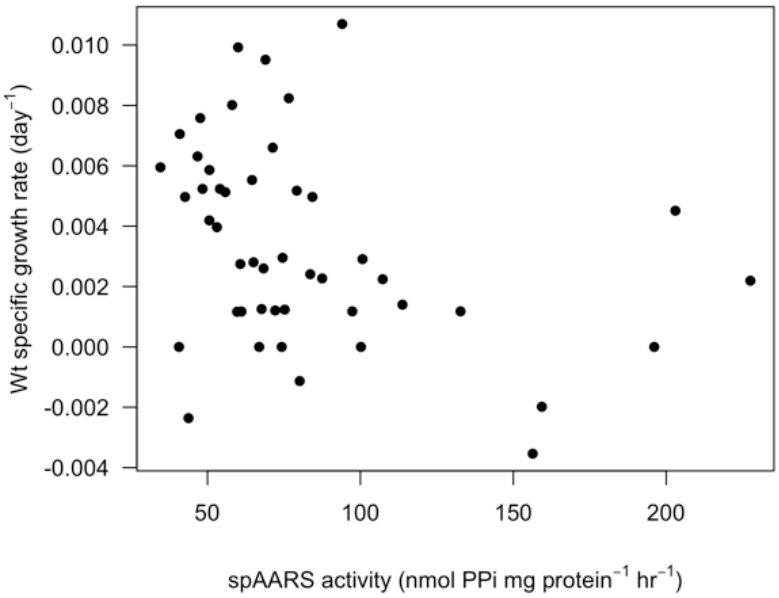

Figure 6.4. IGR-measured weight specific growth rate compared to spAARS measured in the same individuals; R^2=0.096, p=0.019.

The effect of IGR incubation period on spAARS and spETS was tested with data from the three stations where some individuals were immediately frozen in liquid nitrogen in addition to those used in IGR experiments. The best model for log(spAARS) included station as a random effect and incubation as a fixed effect (Figure 6.5a; S6.2 Table). Those that were frozen immediately generally had lower and less variable spAARS activity than those that were incubated in IGR experiments for 12-48 hours before preservation. The best model for spETS activity only included station as a random effect (Figure 6.5b; S6.2 Table).

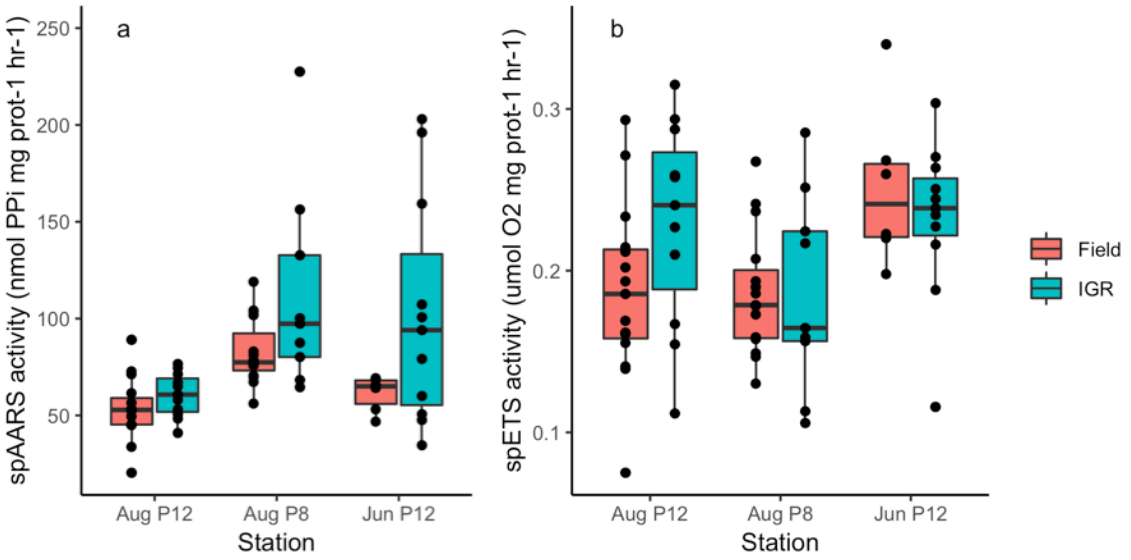

Figure 6.5. (a) Comparison of spAARS and (b) spETS activity in adult female *E. pacifica* that were flash frozen immediately after capture (red) and those that were collected from the same station but incubated for 12-48 hours in IGR experiments (teal). Boxes show the inter-quartile range, bold horizontal line indicates the median, vertical lines show the range of data excluding any outliers, and points show the measurements from each individual.

6.4.2 *NADH oxidation*

Significant changes in absorbance were observed in NADH blanks for all samples, and the change in absorbance in the blanks was closely correlated with the change in absorbance in the assay (Figure 6.6). The change in absorbance observed when only NADH was added ranged from 36-105 % (mean 62 %) of the change in absorbance when the Pyrophosphate Reagent was added. The best model of log(NADH blank slope) included only log(Assay slope) but did not include ETS activity, dry weight, or collection station (S6.3 Table).

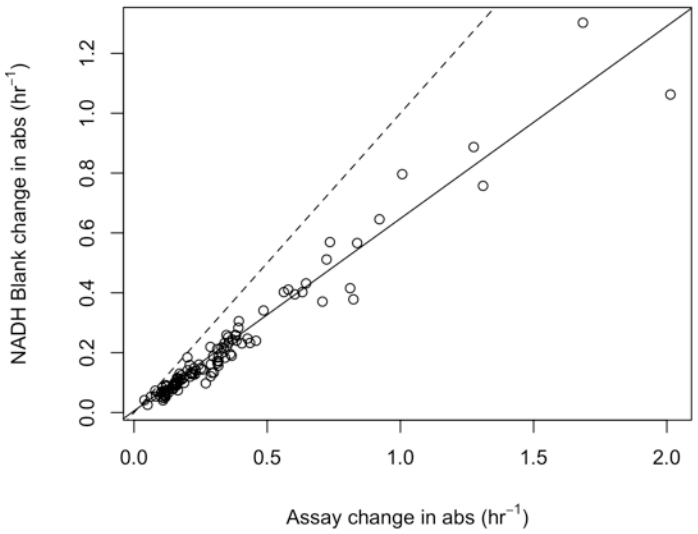

Figure 6.6. Change in absorbance measured in NADH blanks (hr^{-1}) versus change in absorbance measured in the full Assays (R^2=0.89). Regression line shown as solid line; 1:1 line is dashed.

When the assay activity was corrected using the additional NADH blank, log(spAARS) activity showed no relationship with dry weight (R^2=0.04, p=0.18) and weight specific growth rate showed no relationship with spAARS (Figure 6.7; R^2=0.02, p=0.41).

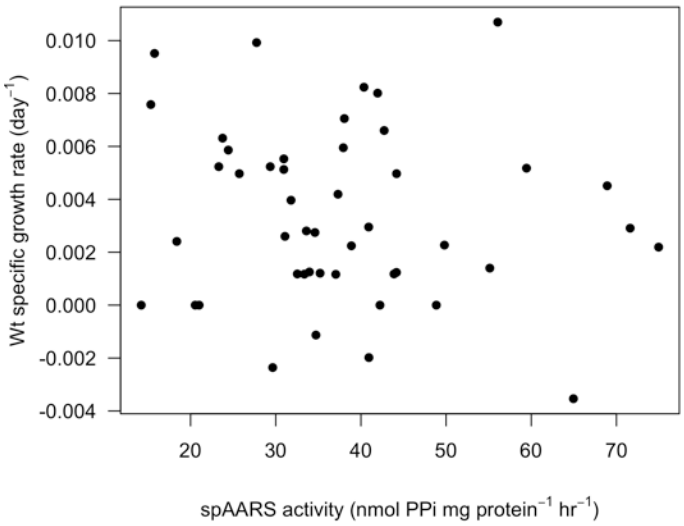

Figure 6.7. Protein specific AARS activity calculated using the NADH Blank to correct activity.

6.5 Discussion

Our data show differences in IGR and AARS activity in individual adult female *E. pacifica* that likely result from the different time scales over which these two measures integrate and the degree to which they were influenced by the incubation period. IGR was best explained by a negative relationship with individual dry weight, while spAARS activity was best explained by differences among experiments, with a weak positive relationship to dry weight. We also found evidence that the AARS assay may be measuring other processes in addition to the PPi-producing reactions that contribute to growth. Significant NADH oxidation was observed in all samples to which only NADH had been added, which suggests additional, unidentified processes contribute to the assay signal.

Crustaceans accommodate growth by molting, so changes in length occur as discrete events while changes in weight occur continuously. The IGR method measures these discrete length increases. A key assumption of the method is that the growth increment is set by

environmental conditions prior to when the krill are collected and is not influenced by conditions during the incubation period. However, a study of *E. superba* showed that percent growth increment decreases in individuals that molt later in the incubation period and that this decrease is more pronounced in individuals with larger growth increments (Tarling et al. 2006). AARS activity indexes protein synthesis, a continuous process linked to changes in weight. The rate at which AARS activity in zooplankton changes is not well constrained, but it responds to food concentrations within 48 hours in copepods (Holmborn et al. 2009), and *Euphausia distinguenda* displays diel variability in both AARS and ETS activity (Herrera et al. 2019). Our data indicate that AARS activity changes on time scales of less than 48 hours. Individuals that were immediately frozen in the field had lower and less variable spAARS activity than those that were used in IGR experiments, revealing the influence of the IGR incubation period on spAARS activity. Interestingly, ETS activity in the same individuals did not differ between capture and post-incubation, indicating that in our study ETS varied over longer timescales or was less sensitive to incubation conditions. It is likely that IGR and AARS do not index growth over identical periods prior to measurement, and further constraining the timescales over which they integrate would increase the utility and improve interpretation of these methods.

Low food conditions can lead to negative relationships between spAARS and growth rate, potentially due to degradation of proteins during starvation or ß-oxidation of fatty acids that also produces PPi that would be measured with the method (Herrera et al. 2012). Food conditions are rarely optimal in the field, and even in highly productive environments such as Puget Sound, they fluctuate widely on diel timescales for organisms that undergo diel vertical migration. Krill are successful in highly variable environments through a variety of strategies, including the capacity for negative growth rates, which are commonly observed (~25 % of the

time) in juvenile and adult krill year-round (Shaw et al. 2010). Potential dependence of AARS activity on sufficient (non-starvation) food conditions makes the timing of sampling an important consideration for field studies. These mature female krill were likely investing significant energy into reproductive output rather than somatic growth, which could potentially decouple spAARS and IGR. However, other studies have shown that spAARS activity and copepod egg production rates are correlated in the laboratory (Holmborn et al. 2009) and in the field (Yebra et al. 2005). The influence of food availability on the relationship between spAARS activity and growth rate deserves further investigation.

The IGR values we measured are within the usual range for individuals of this size (Shaw et al. 2010), although the range we observed is narrower, as would be expected from the narrow spatiotemporal coverage of our sampling. Size specific growth rate of animals generally decreases with increasing body size, as has been previously observed in *E. pacifica* (Shaw et al. 2010), and seen in our IGR data. The positive relationship between log(spAARS) and dry weight was significant; however, the small improvement (< 2) in AICc score when dry weight was included in the model in addition to experiment indicates that dry weight was not an important factor. AARS activity has not been published for this species before but our spAARS values are similar to those of *E. distinguenda* (Herrera et al. 2019) and mixed zooplankton communities (McKinnon et al. 2015).

We observed significant activity in all NADH blanks, indicating that the AARS assay may be measuring other processes in addition to PPi-producing reactions. ETS is one process likely contributing to NADH oxidation but its activity did not explain the observed variability in NADH blanks, so is not the only contributing process. Another potential contribution comes from microbial enzymes released from within or on the krill during homogenization. Although

outside the scope of this study, assay conditions, e.g., pH, could be optimized to minimize possible contribution of prokaryotic enzymes, and a new blank method could improve the specificity of this assay. It is also important to note that the AARS assay is not a traditional enzyme assay as it is meant to measure the activity of many different AARS enzymes at the same time, and it does not include the addition of saturating substrates to measure the maximum rate of reaction (Vmax). The close correlation between the signal detected in the NADH blank and the assay may be due to similar substrate limitation in the reactions affecting each. We are unable to evaluate whether correcting the assay activity with the NADH blank improves its relationship with growth rate using these data due to the differences between the two methods described above, but testing whether the use of this blank improves the relationship between AARS activity and growth rate of zooplankton is an important next step in the development of this method.

6.6 Conclusions

Measuring zooplankton growth rate and estimating secondary production remains a significant challenge in zooplankton ecology but it is advanced by a greater understanding of the advantages and limitations of different methods. IGR and AARS activity index krill responses over different timescales and care should be exercised when applying either as a metric of population growth rate when measured infrequently or among few individuals. AARS activity may track small short-term variations in environmental experience and therefore be useful as a high-resolution index of protein synthesis. Our results also indicate that the AARS assay is measuring processes in addition to protein synthesis that may be contributing additional variability, and provide a potential path to improve the specificity of the AARS assay.

6.7 Acknowledgements

I would like to thank Lidia Yebra, Ted Packard, and May Gómez for guiding me in the enzyme activity methods and for very helpful conversations about the data; Captain Ken Pinnell, Brian Bare, and Jen Nomura of the R/V Clifford A. Barnes for field sampling; Amanda Winans, Katie Keil, Anna Boyar, Anita Montero, and Morgan Beste for help in the field; and Shelly Carpenter and Rachel Lundeen for advice on running assays. This material is based upon work partially supported by the Washington Ocean Acidification Center and University of Washington School of Oceanography student ship time.

6.8 Supporting Information

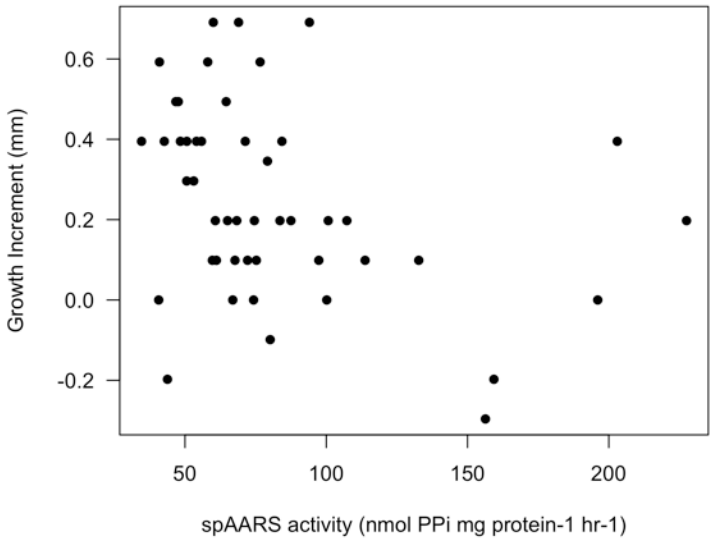

S6.1 Figure. Relationship between growth increment (mm) and spAARS activity. R^2=0.088; p=0.02.

S6.1 Table. AICc scores for linear models of and growth rate (d^{-1}) and spAARS activity after undergoing a log(y) transformation. Best models indicated in bold.

	Growth Rate	log(spAARS)
Response= intercept	-400.7	58.6
Response= exp + intercept	-400.8	**53.9**
Response= dry weight + intercept	**-411.2**	54.7
Response= dry weight + exp + intercept	-404.3	**52.1**

S6.2 Table. AICc scores for linear mixed models of investigating the effect of IGR incubation on spAARS activity after undergoing a log(y) transformation and spETS activity. In the models, fixed effects are shown without parentheses and random effects with parentheses. Best models indicated in bold.

	log(spAARS)	spETS
Response= (station) + intercept	70	**-185.5**
Response= DataType + (station) + intercept	**67.9**	-177.5
Response= DataType * (station) + intercept	67.9	-177.5

S6.3 Table. AICc scores for linear models of change in absorbance in the NADH Blank, after undergoing a log transform. In the models, fixed effects are shown without parentheses and random effects with parentheses. Best model indicated in bold.

	log(NADH Blank)
Response= station + intercept	211.2
Response= dry weight + intercept	158.6
Response= log(Assay) + intercept	**-63.5**
Response= ETS + intercept	180.0
Response= dry weight + log(Assay) + intercept	-62.0
Response= log(Assay) + ETS + intercept	-61.4

Response= dry weight + ETS + intercept	154.7
Response= log(Assay) + station + intercept	-54.2
Response= dry weight + station + intercept	145.8
Response= log(Assay) + ETS + station + intercept	-51.8
Response= dry weight + ETS + station + intercept	144.4
Response= dry weight + log(Assay) + ETS + intercept	-59.8
Response= dry weight + log(Assay) + station + intercept	-52.0
Response= dry weight + log(Assay) + ETS + station + intercept	-49.6

Chapter 7

CONCLUSIONS

This dissertation investigates how OA and co-occurring stressors will affect copepods and krill by combining laboratory experiments and field observations. A key outcome of this research has been to establish a baseline understanding of how *E. pacifica* is influenced by seawater pH in Puget Sound, but it has also presented avenues for further investigation. In this final chapter, I explore important topics that are outside the scope of this dissertation, present open questions that still remain, and identify key research priorities for the future.

7.1 SPATIAL AND SEASONAL CO-OCCURRENCE OF DRIVERS

In the coastal ocean, DO and pH are strongly correlated, so understanding their interactive effects on krill should be a research priority. Temperature is often positively correlated with DO and pH (Reum et al. 2014), which could provide a thermal refuge when krill are exposed to the lowest pH and DO conditions. Low temperatures may increase their ability to tolerate those stressors, but as ocean temperatures continue to rise such refuges will become rarer. A 15-year time-series of krill collected at the shelf break of the Newport Hydrographic Line shows that krill biomass is reduced during warm periods (Peterson et al. 2017). In addition, during the anomalous warm event in 2014-2016, the Blob, *E. pacifica* were nearly absent when Blob

conditions were present on the shelf, and the lengths of adults in 2015 were smaller than during any other year (Peterson et al. 2017).

Temperature, pH, and DO are also seasonally correlated, and there are a few intriguing but sparse examples which indicate that early recruitment may be important for sustaining krill populations in Hood Canal, before low pH and low DO conditions develop. In Chapter 5, I observed fewer furcilia late in the summer in Hood Canal but many more calyptopis and furcilia late in the summer in South Sound. Monthly sampling over the summer and early fall during 2012 and 2013 in Hood Canal show calyptopis and furcilia declined dramatically over the course of the season, while eggs, nauplii, juveniles, and adults remained at consistent densities (Li et al. 2019). This decline is unusual among studies from other locations and may relate to greater sensitivity of furcilia I-III to DO levels. In addition, early life stages are sensitive to low pH (Chapter 2), which would also contribute to this phenomenon.

Regular zooplankton sampling within Puget Sound has increased dramatically in the past five years and these data can be used to test the hypothesis that krill populations in Hood Canal rely on early spawning for successful recruitment. Dr. Keister's lab manages a zooplankton time-series collected throughout Puget Sound that includes stage-specific krill densities. In an initial evaluation, I pooled all samples collected between 2014-2017 by basin and calculated survival rates among stages by multiplying the total counts of each stage by the stage duration (days). There was a slightly lower survival rate from Nauplius 2 to Calyptopis 2 in Southern Hood Canal (3.5%) than in South Sound (4.1%), but otherwise there were few obvious differences. This dataset deserves a more thorough analysis that accounts for temporal and spatial structuring, especially as the length of the time-series increases and a broader range of environmental conditions are characterized. Determining the importance of early recruitment in Hood Canal is a

research priority because shifts in the timing of seasonal hypoxia and low pH conditions could compress the window of favorable conditions for krill larvae throughout broad areas of their range.

7.2 OTHER SOURCES OF MORTALITY

The effects of ocean circulation on individual zooplankton can be an important control on their populations. Krill are relatively strong swimmers, but the currents still move them, and retention is critical to their distribution in the CCE (Santora et al. 2011, 2018). In Puget Sound, the restricted circulation in Hood Canal during stratified conditions may help retain krill, leading to large populations despite the presence of stressful pH and DO conditions. In addition to advective losses, we know little about natural mortality rates, making it difficult to determine how important pH-driven larval mortality is to the overall population persistence. Different size structure of populations in Hood Canal and South Sound suggest that predation pressure may be an important factor, but is difficult to evaluate. Models are powerful tools to investigate these questions but will require field observations to test their assumptions.

7.3 ROLE OF FOOD SOURCES

Nutritional status is an important factor in mediating organism responses to OA and other stressors, but the exact mechanisms involved are not clearly understood (Thomsen et al. 2013, Pedersen et al. 2014). CO_2-induced changes to the nutritional quality of phytoplankton are largely species or strain specific, and depend on other growth conditions. This suggests that bottom-up effects of OA will most likely come from broad shifts in phytoplankton community composition or production. Puget Sound is a highly productive system and krill living in Hood

Canal benefit from abundant prey resources, which may support their tolerance to low pH and DO conditions. In the CCE, upwelling centers are sites of low pH and DO waters, but also intense primary productivity, which provides a food source to potentially mitigate such stressful conditions. Broad changes in food supply should be considered when extrapolating current responses to the future, or extending results from Puget Sound to more food-limited systems.

7.4 Adapting to ocean change

High inter-individual variability in traits appears to be a key attribute of krill, and variable responses among individuals to environmental drivers indicate the potential for adaptation. This variability is likely due to both phenotypic plasticity and heritable variation, but we currently can't distinguish the two influences due to limited genetic information and difficulty breeding this species in captivity. Plasticity allows organisms to persist under changing conditions in the short term, but genetic variation is required for populations to adapt to long-term changes that are outside their current tolerances. Characterizing the evolutionary potential of zooplankton in response to ocean change is still a major challenge, but will be important in determining their likelihood of persistence.

7.5 Biological monitoring and ocean change research

Connecting ocean change research and biological monitoring requires the development of biomarkers that can be applied in a variety of circumstances. ETS activity of krill responded to DO and pH conditions from the collection sites in ways we expected, showing that it can be a useful biological indicator. Although individual responses were a focus of this dissertation, population samples would likely show a clearer environmental signal by averaging inter-

individual variability. AARS activity of krill appears to track short-term physiological changes, and therefore provides a measure of fine-scale influences. It could be useful to answer questions on event timescales, e.g., responses to an upwelling episode or changes over a diel cycle. High sampling intensity would likely be required to establish relationships between AARS activity and broad environmental characteristics as I attempted to do in Chapter 5.

In Chapter 6, I found evidence that the AARS assay measures activity due to other processes in addition to protein synthesis, which is its intended target. The new blank for the assay that I proposed could not be tested with these data because AARS activity was heavily influenced by the incubation period for the Individual Growth Rate (IGR) method, preventing a direct comparison of AARS activity and IGR. Comparing AARS activity measured using the new blank to other methods for estimating growth rate is an important next step to establish whether it improves the relationship between AARS activity and growth rate. In addition, this assay is not measured with the addition of saturating substrates, and therefore does not yield a measure of maximum enzyme activity, Vmax. This is an unusual way of measuring enzyme activity, because measurements will be influenced by both enzyme and substrate concentrations, both of which are unknown. A second important area of inquiry for this method is determining what effect this has on the interpretation of AARS activity measurements in zooplankton.

Zooplankton will be affected by OA and other ocean changes through a variety of pathways, with many potential interactions that could lead to unexpected outcomes. Therefore, *in situ* biological monitoring is an important strategy to minimize the risk of ecological surprises that could disrupt socio-economic systems, for example those that depend on capture fisheries. The ocean change research community can provide guidance regarding how biological monitoring should be structured, while biological monitoring can generate data to test

hypotheses and refine our understanding of responses to ocean change. The field will be best advanced by an iterative relationship between these two approaches.

BIBLIOGRAPHY

Aguilera, V. M., C. A. Vargas, M. A. Lardies, and M. J. Poupin. 2016. Adaptive variability to low-pH river discharges in Acartia tonsa and stress responses to high pCO2 conditions. Mar. Ecol. **37**: 215–226.

Aguilera, V. M., C. A. Vargas, P. H. Manríquez, J. M. Navarro, and C. Duarte. 2013. Low-pH Freshwater Discharges Drive Spatial and Temporal Variations in Life History Traits of Neritic Copepod Acartia tonsa. Estuaries and Coasts **36**: 1084–1092.

Anderson, T. R., and D. W. Pond. 2000. Stoichiometric theory extended to micronutrients: Comparison of the roles of essential fatty acids, carbon, and nitrogen in the nutrition of marine copepods. Limnol. Oceanogr. **45**: 1162–1167.

Atkinson, A., R. S. Shreeve, A. G. Hirst, P. Rothery, G. A. Tarling, D. W. Pond, R. E. Korb, E. J. Murphy, and J. L. Watkins. 2006. Natural growth rates in Antarctic krill (Euphausia superba): II. Predictive models based on food, temperature, body length, sex, and maturity stage. Limnol. Oceanogr. **51**: 973–987.

Awai, T., N. Ichihashi, and T. Yomo. 2015. Activities of 20 aminoacyl-tRNA synthetases expressed in a reconstituted translation system in Escherichia coli. Biochem. Biophys. Reports **3**: 140–143.

Bailey, A., P. Thor, H. I. Browman, D. M. Fields, J. Runge, A. Vermont, R. Bjelland, C. Thompson, S. Shema, C. M. F. Durif, and H. Hop. 2016. Early life stages of the Arctic copepod Calanus glacialis are unaffected by increased seawater pCO2. ICES J. Mar. Sci. **74**: 996–1004.

Bates, D., M. Maechler, Bolker B, and S. Walker. 2014. lme4: Linear mixed-effects models using Eigen and S4.

Bell, M. V., J. R. Dick, T. R. Anderson, and D. W. Pond. 2007. Application of liposome and stable isotope tracer techniques to study polyunsaturated fatty acid biosynthesis in marine zooplankton. J. Plankton Res. **29**: 417–422.

Bermúdez, J. R., U. Riebesell, A. Larsen, and M. Winder. 2016a. Ocean acidification reduces transfer of essential biomolecules in a natural plankton community. Sci. Rep. **6**: 27749.

Bermúdez, R., Y. Feng, M. Y. Roleda, A. O. Tatters, D. A. Hutchins, T. Larsen, P. W. Boyd, C. L. Hurd, U. Riebesell, and M. Winder. 2015. Long-term conditioning to elevated pCO_2 and warming influences the fatty and amino acid composition of the diatom Cylindrotheca fusiformis. PLoS One **10**: e0123945.

Bermúdez, R., M. Winder, A. Stuhr, A.-K. Almén, J. Engström-Öst, and U. Riebesell. 2016b. Effect of ocean acidification on the structure and fatty acid composition of a natural plankton community in the Baltic Sea. Biogeosciences **13**: 6625–6635.

Bi, R., C. Arndt, and U. Sommer. 2014. Linking elements to biochemicals: effects of nutrient supply ratios and growth rates on fatty acid composition of phytoplankton species. J. Phycol. **50**: 117–130.

Bi, R., S. Ismar, U. Sommer, and M. Zhao. 2017. Environmental dependence of the correlations between stoichiometric and fatty acid-based indicators of phytoplankton nutritional quality. Limnol. Oceanogr. **62**: 334–347.

Bligh, E. G., and W. J. Dyer. 1959. A rapid method of total lipid extraction and purification. Can. J. Biochem. Physiol. **37**: 911–917.

Boniecki, M. T., M. T. Vu, A. K. Betha, and S. A. Martinis. 2008. CP1-dependent partitioning of pretransfer and posttransfer editing in leucyl-tRNA synthetase. Proc. Natl. Acad. Sci. **105**: 19223–19228.

Breitburg, D., L. A. Levin, A. Oschlies, M. Grégoire, F. P. Chavez, D. J. Conley, V. Garçon, D. Gilbert, D. Gutiérrez, K. Isensee, G. S. Jacinto, K. E. Limburg, I. Montes, S. W. A. Naqvi, G. C. Pitcher, N. N. Rabalais, M. R. Roman, K. A. Rose, B. A. Seibel, M. Telszewski, M. Yasuhara, and J. Zhang. 2018. Declining oxygen in the global ocean and coastal waters. Science **359**: eaam7240.

Brett, M. T., and D. Müller-Navarra. 1997. The role of highly unsaturated fatty acids in aquatic foodweb processes. Freshw. Biol. **38**: 483–499.

Brinton, E. 1962. The distribution of Pacific euphausiids, *In* Bulletin of the Scripps Institution of Oceanography, La Jolla, California. University of California Press.

Burnham, K. P., and D. R. Anderson. 2002. Model selection and multimodel inference: a practical information-theoretic approach, 2nd ed. Springer.

Byrne, M. 2011. Impact of ocean warming and ocean acidification on marine invertebrate life history stages: vulnerabilities and potential for persistence in a changing ocean, p. 1–42. *In* Oceanography and Marine Biology: An Annual Review.

Caldeira, K., and M. E. Wickett. 2003. Anthropogenic carbon and ocean pH. Nature **425**: 365.

Carpenter, J. H. 1965. The Chesapeake Bay Institute technique for the Winkler dissolved oxygen method. Limnol. Oceanogr. **10**: 141–143.

Chan, F., J. A. Barth, C. A. Blanchette, R. H. Byrne, F. Chavez, O. Cheriton, R. A. Feely, G. Friederich, B. Gaylord, T. Gouhier, S. Hacker, T. Hill, G. Hofmann, M. A. McManus, B. A. Menge, K. J. Nielsen, A. Russell, E. Sanford, J. Sevadjian, and L. Washburn. 2017. Persistent spatial structuring of coastal ocean acidification in the California Current System. Sci. Rep. **7**: 2526.

Chan, F., J. A. Barth, J. Lubchenco, A. Kirincich, H. Weeks, W. T. Peterson, and B. A. Menge.

2008. Emergence of Anoxia in the California Current Large Marine Ecosystem. Science **319**: 920–920.

Chang, G., F. Pan, Y. Lin, and H. Wang. 1984. Continuous spectrophotometric assay for aminoacyl-tRNA synthetases. Anal. Biochem. **142**: 369–372.

Cooper, H. L., D. C. Potts, and A. Paytan. 2016a. Effects of elevated pCO_2 on the survival, growth, and moulting of the Pacific krill species, *Euphausia pacifica*. ICES J. Mar. Sci. J. **74**: fsw021.

Cooper, H. L., D. C. Potts, and A. Paytan. 2016b. Metabolic responses of the North Pacific krill, Euphausia pacifica, to short- and long-term pCO2 exposure. Mar. Biol. **163**: 207.

Cornwall, C. E., and C. L. Hurd. 2016. Experimental design in ocean acidification research: problems and solutions. ICES J. Mar. Sci. fsv118.

Cowles, T. J., R. J. Olson, and S. W. Chisholm. 1988. Food selection by copepods: discrimination on the basis of food quality. Mar. Biol. **100**: 41–49.

Cripps, G., K. J. Flynn, and P. K. Lindeque. 2016. Ocean acidification affects the phyto-zoo plankton trophic transfer efficiency. PLoS One **11**: e0151739.

Cripps, G., P. Lindeque, and K. Flynn. 2014a. Parental exposure to elevated pCO_2 influences the reproductive success of copepods. J. Plankton Res. **36**: 1165–1174.

Cripps, G., P. Lindeque, and K. J. Flynn. 2014b. Have we been underestimating the effects of ocean acidification in zooplankton? Glob. Chang. Biol. **20**: 3377–85.

Dickson, A. G. 1990. Standard potential of the reaction: AgCl(s) + 1/2 H_2(g) = Ag(s) + HCl(aq), and the standard acidity constant of the ion HSO_4^- in synthetic sea water from 273.15 to 318.15 K. J. Chem. Thermodyn. **22**: 113–127.

Dickson, A. G., and F. J. Millero. 1987. A comparison of the equilibrium constants for the

dissociation of carbonic acid in seawater media. Deep Sea Res. Part A, Oceanogr. Res. Pap. **34**: 1733–1743.

Dickson, A. G., C. L. Sabine, and J. R. Christian. 2007. Guide to best practices for ocean CO_2 measurements. PICES Spec. Publ. **3**: 191.

Doney, S. C., M. Ruckelshaus, J. E. Duffy, J. P. Barry, F. Chan, C. A. English, H. M. Galindo, J. M. Grebmeier, A. B. Hollowed, N. Knowlton, J. Polovina, N. N. Rabalais, W. J. Sydeman, and L. D. Talley. 2012. Climate change impacts on marine ecosystems. Ann. Rev. Mar. Sci. **4**: 11–37.

Dupont, S., B. Lundve, and M. Thorndyke. 2010a. Near future ocean acidification increases growth rate of the lecithotrophic larvae and juveniles of the sea star Crossaster papposus. J. Exp. Zool. B. Mol. Dev. Evol. **314**: 382–9.

Dupont, S., O. Ortega-Martínez, and M. Thorndyke. 2010b. Impact of near-future ocean acidification on echinoderms. Ecotoxicology **19**: 449–62.

Durbin, E. G., and A. G. Durbin. 1992. Effects of temperature and food abundance on grazing and short-term weight change in the marine copepod Acartia hudsonica. Limnol. Oceanogr. **37**: 361–378.

Durbin, E. G., A. G. Durbin, and R. G. Campbell. 1992. Body size and egg production in the marine copepod Acartia hudsonica during a winter-spring diatom bloom in Narragansett Bay. Limnol. Ocean. **37**: 342–360.

Ekau, W., H. Auel, H.-O. Pörtner, and D. Gilbert. 2010. Impacts of hypoxia on the structure and processes in pelagic communities (zooplankton, macro-invertebrates and fish). Biogeosciences **7**: 1669–1699.

Engström-Öst, J., T. Holmborn, A. Brutemark, H. Hogfors, A. Vehmaa, and E. Gorokhova.

2014. The effects of short-term pH decrease on the reproductive output of the copepod Acartia bifilosa – a laboratory study. Mar. Freshw. Behav. Physiol. **47**: 173–183.

Ericson, J. A., N. Hellessey, S. Kawaguchi, S. Nicol, P. D. Nichols, N. Hoem, and P. Virtue. 2018. Adult Antarctic krill proves resilient in a simulated high CO_2 ocean. Commun. Biol. **1**: 190.

Feely, R. A., S. R. Alin, J. Newton, C. L. Sabine, M. Warner, A. Devol, C. Krembs, and C. Maloy. 2010. The combined effects of ocean acidification, mixing, and respiration on pH and carbonate saturation in an urbanized estuary. Estuar. Coast. Shelf Sci. **88**, doi:10.1016/j.ecss.2010.05.004

Feely, R. A., C. L. Sabine, J. M. Hernandez-Ayon, D. Ianson, and B. Hales. 2008. Evidence for upwelling of corrosive "acidified" water onto the continental shelf. Science **320**: 1490–1492.

Feely, R., S. Doney, and S. Cooley. 2009. Ocean Acidification: Present Conditions and Future Changes in a High-CO_2 World. Oceanography **22**: 36–47.

Feinberg, L. R., C. T. Shaw, and W. T. Peterson. 2006. Larval development of *Euphausia pacifica* in the laboratory: variability in developmental pathways. Mar. Ecol. Prog. Ser. **316**: 127–137.

Feinberg, L. R., C. T. Shaw, and W. T. Peterson. 2007. Long-term laboratory observations of Euphausia pacifica fecundity: comparison of two geographic regions. Mar. Ecol. Prog. Ser. **341**: 141–152.

Feinberg, L. R., C. T. Shaw, W. T. Peterson, M. Decima, Y. Okazaki, and S.-J. Ju. 2013. Euphausia pacifica brood sizes: a North Pacific synthesis. J. Plankton Res. **35**: 1192–1206.

Field, J. C., and R. C. Francis. 2006. Considering ecosystem-based fisheries management in the California Current. Mar. Policy **30**: 552–569.

Finkel, Z. V., J. Beardall, K. J. Flynn, A. Quigg, T. A. V. Rees, and J. A. Raven. 2010. Phytoplankton in a changing world: cell size and elemental stoichiometry. J. Plankton Res. **32**: 119–137.

Fitzer, S. C., G. S. Caldwell, A. J. Close, A. S. Clare, R. C. Upstill-Goddard, and M. G. Bentley. 2012. Ocean acidification induces multi-generational decline in copepod naupliar production with possible conflict for reproductive resource allocation. J. Exp. Mar. Bio. Ecol. **418**–**419**: 30–36.

Folch, J., M. Lees, and G. H. Sloane Stanley. 1957. A simple method for the isolation and purification of total lipides from animal tissues. J. Biol. Chem. **226**: 497–509.

Frost, B. W. 1972. Effects of Size and Concentration of Food Particles on the Feeding Behavior of the Marine Planktonic Copepod Calanus pacificus. Limnol. Oceanogr. **17**: 805–815.

Galloway, A. W. E., and M. Winder. 2015. Partitioning the Relative Importance of Phylogeny and Environmental Conditions on Phytoplankton Fatty Acids. PLoS One **10**: e0130053.

Garzke, J., T. Hansen, S. M. H. Ismar, and U. Sommer. 2016. Combined effects of ocean warming and acidification on copepod abundance, body size and fatty acid content. PLoS One **11**: e0155952.

Garzke, J., U. Sommer, and S. M. H. Ismar. 2017. Is the chemical composition of biomass the agent by which ocean acidification influences on zooplankton ecology? Aquat. Sci. **79**: 733–748.

Gaylord, B., K. J. Kroeker, J. M. Sunday, K. M. Anderson, J. P. Barry, N. E. Brown, S. D. Connell, S. Dupont, K. E. Fabricius, J. M. Hall-Spencer, T. Klinger, M. Milazzo, P. L.

Munday, B. D. Russell, E. Sanford, S. J. Schreiber, V. Thiyagarajan, M. L. H. Vaughan, S. Widdicombe, and C. D. G. Harley. 2015. Ocean acidification through the lens of ecological theory. Ecology **96**: 3–15.

Gobler, C. J., H. R. Clark, A. W. Griffith, and M. W. Lusty. 2017. Diurnal Fluctuations in Acidification and Hypoxia Reduce Growth and Survival of Larval and Juvenile Bay Scallops (Argopecten irradians) and Hard Clams (Mercenaria mercenaria). Front. Mar. Sci. **3**: 282.

Gomez-Gutierrez, J. 2002. Hatching mechanism and delayed hatching of the eggs of three broadcast spawning euphausiid species under laboratory conditions. J. Plankton Res. **24**: 1265–1276.

Gómez, M., S. Torres, and S. Hernández-León. 1996. Modification of the electron transport system (ETS) method for routine measurements of respiratory rates of zooplankton. South African J. Mar. Sci. **17**: 15–20.

Gruber, N., C. Hauri, Z. Lachkar, D. Loher, T. L. Frölicher, and G.-K. Plattner. 2012. Rapid progression of ocean acidification in the California Current System. Science **337**: 220–3.

Guerra, C. 2006. Growth rates and nutritional condition of Krill Larvae (Euphausia superba) in the antarctic autumn of the Sea of Lazarev, Antartica.

Guillard, R. R. L., and J. H. Ryther. 1962. Studies of marine planktonic diatoms. Can. J. Microbiol. **8**: 229–239.

Harris, R. P., P. H. Wiebe, J. Lenz, H. R. Skjoldal, and M. Huntley. 2000. Zooplankton methodology manual, Academic.

Hauri, C., N. Gruber, M. Vogt, S. C. Doney, R. A. Feely, Z. Lachkar, A. Leinweber, A. M. P. McDonnell, M. Munnich, and G. K. Plattner. 2013. Spatiotemporal variability and long-

term trends of ocean acidification in the California Current System. Biogeosciences **10**: 193–216.

Herrera, A., T. Packard, A. Santana, and M. Gómez. 2011. Effect of starvation and feeding on respiratory metabolism in Leptomysis lingvura (G.O. Sars, 1866). J. Exp. Mar. Bio. Ecol. **409**: 154–159.

Herrera, I. 2014. The use of AARS activity as a proxy for zooplankton and ichthyoplankton growth rates. University of Las Palmas de Gran Canaria.

Herrera, I., L. Yebra, T. Antezana, A. Giraldo, J. Färber-Lorda, and S. Hernández-León. 2019. Vertical variability of *Euphausia distinguenda* metabolic rates during diel migration into the oxygen minimum zone of the Eastern Tropical Pacific off Mexico. J. Plankton Res. **41**: 165–176.

Herrera, I., L. Yebra, and S. Hernández-Léon. 2012. Effect of temperature and food concentration on the relationship between growth and AARS activity in Paracartia grani nauplii. J. Exp. Mar. Bio. Ecol. **416**: 101–109.

Hildebrandt, N., B. Niehoff, and F. J. Sartoris. 2014. Long-term effects of elevated CO_2 and temperature on the Arctic calanoid copepods *Calanus glacialis* and *C. hyperboreus*. Mar. Pollut. Bull. **80**: 59–70.

Hofmann, G. E., J. P. Barry, P. J. Edmunds, R. D. Gates, D. A. Hutchins, T. Klinger, and M. A. Sewell. 2010. The effect of ocean acidification on calcifying organisms in marine ecosystems: An organism-to-ecosystem perspective. Annu. Rev. Ecol. Evol. Syst. **41**: 127–147.

Hofmann, G. E., J. E. Smith, K. S. Johnson, U. Send, L. A. Levin, F. Micheli, A. Paytan, N. N. Price, B. Peterson, Y. Takeshita, P. G. Matson, E. D. Crook, K. J. Kroeker, M. C. Gambi, E.

B. Rivest, C. A. Frieder, P. C. Yu, and T. R. Martz. 2011. High-Frequency Dynamics of Ocean pH: A Multi-Ecosystem Comparison. PLoS One **6**: e28983.

Holmborn, T., K. Dahlgren, C. Holeton, H. Hogfors, and E. Gorokhova. 2009. Biochemical proxies for growth and metabolism in *Acartia bifilosa* (Copepoda, Calanoida). Limnol. Oceanogr. Methods **7**: 785–794.

Hönisch, B., A. Ridgwell, D. N. Schmidt, E. Thomas, S. J. Gibbs, A. Sluijs, R. Zeebe, L. Kump, R. C. Martindale, S. E. Greene, W. Kiessling, J. Ries, J. C. Zachos, D. L. Royer, S. Barker, T. M. Marchitto, R. Moyer, C. Pelejero, P. Ziveri, G. L. Foster, and B. Williams. 2012. The geological record of ocean acidification. Science **335**: 1058–63.

IPCC. 2011. Workshop Report of the Intergovernmetal Panel on Climate Change Workshop on Impacts of Ocean Acidification on Marine Biology and Ecosystems, C.B. Field, V. Barros, T.F. Stocker, D. Qin, K.J. Mach, G.-K. Plattner, M.D. Mastrandrea, M. Tignor, K.L. Ebi, and And [eds.]. IPCC Working Group II Technical Support Unit.

IPCC. 2014. Summary for Policymakers. Climate Change 2014: Synthesis Report. Contribution of Working Groups I, II and III to the Fifth Assessment Report of the Intergovernmental Panel on Climate Change, Geneva, Switzerland.

Isari, S., M. Antó, and E. Saiz. 2013. Copepod Foraging on the Basis of Food Nutritional Quality: Can Copepods Really Choose? PLoS One **8**: e84742.

Isari, S., S. Zervoudaki, J. Peters, G. Papantoniou, C. Pelejero, and E. Saiz. 2016. Lack of evidence for elevated CO2-induced bottom-up effects on marine copepods: a dinoflagellate-calanoid prey-predator pair. ICES J. Mar. Sci. **73**: 650–658.

Jacob, B. G., P. von Dassow, J. E. Salisbury, J. M. Navarro, and C. A. Vargas. 2017. Impact of low pH/high pCO2 on the physiological response and fatty acid content in diatom Skeletonema pseudocostatum. J. Mar. Biol. Assoc. United Kingdom **97**: 1–9.

Jaffe, J. S., M. D. Ohman, and A. De Robertis. 1999. Sonar estimates of daytime activity levels of *Euphausia pacifica* in Saanich Inlet. Can. J. Fish. Aquat. Sci. **56**: 2000–2010.

Jónasdóttir, S. H. 1994. Effects of food quality on the reproductive success of Acartia tonsa and Acartia hudsonica: laboratory observations. Mar. Biol. **121**: 67–81.

Jónasdóttir, S. H., D. Fields, and S. Pantoja. 1995. Copepod egg production in Long Island Sound,USA, as a function of the chemical composition of seston. Mar. Ecol. Prog. Ser. **119**: 87–98.

Jónasdóttir, S., A. Visser, and C. Jespersen. 2009. Assessing the role of food quality in the production and hatching of *Temora longicornis* eggs. Mar. Ecol. Prog. Ser. **382**: 139–150.

Kawaguchi, S., A. Ishida, R. King, B. Raymond, N. Waller, A. Constable, S. Nicol, M. Wakita, and A. Ishimatsu. 2013. Risk maps for Antarctic krill under projected Southern Ocean acidification. Nat. Clim. Chang. **3**: 843–847.

Kawaguchi, S., H. Kurihara, R. King, L. Hale, T. Berli, J. P. Robinson, A. Ishida, M. Wakita, P. Virtue, S. Nicol, and A. Ishimatsu. 2011. Will krill fare well under Southern Ocean acidification? Biol. Lett. **7**: 288–291.

Kelly, M. W., J. L. Padilla-Gamiño, and G. E. Hofmann. 2013. Natural variation and the capacity to adapt to ocean acidification in the keystone sea urchin *Strongylocentrotus purpuratus*. Glob. Chang. Biol. **19**: 2536–46.

King, A., B. Jenkins, J. Wallace, Y. Liu, G. Wikfors, L. Milke, and S. Meseck. 2015. Effects of CO_2 on growth rate, C:N:P, and fatty acid composition of seven marine phytoplankton species. Mar. Ecol. Prog. Ser. **537**: 59–69.

Kiørboe, T., F. Møhlenberg, and K. Hamburger. 1985. Bioenergetics of the planktonic copepod *Acartia tonsa*: relation between feeding, egg production and respiration, and composition of specific dynamic action. Mar. Ecol. Prog. Ser. **26**: 85–97.

Kleinbaum, D., and M. Klein. 2005. Survival analysis: a self-learning text, 2nd ed. Springer.

Kroeker, K. J., R. L. Kordas, R. Crim, I. E. Hendriks, L. Ramajo, G. S. Singh, C. M. Duarte, and J. P. Gattuso. 2013. Impacts of ocean acidification on marine organisms: quantifying sensitivities and interaction with warming. Glob. Chang. Biol. **19**: 1884–1896.

Kurihara, H. 2008. Effects of CO_2-driven ocean acidification on the early developmental stages of invertebrates. Mar. Ecol. Prog. Ser. **373**: 275–284.

Kurihara, H., and A. Ishimatsu. 2008. Effects of high CO_2 seawater on the copepod (*Acartia tsuensis*) through all life stages and subsequent generations. Mar. Pollut. Bull. **56**: 1086–1090.

Langer, G., G. Nehrke, I. Probert, J. Ly, and P. Ziveri. 2009. Strain-specific responses of *Emiliania huxleyi* to changing seawater carbonate chemistry. Biogeosciences **6**: 2637–2646.

Leu, E., M. Daase, K. G. Schulz, A. Stuhr, and U. Riebesell. 2013. Effect of ocean acidification on the fatty acid composition of a natural plankton community. Biogeosciences **10**: 1143–1153.

Lewis, C. N., K. A. Brown, L. A. Edwards, G. Cooper, and H. S. Findlay. 2013. Sensitivity to ocean acidification parallels natural pCO2 gradients experienced by Arctic copepods under winter sea ice. Proc. Natl. Acad. Sci. U. S. A. **110**: E4960-7.

Lewis, E., and D. W. R. Wallace. 2012. Program developed for CO_2 system calculations. ORNL/CDIAC-105. Carbon Dioxide Information Analysis Center, Oak Ridge National Laboratory, US Department of Energy, Oak Ridge, Tennessee.

Li, L., J. E. Keister, T. E. Essington, and J. Newton. 2019. Vertical distributions and abundances of life stages of the euphausiid *Euphausia pacifica* in relation to oxygen and temperature in a seasonally hypoxic fjord. J. Plankton Res. **41**: 188–202.

Li, W., and K. Gao. 2012. A marine secondary producer respires and feeds more in a high CO_2 ocean. Mar. Pollut. Bull. **64**: 699–703.

Liu, H.-L., and S. Sun. 2010. Diel vertical distribution and migration of a euphausiid *Euphausia pacifica* in the Southern Yellow Sea. Deep Sea Res. Part II Top. Stud. Oceanogr. **57**: 594–605.

Love, B. A., M. B. Olson, and T. Wuori. 2017. Technical Note: A minimally invasive experimental system for pCO_2 manipulation in plankton cultures using passive gas exchange (atmospheric carbon control simulator). Biogeosciences **14**: 2675–2684.

Lowe, A. T., J. Bos, and J. Ruesink. 2019. Ecosystem metabolism drives pH variability and modulates long-term ocean acidification in the Northeast Pacific coastal ocean. Sci. Rep. **9**: 963.

Lueker, T. 2000. Ocean pCO_2 calculated from dissolved inorganic carbon, alkalinity, and equations for K1 and K2: validation based on laboratory measurements of CO_2 in gas and seawater at equilibrium. Mar. Chem. **70**: 105–119.

Maas, A. E., K. F. Wishner, and B. A. Seibel. 2012. The metabolic response of pteropods to acidification reflects natural CO_2-exposure in oxygen minimum zones. Biogeosciences **9**: 747–757.

Malzahn, A. M., F. Hantzsche, K. L. Schoo, M. Boersma, and N. Aberle. 2010. Differential effects of nutrient-limited primary production on primary, secondary or tertiary consumers. Oecologia **162**: 35–48.

Mangan, S., M. A. Urbina, H. S. Findlay, R. W. Wilson, and C. Lewis. 2017. Fluctuating seawater pH/pCO_2 regimes are more energetically expensive than static pH/pCO_2 levels in the mussel *Mytilus edulis*. Proceedings. Biol. Sci. **284**, doi:10.1098/rspb.2017.1642

McConville, K., C. Halsband, E. S. Fileman, P. J. Somerfield, H. S. Findlay, and J. I. Spicer. 2013. Effects of elevated CO_2 on the reproduction of two calanoid copepods. Mar. Pollut. Bull. **73**: 428–34.

McElhany, P., and D. S. Busch. 2012. Appropriate pCO_2 treatments in ocean acidification experiments. Mar. Biol. **160**: 1807–1812.

McKinnon, A. D., J. Doyle, S. Duggan, M. Logan, C. Lønborg, and R. Brinkman. 2015. Zooplankton Growth, Respiration and Grazing on the Australian Margins of the Tropical Indian and Pacific Oceans. PLoS One **10**: e0140012.

McLaskey, A., J. Keister, P. McElhany, M. Brady Olson, D. Shallin Busch, M. Maher, and A. Winans. 2016. Development of *Euphausia pacifica* (krill) larvae is impaired under pCO_2 levels currently observed in the Northeast Pacific. Mar. Ecol. Prog. Ser. **555**: 65–78.

Mehrbach, C., C. H. Culberson, J. E. Hawley, and R. M. Pytkowicx. 1973. Measurement of the apparent dissociation constants of carbonic acid in seawater at atmospheric pressure. Limnol. Oceanogr. **18**: 897–907.

Melzner, F., P. Stange, K. Trübenbach, J. Thomsen, I. Casties, U. Panknin, S. N. Gorb, and M. A. Gutowska. 2011. Food supply and seawater pCO_2 impact calcification and internal shell dissolution in the blue mussel *Mytilus edulis*. PLoS One **6**: e24223.

Meyers, M. T. 2016. Ocean acidification effects on the nutritional quality of phytoplankton for copepod reproduction. M.Sc. Thesis, San Francisco State University.

Miller, J. J., M. Maher, E. Bohaboy, C. S. Friedman, and P. McElhany. 2016. Exposure to low pH reduces survival and delays development in early life stages of Dungeness crab (*Cancer magister*). Mar. Biol. **163**: 118.

Newton, J. A., S. L. Albertson, K. Van Voorhis, C. Maloy, and E. Siegel. 2002. Washington State marine water quality in 1998 through 2000. Washingt. State Dep. Ecol. Environmen.

Nicol, S. 2000. Understanding krill growth and aging: the contribution of experimental studies. Can. J. Fish. Aquat. Sci. **57**: 168–177.

O'Donnell, M. J., M. N. George, and E. Carrington. 2013. Mussel byssus attachment weakened by ocean acidification. Nat. Clim. Chang. **3**: 587–590.

Olson, M. B., T. A. Wuori, B. A. Love, and S. L. Strom. 2017. Ocean acidification effects on haploid and diploid *Emiliania huxleyi* strains: Why changes in cell size matter. J. Exp. Mar. Bio. Ecol. **488**: 72–82.

Orr, J. C., V. J. Fabry, O. Aumont, L. Bopp, S. C. Doney, R. A. Feely, A. Gnanadesikan, N. Gruber, A. Ishida, F. Joos, R. M. Key, K. Lindsay, E. Maier-Reimer, R. Matear, P. Monfray, A. Mouchet, R. G. Najjar, G. K. Plattner, K. B. Rodgers, C. L. Sabine, J. L. Sarmiento, R. Schlitzer, R. D. Slater, I. J. Totterdell, M. F. Weirig, Y. Yamanaka, and A. Yool. 2005. Anthropogenic ocean acidification over the twenty-first century and its impact on calcifying organisms. Nature **437**, doi:10.1038/nature04095

Osma, N., I. Fernández-Urruzola, M. Gómez, S. Montesdeoca-Esponda, and T. T. Packard. 2016. Predicting in vivo oxygen consumption rate from ETS activity and bisubstrate enzyme kinetics in cultured marine zooplankton. Mar. Biol. **163**: 146.

Owens, T. G., and F. D. King. 1975. The measurement of respiratory electron-transport-system activity in marine zooplankton. Mar. Biol. **30**: 27–36.

Packard, T. T., and J. P. Christensen. 2004. Respiration and vertical carbon flux in the Gulf of Maine water column. J. Mar. Res. **62**: 93–115.

Packard, T. T., A. H. Devol, and F. D. King. 1975. The effect of temperature on the respiratory electron transport system in marine plankton. Deep Sea Res. Oceanogr. Abstr. **22**: 237–249.

Packard, T. T., and B. Williams. 1981. Rates of respiratory oxygen consumption and electron transport in surface seawater from the northwest Atlantic. Oceanol. acta **4**: 351–358.

Pan, T.-C. F., S. L. Applebaum, and D. T. Manahan. 2015. Experimental ocean acidification alters the allocation of metabolic energy. Proc. Natl. Acad. Sci. U. S. A. **112**: 4696–701.

Parker, L. M., P. M. Ross, W. A. O'Connor, L. Borysko, D. A. Raftos, and H.-O. Pörtner. 2012. Adult exposure influences offspring response to ocean acidification in oysters. Glob. Chang. Biol. **18**: 82–92.

Parrish, C. C., V. M. French, and M. J. Whiticar. 2012. Lipid class and fatty acid composition of copepods (C*alanus finmarchicus, C. glacialis, Pseudocalanus* sp., *Tisbe furcata* and *Nitokra lacustris*) fed various combinations of autotrophic and heterotrophic protists. J. Plankton Res. **34**: 356–375.

Pechenik, J. 2006. Larval experience and latent effects--metamorphosis is not a new beginning. Integr. Comp. Biol. **46**: 323–333.

Pedersen, S. A., O. J. Håkedal, I. Salaberria, A. Tagliati, L. M. Gustavson, B. M. Jenssen, A. J. Olsen, and D. Altin. 2014a. Multigenerational exposure to ocean acidification during food limitation reveals consequences for copepod scope for growth and vital rates. Environ. Sci. Technol. **48**: 12275–84.

Pedersen, S. A., V. T. Våge, A. J. Olsen, K. M. Hammer, and D. Altin. 2014b. Effects of elevated carbon dioxide (CO_2) concentrations on early developmental stages of the marine copepod *Calanus finmarchicus gunnerus* (Copepoda: Calanoidae). Journal of Toxicology and Environmental Health - Part A: Current Issues.

Pelletier, G., M. Roberts, M. Keyzers, and S. R. Alin. 2018. Seasonal variation in aragonite saturation in surface waters of Puget Sound – a pilot study. Elem Sci Anth **6**: 5.

Peterson, W. T., J. L. Fisher, P. T. Strub, X. Du, C. Risien, J. Peterson, and C. T. Shaw. 2017. The pelagic ecosystem in the Northern California Current off Oregon during the 2014-2016 warm anomalies within the context of the past 20 years. J. Geophys. Res. Ocean. **122**: 7267–7290.

Pinchuk, A. I., and R. R. Hopcroft. 2007. Seasonal variations in the growth rates of euphausiids (*Thysanoessa inermis, T. spinifera,* and *Euphausia pacifica*) from the northern Gulf of Alaska. Mar. Biol. **151**: 257–269.

Pond, D., R. Harris, R. Head, and D. Harbour. 1996. Environmental and nutritional factors determining seasonal variability in the fecundity and egg viability of *Calanus helgolandicus* in coastal waters off Plymouth, UK. Mar. Ecol. Prog. Ser. **143**: 45–63.

R Core Development Team. 2014. R: A language and environment for statistical computing.

Ramajo, L., E. Pérez-León, I. E. Hendriks, N. Marbà, D. Krause-Jensen, M. K. Sejr, M. E. Blicher, N. A. Lagos, Y. S. Olsen, and C. M. Duarte. 2016. Food supply confers calcifiers resistance to ocean acidification. Sci. Rep. **6**: 19374.

Reinfelder, J. R. 2012. Carbon dioxide regulation of nitrogen and phosphorus in four species of marine phytoplankton. Mar. Ecol. Prog. Ser. **466**: 57–67.

Ren, A. S., F. Chai, H. Xue, D. M. Anderson, and F. P. Chavez. 2018. A Sixteen-year Decline in Dissolved Oxygen in the Central California Current. Sci. Rep. **8**: 7290.

Reum, J. C. P., S. R. Alin, R. A. Feely, J. Newton, M. Warner, and P. McElhany. 2014. Seasonal carbonate chemistry covariation with temperature, oxygen, and salinity in a fjord estuary: implications for the design of ocean acidification experiments. PLoS One **9**: e89619.

Riebesell, U., V. J. Fabry, L. Hansson, and J.-P. Gattuso. 2010. Guide to Best Practices in Ocean Acidification Research and Data Reporting,.

Riebesell, U., and P. Tortell. 2011. Effects of ocean acidification on pelagic organisms and ecosystems, p. 99–121. *In* J.-P. Gattuso and L. Hansson [eds.], Ocean acidification. Oxford University Press.

Ries, J. B., A. L. Cohen, and D. C. McCorkle. 2009. Marine calcifiers exhibit mixed responses to CO_2-induced ocean acidification. Geology **37**: 1131–1134.

Ross, R. M. 1981. Laboratory culture and development of *Euphausia-pacifica*. Limnol. Oceanogr. **26**: 235–246.

Ross, R. M., L. B. Quetin, K. S. Baker, M. Vernet, and R. C. Smith. 2000. Growth limitation in young *Euphausia superba* under field conditions. Limnol. Oceanogr. **45**: 31–43.

Rossoll, D., R. Bermudez, H. Hauss, K. G. Schulz, U. Riebesell, U. Sommer, and M. Winder. 2012. Ocean Acidification-Induced Food Quality Deterioration Constrains Trophic Transfer. PLoS One **7**: e34737.

Runge, J. A., D. M. Fields, C. R. S. Thompson, S. D. Shema, R. M. Bjelland, C. M. F. Durif, A. B. Skiftesvik, and H. I. Browman. 2016. End of the century CO_2 concentrations do not have a negative effect on vital rates of *Calanus finmarchicus*, an ecologically critical planktonic species in North Atlantic ecosystems. ICES J. Mar. Sci. **73**: 937–950.

Saba, G. K., O. Schofield, J. J. Torres, E. H. Ombres, and D. K. Steinberg. 2012. Increased feeding and nutrient excretion of adult Antarctic krill, *Euphausia superba*, exposed to enhanced carbon dioxide (CO_2). PLoS One **7**: e52224.

Santora, J. A., W. J. Sydeman, I. D. Schroeder, C. S. Reiss, B. K. Wells, J. C. Field, A. M. Cossio, and V. J. Loeb. 2012. Krill space: a comparative assessment of mesoscale structuring in polar and temperate marine ecosystems. ICES J. Mar. Sci. **69**: 1317–1327.

Santora, J. A., W. J. Sydeman, I. D. Schroeder, B. K. Wells, and J. C. Field. 2011. Mesoscale structure and oceanographic determinants of krill hotspots in the California Current: Implications for trophic transfer and conservation. Prog. Oceanogr. **91**: 397–409.

Santora, J. A., R. Zeno, J. G. Dorman, and W. J. Sydeman. 2018. Submarine canyons represent an essential habitat network for krill hotspots in a Large Marine Ecosystem. Sci. Rep. **8**: 7579.

Schoo, K. L., A. M. Malzahn, E. Krause, and M. Boersma. 2013. Increased carbon dioxide availability alters phytoplankton stoichiometry and affects carbon cycling and growth of a marine planktonic herbivore. Mar. Biol. **160**: 2145–2155.

Shaw, C. T., W. T. Peterson, and L. R. Feinberg. 2010. Growth of *Euphausia pacifica* in the upwelling zone off the Oregon coast. Deep Sea Res. Part II Top. Stud. Oceanogr. **57**: 584–593.

Smith, P. K., R. I. Krohn, G. T. Hermanson, A. K. Mallia, F. H. Gartner, M. D. Provenzano, E. K. Fujimoto, N. M. Goeke, B. J. Olson, and D. C. Klenk. 1985. Measurement of protein using bicinchoninic acid. Anal. Biochem. **150**: 76–85.

Sperfeld, E., A. Mangor-Jensen, and P. Dalpadado. 2014. Effect of increasing sea water pCO_2 on the northern Atlantic krill species *Nyctiphanes couchii*. Mar. Biol. **161**: 2359–2370.

Stumpp, M., M. Hu, I. Casties, R. Saborowski, M. Bleich, F. Melzner, and S. Dupont. 2013. Digestion in sea urchin larvae impaired under ocean acidification. Nat. Clim. Chang. **3**: 1044–1049.

Sunday, J. M., K. E. Fabricius, K. J. Kroeker, K. M. Anderson, N. E. Brown, J. P. Barry, S. D. Connell, S. Dupont, B. Gaylord, J. M. Hall-Spencer, T. Klinger, M. Milazzo, P. L. Munday, B. D. Russell, E. Sanford, V. Thiyagarajan, M. L. H. Vaughan, S. Widdicombe, and C. D. G. Harley. 2016. Ocean acidification can mediate biodiversity shifts by changing biogenic habitat. Nat. Clim. Chang. **7**: 81–85.

Swiney, K. M., W. C. Long, and R. J. Foy. 2016. Effects of high pCO_2 on Tanner crab reproduction and early life history—Part I: long-term exposure reduces hatching success and female calcification, and alters embryonic development. ICES J. Mar. Sci. J. du Cons. **73**: 825–835.

Tarling, G. A., R. S. Shreeve, A. G. Hirst, A. Atkinson, D. W. Pond, E. J. Murphy, and J. L. Watkins. 2006. Natural growth rates in Antarctic krill (*Euphausia superba*): I. Improving methodology and predicting intermolt period. Limnol. Oceanogr. **51**: 959–972.

Tester, P. A., and J. T. Turner. 1990. How long does it take copepods to make eggs? J. Exp. Mar. Bio. Ecol. **141**: 169–182.

Therneau, T. 2014. A Package for Survival Analysis in S.

Thomsen, J., I. Casties, C. Pansch, A. Körtzinger, and F. Melzner. 2013. Food availability outweighs ocean acidification effects in juvenile *Mytilus edulis*: laboratory and field experiments. Glob. Chang. Biol. **19**: 1017–27.

Thor, P., A. Bailey, S. Dupont, P. Calosi, J. E. Søreide, P. De Wit, E. Guscelli, L. Loubet-Sartrou, I. M. Deichmann, M. M. Candee, C. Svensen, A. L. King, and R. G. J. Bellerby.

2018a. Contrasting physiological responses to future ocean acidification among Arctic copepod populations. Glob. Chang. Biol. **24**: e365–e377.

Thor, P., and S. Dupont. 2015. Transgenerational effects alleviate severe fecundity loss during ocean acidification in a ubiquitous planktonic copepod. Glob. Chang. Biol. **21**: 2261–71.

Thor, P., and E. O. Oliva. 2015. Ocean acidification elicits different energetic responses in an Arctic and a boreal population of the copepod *Pseudocalanus acuspes*. Mar. Biol. **162**: 799–807.

Thor, P., F. Vermandele, M.-H. Carignan, S. Jacque, and P. Calosi. 2018b. No maternal or direct effects of ocean acidification on egg hatching in the Arctic copepod *Calanus glacialis*. PLoS One **13**: e0192496.

Torstensson, A., M. Hedblom, J. Andersson, M. X. Andersson, and A. Wulff. 2013. Synergism between elevated pCO_2 and temperature on the Antarctic sea ice diatom *Nitzschia lecointei*. Biogeosciences **10**: 6391–6401.

Tremblay, N., and D. Abele. 2016. Response of three krill species to hypoxia and warming: an experimental approach to oxygen minimum zones expansion in coastal ecosystems. Mar. Ecol. **37**: 179–199.

Uppström, L. 1974. The boron chlorinity ratio of deep-sea water from the Pacific Ocean. Deep. Res. Oceanogr. Abstr. **21**: 161–162.

Uye, S.-I. 1981. Fecundity studies of neritic calanoid copepods *Acartia clausi* Giesbrecht and *A. steueri* Smirnov: A simple empirical model of daily egg production. J. Exp. Mar. Bio. Ecol. **50**: 255–271.

Vehmaa, A., A. Brutemark, and J. Engstrom-Ost. 2012. Maternal Effects May Act as an Adaptation Mechanism for Copepods Facing pH and Temperature Changes. PLoS One **7**: 8.

Wang, T., S. Tong, N. Liu, F. Li, M. L. Wells, and K. Gao. 2017. The fatty acid content of plankton is changing in subtropical coastal waters as a result of OA: Results from a mesocosm study. Mar. Environ. Res. **132**: 51–62.

Whiteley, N. M. 2011. Physiological and ecological responses of crustaceans to ocean acidification. Mar. Ecol. Ser. **430**: 257–271.

Wittmann, A. C., and H.-O. Pörtner. 2013. Sensitivities of extant animal taxa to ocean acidification. Nat. Clim. Chang. **3**: 995–1001.

Wootton, J. T. 1994. The Nature and Consequences of Indirect Effects in Ecological Communities. Annu. Rev. Ecol. Syst. **25**: 443–466.

Wynn-Edwards, C., R. King, A. Davidson, S. Wright, P. Nichols, S. Wotherspoon, S. Kawaguchi, and P. Virtue. 2014. Species-Specific Variations in the Nutritional Quality of Southern Ocean Phytoplankton in Response to Elevated pCO_2. Water **6**: 1840–1859.

Yebra, L., E. Berdalet, R. Almeda, V. Pérez, A. Calbet, and E. Saiz. 2011. Protein and nucleic acid metabolism as proxies for growth and fitness of *Oithona davisae* (Copepoda, Cyclopoida) early developmental stages. J. Exp. Mar. Bio. Ecol. **406**: 87–94.

Yebra, L., R. P. Harris, and T. Smith. 2005. Comparison of five methods for estimating growth of *Calanus helgolandicus* later developmental stages (CV-CVI). Mar. Biol. **147**: 1367–1375.

Yebra, L., and S. Hernández-León. 2004. Aminoacyl-tRNA synthetases activity as a growth index in zooplankton. J. Plankton Res. **26**: 351–356.

Yebra, L., A. G. Hirst, S. Hernandez-Leon, and R. P. Harris. 2006. Assessment of *Calanus finmarchicus* growth and dormancy using the aminoacyl-tRNA synthetases method. J. Plankton Res. **28**: 1191–1198.

Yebra, L., T. Kobari, A. R. Sastri, F. Gusmão, and S. Hernández-León. 2017. Advances in Biochemical Indices of Zooplankton Production. Adv. Mar. Biol. **76**: 157–240.

Zhang, D., S. Li, G. Wang, and D. Guo. 2011. Impacts of CO2-driven seawater acidification on survival, egg production rate and hatching success of four marine copepods. Acta Oceanol. Sin. **30**: 86–94.